THE NEARSHORE DYNAMICS OF MATROOS BAY

– FIELD AND THEORETICAL INVESTIGATIONS

A thesis submitted in fulfillment of
the requirements of the degree
Master of Science
at
The University of Cape Town
by
Bruce William Gunn.

April
1977.

Supervisor: Professor T.F.W. Harris.

CONTENTS

LIST OF TABLES

LIST OF FIGURES

LIST OF PLATES

ACKNOWLEDGEMENTS

This research was carried out under the supervision of Professor T.F.W. Harris. His assistance and encouragement have been greatly appreciated. I take this opportunity of expressing, to him, my sincerest thanks.

Thanks must also be expressed to all those that assisted with the field work and data processing. Mr. J. Ravenscroft and Miss S. Leach must be mentioned, in particular, for their assistance.

All credit for the drafting in this report must go to Mr. A. Britten-Jones and for the typing to Miss S. Leach. The many hours of work performed by these two people have been much appreciated.

Wind and wave records were supplied by the ESCOM Research Unit.

Financial support for this study was supplied by the National Program for Environmental Sciences.

ABSTRACT

Field and theoretical investigations were made of the near-shore circulation of Matroos Bay, a small embayment on the south-western coast of Africa. The field study revealed two dominant circulation types, denoted "anticlockwise" and "clockwise". The anticlockwise circulation type was characterized by longshore currents flowing from the back of the bay to the northern headland where a rip current was located. The clockwise circulation type was characterized by longshore currents flowing from the northern headland to the back of the bay where a rip current was situated. Anticlockwise circulation types were primarily found to occur during periods of low waves, the clockwise circulation during periods of high waves. Winds and coastal currents were found not to have a major influence on the circulation within the bay.

The theoretical study was based on a model of longshore currents in a semi-circular bay (O'Rourke and Le Blond, 1972). This study showed that a change of the height of the wave could lead to a change in the direction of flow of the longshore current. In agreement with the field study, a low wave height was found to result in an anti-clockwise circulation type, a high wave height resulting in a clockwise circulation type. The change from one circulation type to the other depended on the relative strength of two opposing mechanisms. One mechanism arose from the obliquity of the wave approach to the shore. This mechanism generated longshore currents towards the back of the bay and was dominant during high waves. The other mechanism resulted from the non-uniformity of the wave height around the bay and generated longshore currents flowing from the back of the bay.

Coastal currents were measured as part of the field study. A fair correlation was observed between the direction of the coastal current and that of the wind, particularly if the winds were moderate to strong.

Temperature and salinity measurements were also made. These properties showed seasonal variations in accord with the principles of upwelling. Surface water was found to have a salinity similar to that found at a depth of 400 to 600 metres in the South Atlantic Ocean. The water was upwelled from a greater depth during the summer than during the winter. Heating of the water was found to be greater in summer than in winter whilst dilution of the water, due to rainfall, was found to be negligible, even during winter.

The interchange of water between the bay and the coastal circulation was found to be dependent on the circulation type.

1. INTRODUCTION AND LITERATURE REVIEW

The nearshore region of the ocean is probably the most familiar region of the ocean to the majority of people yet it remains perhaps the least understood, and, until the last few decades, the least studied region. It was initially military and, more recently, economic and environmental considerations that have forced us to devote more time to this complex but intriguing area.

For the purpose of this study the terminology of Shepard and Inman (1950) will be followed as this has now come into fairly common practice. They define "(1) the nearshore system associated with the wave motion in and near the breaker zone, and (2) the current system which is more pronounced in deeper water adjacent to the surf zone .... coastal currents .... not related genetically to the waves and the resulting surf". Although the importance of the circulation about a vertical axis had been pointed out some years earlier (Shepard et al, 1941), it was again Shepard and Inman (1950) who detailed the nearshore system as being composed of "(1) Shoreward mass transport of water .... (2) Longshore currents of movement along the shore, largely confined to the surf zone. These currents are caused by (a) waves approaching the beach at an angle and (b) the rise in water level due to mass transport by waves. (3) Seaward return flows;(a) Rip currents .... (b) Uniform return flow. (4) Rip heads".

This investigation will be concerned with the circulation within a bay, Matroos Bay (see frontispiece). This is a bay approximately 1500 metres wide with an open mouth, exposed to the South Atlantic Ocean. The circulation within the whole bay will be considered, in particular, the wave driven circulation comprising the nearshore system

of the bay. Forcing of this wave driven circulation primarily occurs around the edges of the bay where the waves break and drive longshore currents. Two distinct mechanisms are involved in this process; one, the action of the waves breaking at an angle to the contours, and two, the gradient of the wave height around the shoreline as induced by refraction processes. Dominance of either one or the other of these processes can result in a shift in the position of the rip currents with different nearshore circulations resulting.

In dealing with a prototype situation it is not possible to eliminate all but one of the driving forces acting and study the effect of that force in isolation. Usually several forces will be present at any time. To determine the response of the system to any one force it is necessary to be able to identify possible influence of the forces that are present. In considering the wave driven nearshore circulation within Matroos Bay it is necessary to establish whether other driving forces will have an effect on the nearshore circulation. The driving forces that will be considered are the wind and the coastal current.

Matroos Bay is located in the Benguela upwelling region off the south-western coast of Africa. Upwelling occurs as a response to the strong south-easterly winds that blow throughout much of the year. A rapid drop in the temperature and salinity of the water is experienced near the coast as a result of upwelling. Temperature and salinity measurements were made throughout this study to try to establish whether upwelling was occuring within Matroos Bay, and if so, whether temperature and salinity changes so produced could be used as a natural tracer of nearshore and coastal water movement. It was also possible to investigate the response time of the temperatures and salinities to the wind.

As mentioned earlier, the principle aim of this investigation was to determine the circulation within the bay and to establish what were the driving forces of the circulation. Before considering the methods and results of this study it is as well to review the development of our knowledge of nearshore circulation.

Nearshore circulation - a literature review: The first attempts at deriving a predictive equation for longshore current velocity due to obliquely incident waves were performed by Putnam, Munk and Traylor (1949). The equations they derived were based on momentum and energy considerations of solitary waves incident on a plane beach. In subsequent years field and laboratory studies on longshore currents were made (Shepard and Inman, 1950, 1951; Inman and Quinn, 1952; Galvin and Eagleson, 1965; Brebner and Kampuis, 1963) and several more formulae for longshore currents were proposed (Inman and Quinn, 1952; Inman and Bagnold, 1963; Bruun, 1963; Galvin and Eagleson, 1965; Eagleson, 1965). In fact, Sonu et al (1966) were able to list no less than 12 formulae based on either general or specific conditions. They mention that "these formulae contain widely varied contributions of the component variables. For instance, note the angle of incidence, ϕ, ... is taken as a sine function in some formulae, as a cosine in others, with ϕ or 2ϕ, carrying different exponents. Thus, the question arises as to which of these formulae gives the best approximation to phenomena observed in the field". Perhaps the answer to this question was provided at the time by Galvin's (1967) review when he concluded "there is still no adequate theoretical prediction of longshore current velocity".

He also concludes that "longshore currents are considerably more complicated than the models on which theoretical studies have been based. Important factors not accounted for in the theories include breaker type, nearshore hydrography and the nearshore current system".

With the introduction of the concept of radiation stress (Longuet-Higgins and Steward, 1960, 1961, 1962, 1964) advances were to come. Bowen (1969) and Longuet-Higgins (1970a, b) independently proposed formulae for the prediction of longshore currents by considering the longshore momentum flux. Both of these papers derive an expression for the longshore current by balancing the driving force (gradient of radiation stress) to the bottom and lateral frictions. They differ in the details of the representaion of the friction terms. This formulation appears to be physically the most realistic yet developed for longshore current generation by oblique wave incidence and is more consistent with the laboratory and field measurements than were earlier formulae. Even so, there is considerable scatter in a plot of predicted and observed longshore current velocities, $\langle v \rangle$, (figure 1.1). The agreement between the predicted and observed velocity is improved (figure 1.2) if the modified formulae of Komar and Inman (1970) is used,

$$\langle v \rangle = 2.7 \quad u_m \quad \sin \phi_b \quad \cos \phi_b \qquad 1.1$$

The scatter observed, particularly amongst the earlier measurements, may be due to insufficient detail concerning where in the nearshore system the longshore current was measured. In fact, Komar (1975) points out that the measured longshore current could be caused by an oblique wave approach and a longshore variation of wave height, although the longshore gradient of the wave height was not measured.

It is surprising that the generation of longshore currents by a longshore gradient of wave height has received little attention since it was first mentioned by Shepard and Inman (1950). In their study of the nearshore circulation near Scripps Beach, they found that refraction resulting from offshore topographic features causes longshore variations in wave height with longshore currents flowing from areas of high waves to areas of low waves. The most

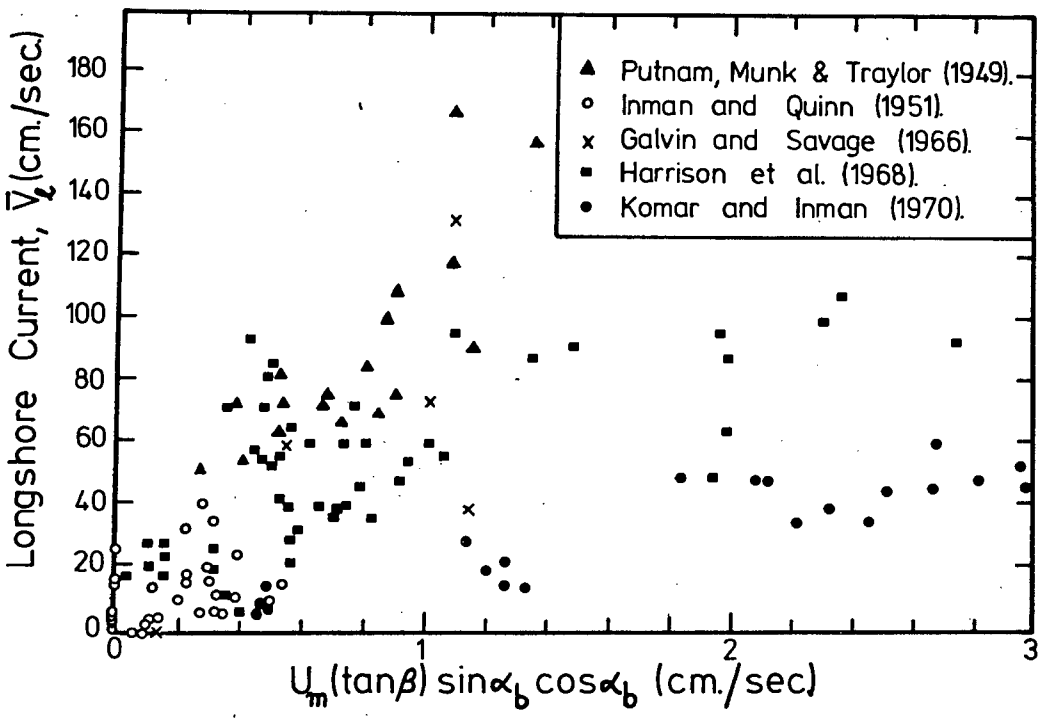

Fig. 1.1 Examination of the longshore current relationship deduced by Longuet-Higgins (1970a). [after Komar and Inman, (1970)].

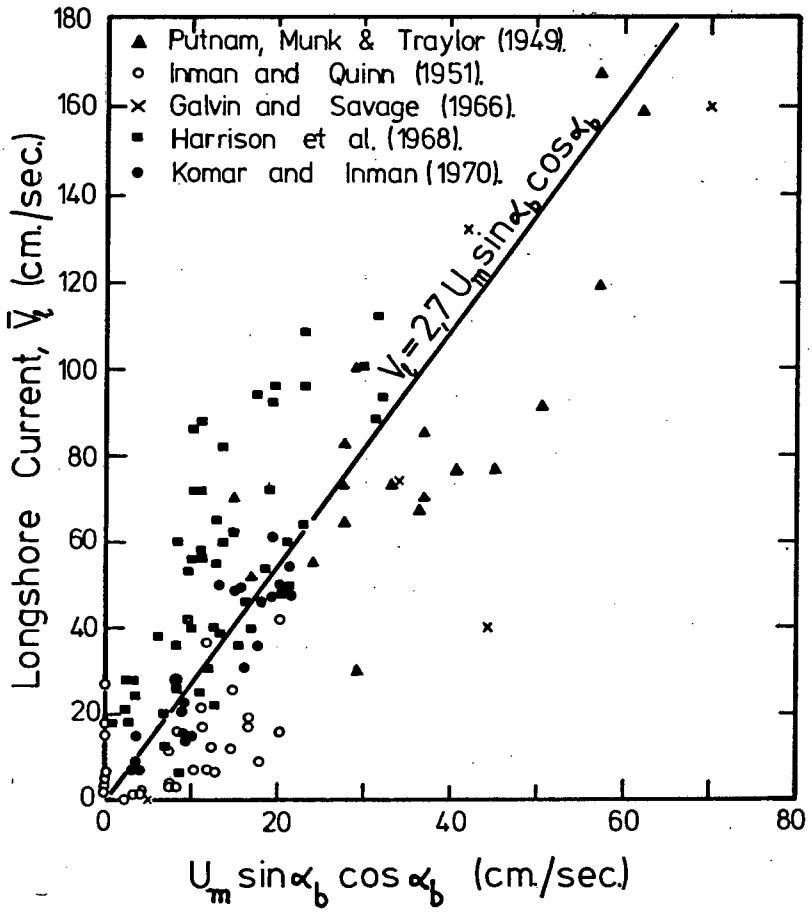

Fig. 1.2 The longshore current relationship deduced by Komar and Inman (after Komar & Inman, 1970).

complete equations for the longshore current on a plane beach have been derived by Le Blond (1972) and Komar (1975). In the equations developed the forcing of the longshore currents by oblique incidence and longshore wave height gradients are balanced by bottom friction and lateral mixing.

Harris (1964) observed that rip currents occuring in regions of low wave height were regularly spaced along a beach. He suggested that edge waves may be possible for the regular spacing observed. Using the concept of radiation stresses, Bowen (1967) showed theoretically that wave height variations could lead to nearshore circulations in which a longshore current flowed from regions of high to regions of low waves. Rip currents developed at the low wave regions. He proposed that if topographically induced wave height variations were not present the incoming waves would excite edge waves that would give rise to wave height variations. He was able to find good agreement between the wavelength of the edge waves and the spacing of the rip currents in both laboratory and field measurements. Similar results are presented by Bowen (1969b) and Bowen and Inman (1969).

Dalrymple (1975) showed that wave trains of similar period but different direction could result in longshore wave height differences and hence rip current spacing whilst Le Blond and Tang (1974) proposed a spacing mechanism based on minimization of energy dissipation. Gourlay (1974) illustrated that refraction-diffraction around a breakwater could lead to longshore wave height gradients. This gradient would generate a longshore current flow from the more exposed region to the sheltered region in the lee of the breakwater. This mechanism may however be considered to be related to the topographic influences pointed out by Shepard and Inman (1950).

Hino (1972, 1973, 1974) has developed a theory for nearshore currents in which instability mechanisms are responsible for the spacing of the rip currents. To reconcile the different ideas regarding rip current spacing Sasaki and Horikawa (1975) introduce domains for which the theories of Bowen and Inman (1969) and Hino (1972, 1973, 1974) are applicable. The basis by which the regions are divided is the "Iribarren No.", $\jmath$

$$\jmath = \frac{\tan \beta}{\sqrt{H/L_o}} \qquad 1.2$$

which is approximately the reciprocal of the number of waves in the surf zone (Battjes, 1974). They find the edge wave theory of Bowen and Inman (1969) to be applicable for $\jmath > 1$ i.e. steep beaches; the instability theory of Hino (1972, 1973, 1974) to be applicable for $1 > \jmath > .23$, for medium slope beaches; and propose an Infragravity wave domain for $\jmath < .23$, i.e. shallow beaches.

The authors suggest that edge waves are responsible for the spacing of the rip currents in both the edge wave and the infragravity wave domains. The difference between the two domains is the period responsible for the excitation of the edge wave. In the edge wave domain, edge waves respond to periods of the order of 10 seconds whilst in the infragravity wave domain the response is to periods of 50 seconds to 5 minutes.

The positioning of the nearshore cell, and in particular of the rip current, was shown to be dependent on the bottom topography within the surf zone by field observations of Sonu (1973). Subsequent work by Noda (1972, 1974) has shown that the bottom topography within the surf zone can play a major role in determining the rip current position. This concept is of course not applicable on a plane beach and serves to illustrate the role of yet another possible complication to nearshore circulation processes.

Thus several possible mechanisms exist which could determine the spacing of the rip currents and hence also the size of the nearshore circulation cells and the resultant longshore current growth. As with most physical processes, more than one of these mechanisms may be present at any time with a complex pattern resulting. An example of such a situation may be demonstrated in figure 6 of Shepard and Inman (1950) (reproduced here as figure 1.3). Two small rip currents were found between large rips that extended some 500 to 1,000 feet offshore. The complexity arises as a result not only of the number of mechanisms operating, but, also, of the different scales of the mechanisms. Both mathematical and numerical models may be used to study the effect of one particular forcing mechanism, thus reducing the complexity of a problem.

Whilst rip currents have been studied as part of the nearshore circulation system, they have also received individual attention in some cases. In an early study Shepard et al (1941) found the intensity of the current to be related to the height of the incoming waves. The position of the current was found to coincide with the centre of beach cusps. Bowen (1969a) and Bowen and Inman (1969) construct a theory for the entire circulation cell where they show that the width of the rip current was reduced with increasing Reynolds Number of the flow. The rip itself was, however, driven by the inflowing longshore currents and the dynamics of the rip current itself was not clearly illustrated. Arthur (1962) showed also that the width of the rip would decrease with increasing depth due to the nonlinear terms in the equations of motion. Tam (1973) proposed a model whereby the rip current derived its energy from the feeder currents, balancing this only by horizontal mixing.

Thus, three ways by which the topography may play a role in influencing the nearshore circulation have been mentioned:

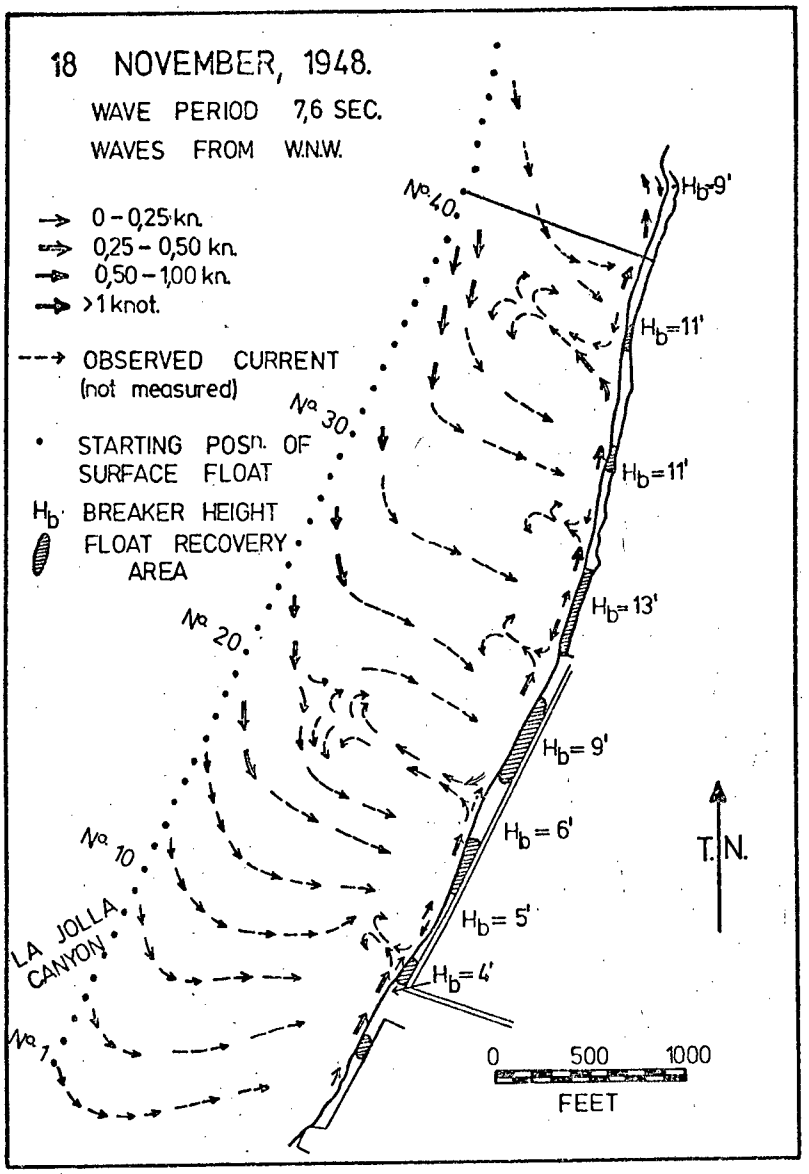

Fig. 1.3 Typical nearshore circulation pattern resulting from waves less than ten second period approaching normal to Scripps Beach and a southerly flowing coastal current (after Shepard & Inman, 1950).

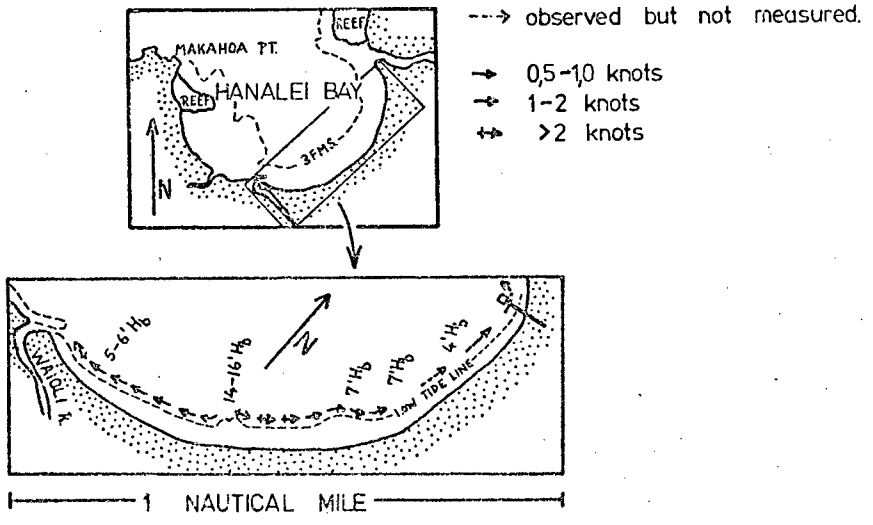

Fig. 1.4 Current system during large breakers at Hanalei, Kauai (after Shepard & Inman, 1950).

one, the effect of the offshore topography; two, the influence of headlands and nearshore beach slope on rip current spacing, e.g. edge waves; and three, by topographic control of the circulation by submarine features within the surf zone.

Although this study was not concerned with sediment movement it is as well to remember that the bottom may be affected by the circulation, as well as affecting the circulation. As a result of this, equilibrium may or may not be achieved by a particular wave condition. In laboratory experiments, Komar (1975) observed cusps to develop in the lee of rip currents shortly after the commencement of wave activity. Approximately half an hour after the start of the experiment the rip currents ceased and the shoreline remained stable. He points out that the oblique incidence of the waves on the sides of the cusp was probably balanced by wave height differences resulting from edge waves. Any small changes in wave parameters could now result in a dominance of either mechanism with rip currents resulting at the apex of the cusp, the centre of the embayment or possibly from the side of the cusp. Such variations have been observed in practice, e.g. Komar (1971).

In a large bay the driving mechanism along the sides of the headlands will be qualitatively similar to those on the sides of the cusps. There will, however, be important differences; for example, the scale will be fixed, not variable as with cusps, and the topography may be considered stationary.

The first report of wave driven currents in an embayment was given by Shepard and Inman (1950). They found longshore currents flowing from the centre to the edges of Hanalei Bay in response to a gradient in the wave height (figure 1.4). Cresentic sand bars observed by Clos-Arceduc

(1962) in the Mediterranean had a wavelength of about 600 m. These sand bars were believed to have resulted from circulation cells, the wavelength of which was either related to the surf beats or to an edge wave subharmonic to the incoming wave period.

Theoretically, the wave-driven circulation in a semi-circular bay has been considered by O'Rourke and Le Blond (1972). In their study they derive expressions for the stream functions within a bay and show that the forcing term contains contributions resulting from the variation in angle of incidence along the beach, the oblique incidence of waves and longshore inhomogeneities of the incoming wave field. The form of their solutions will be considered later.

In conclusion, it may be stated that the radiation stress theory has assisted greatly our understanding of nearshore water movements, in particular, of longshore currents. Many problems, such as wave-current interactions, non-linearities and time dependence, still await a satisfactory treatment but advances are being made (James, 1974a,b; Noda, 1974; Le Blond and Tang, 1974).

In the light of recent developments many of the older sets of laboratory and field data are found to lack details of important parameters. Theoretical models still rely on inapplicable approximations and wave theories. This provides much scope for further research.

This study is primarily concerned with the gross circulation patterns within a bay and the driving forces of this circulation, not with smaller scale phenomena or sediment movement.

2. LOCATION AND BATHYMETRY OF THE FIELD SITE

The data used for this study were collected on the south-western coastline of Cape Province, South Africa, at Matroos Bay (Matroosbaai), 33°36' S, 18°21' E, (3719000x, 60000y) (figure 2.1). The coastline in this region consists of rocky headlands with sandy beaches forming a series of embayments of varying width and breadth. Matroos Bay is one such embayment covering an area of .75 x 10^6 square metres and having a south-westerly aspect exposed to the South Atlantic Ocean.

Figure 2.2 illustrates the bathymetry of the area 40 kilometres to the north and south of Matroos Bay. Offshore from Matroos Bay no major topographic disturbances occur. Contours in this region lie generally in a north-north-west to south-south-easterly direction and are thus almost parallel to the coastline. The average slope of the sea floor to the 100 metre contour is approximately 1:70.

The bathymetry of Matroos Bay itself is presented in figure 2.3. The measurements of the depth were obtained by echo sounder and reduced to depths relative to the South African Geodetic Survey Datum (Mean Sea Level) by elimination of tidal effects. Tidal records were obtained from Granger Bay, near Cape Town Harbour, and were assumed to be representative of the tides at Matroos Bay both in elevation and phase (see section 3.2.2.).

Matroos Bay is approximately 1500 metres wide between the headlands and 500 metres in breadth. The headlands are composed of rock as is the only major feature of the bathymetry, a reef or "blinder" reaching almost to the surface, situated some 400 metres west of the southern headland (see frontispiece). The coastline within the bay is sand

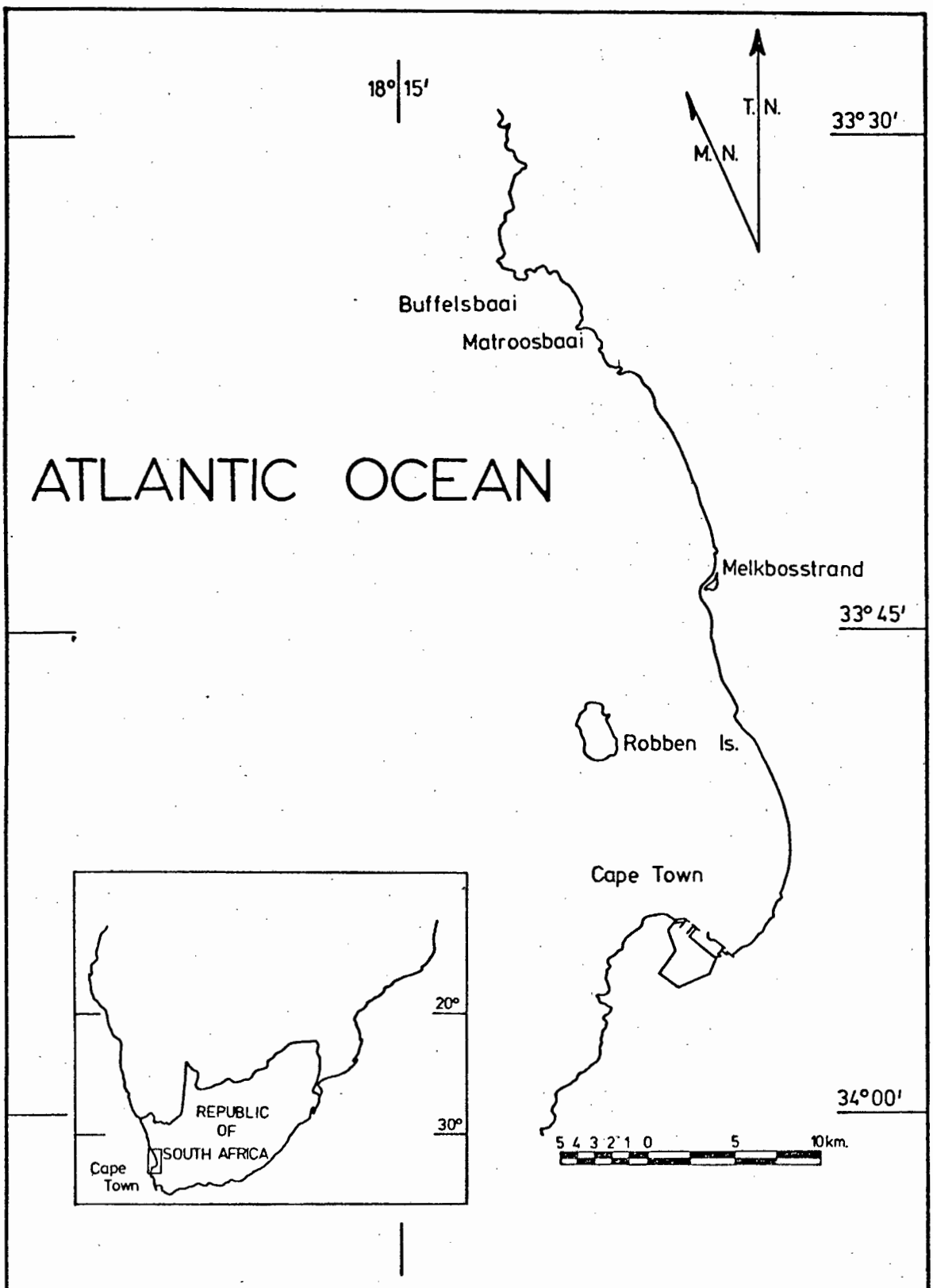

Fig. 2.1 Location plan for Matroosbaai.

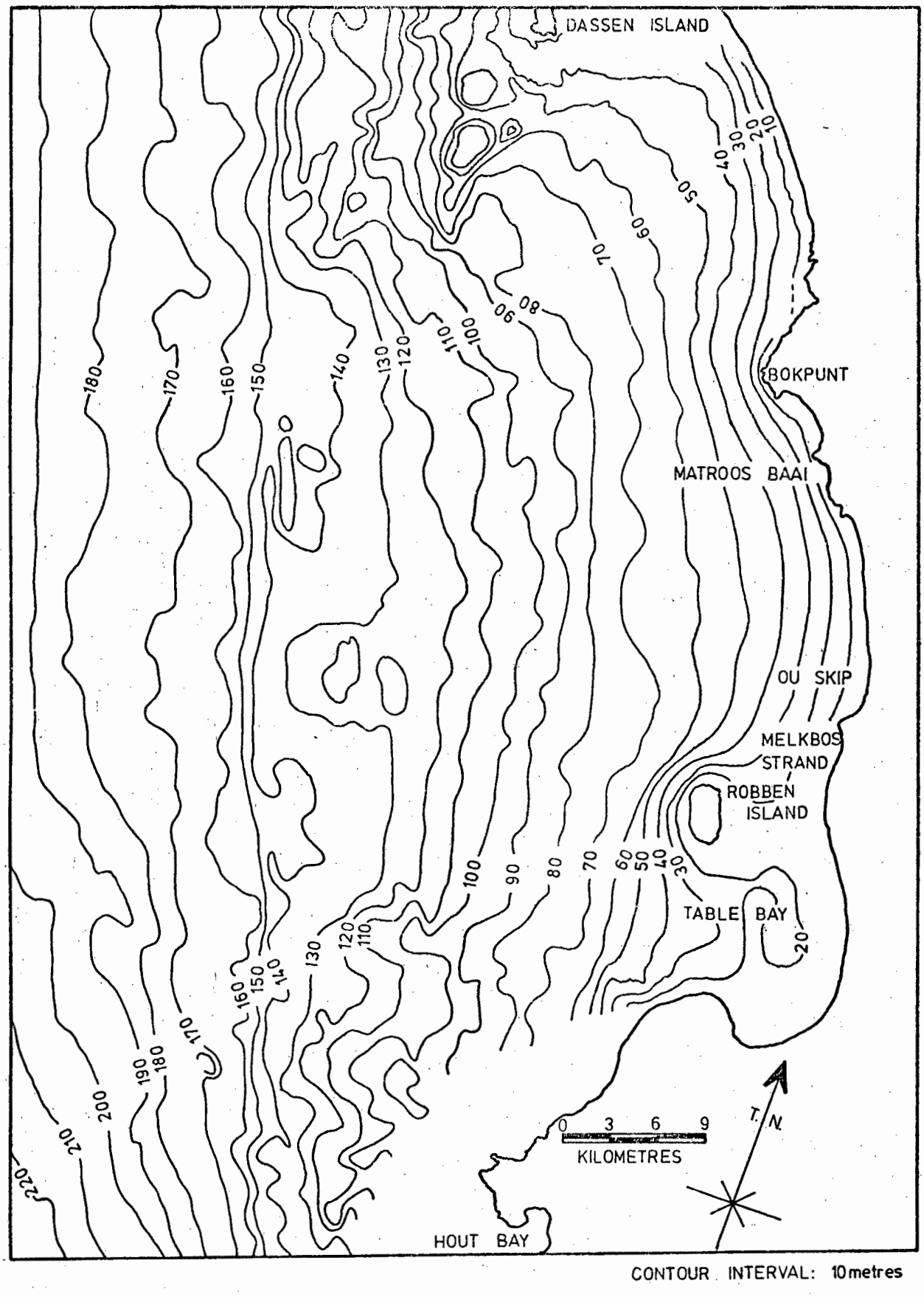

Fig. 2.2 Bathymetric contours between Dassen Island and Hout Bay.

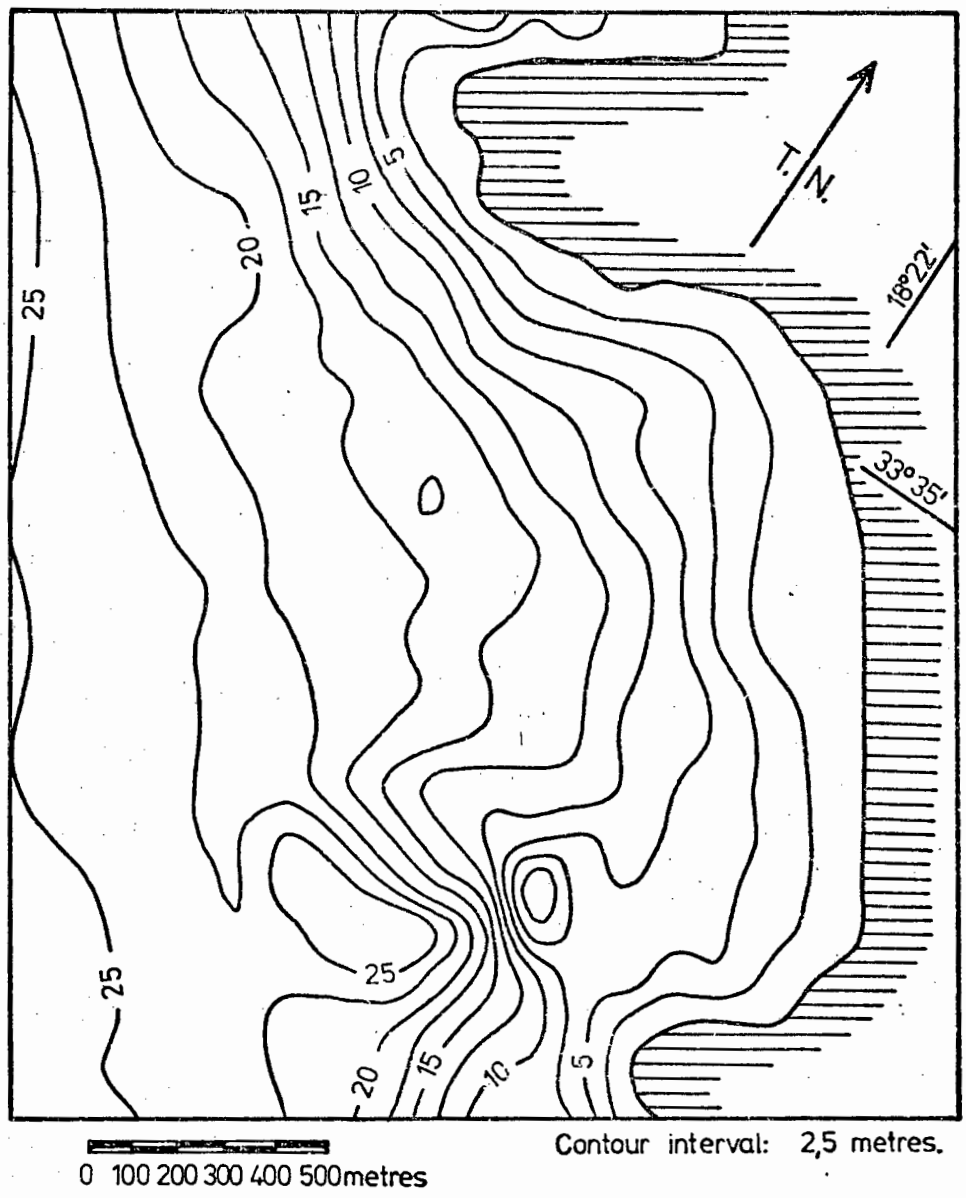

Fig. 2.3 Bathymetric map of Matroosbaai.

as is the sea-bed in most of the bay. It is thus subject to movement and scouring at times and the contours near the coastline may show slight variations. The coastline of the bay may be described as consisting of two arcs from the rocky headlands to the sandy beach with an almost straight, sandy beach in between. Occasionally cusps would form or channels would be eroded but these temporary features were not rigorously investigated.

The sea bottom normal to the centre of the bay had a typical slope of 1:50 and thus reached a depth of approximately 10 metres between the headlands.

Diagrams of Matroos Bay presented in this report cover an area of 2000 x 23000 metres rotated 31.5° anticlockwise, about an origin at (37121300x, 59400y).

3. REVIEW OF METEOROLOGICAL AND OCEANOGRAPHIC CONDITIONS

3.1. Meteorological Conditions

3.1.1. Large scale features

General: The climate of the south-western corner of Africa may be described as Mediterranean, with dry summers and wet winters being experienced. This situation is brought about largely due to the influence of the South Atlantic high pressure system and its latitudinal variations.

The South Atlantic Anticyclonic Cell: During summer the latitudinal axis of this cell lies at approximately 30°S, bringing strong persistent winds from the south-east over the waters off south-western Africa. The strongest winds induced by this circulation system are to be found in the latitudes 25° - 30°S.

During winter the anticyclonic cell intensifies slightly and moves north to about 26°S. This allows the Cape region to come under the influence of depressions in the westerlies which move eastwards from the South-west Atlantic bringing north-westerly winds and rain (Hart and Currie, 1960; Taljaard, 1972).

Summer conditions in the Cape are characterised by persistent strong "south-easters" whilst in winter south-easterly winds of lesser strength and north-westerly fronts occur with a period of about one week.

Cyclone Distribution: The distribution of cylone centres for all seasons shows a maximum from South America through Gough Island to Antarctica. Another maxima is located around the Antarctic Continental Trough (Taljaard, 1972). Recent

studies by Shillington and Harris (1974) have shown that many of the waves observed breaking on the western Cape beaches may be traced to storms in the vicinity of Gough Island, some 1500 nautical miles to the west-south-west of Cape Town.

3.1.2. Local meteorological features

Summer Wind Conditions - The "South-easter": During summer the Cape weather is fine and dry with the "South-easter" blowing, showing a diurnal variation in strength and direction.

Unfortunately, no systematic quantitative observations of the wind distribution off the Cape coast have been made. Qualitative observations suggest that the maximum wind speeds are found near the coast and that there is a sharp fall in wind speed and a veering to the south-west occuring about 50 kilometres offshore (Bang, 1973). Stander (1967) has also found, off the coast of South West Africa, that the wind becomes more constant away from the coast and tends to the south-west. The South-easter may thus be regarded as covering an area from approximately 80 kilometres offshore to 50 kilometres onshore and with a vertical extent of only about 1000 to 1500 metres. A subsidence inversion with a lower base at approximately 1000 metres provides a restriction to vertical motion and renders the South-easter subject to topographical control. This topographical influence has important implications for the upwelling observed off the Cape coast (Bang, 1973).

The observed speed of the South-easter is generally greater than the geostrophic velocity estimated from the surface pressure synoptic charts. Bang (1973) suggested that "the Cape South-easter can be regarded as a trade wind boosted by the local pressure gradient which is, in turn, a complex

function of the diurnal and seasonal land/sea temperature gradients". In many aspects there is a similarity between the South-easter being boosted by the sea breeze in the Cape region and the continental sea breeze of the Australian mainland being boosted by the local sea breeze system in the South Australian Gulf System, as postulated by Physick (1974). The anticlockwise rotation and afternoon strengthening of the sea-breeze system on the western Cape may help to explain the diurnal variation of the observed winds. Some feedback may occur in such a system with the colder coastal water temperatures resulting from the upwelling enhancing land/sea temperature differences during the day and suppressing this difference during the night. Bang (pers. comm.) has further suggested that diurnal variations in the level of the subsidence inversion may give rise to variations in the speed of the wind.

Van Ieperen (1971) obtained a two year wind record at Rietvlei, on the eastern side of Table bay, 27 kilometres to the south of Matroos Bay. South to south-east winds were dominant during spring (49%), summer (58%) and autumn (38%). Over half the winds experienced from these directions had a speed in excess of 7 $m.sec^{-1}$.

A similar distribution of wind speed and direction has been found at Melkbosstrand, 12 kilometres south of Matroos Bay (Mallory, 1976a) and at Cape Columbine, 80 kilometres to the north (CSIR, 1976b).

The Winter Wind Distribution: During winter the wind directions alternate between south-east and north-west. Winds from these directions are observed with approximately equal frequency. Van Ieperen (1971) found the strongest winds during winter were generally from the north-west to west-south-west.

Rainfall: Rainfall statistics from Melkbosstrand show a clear winter rainfall maxima of 60 to 70 mm.month^{-1} and summer minima of only 10 - 15 mm.month^{-1}. Dilution of the coastal water resulting from rainfall and runoff is expected to be more noticeable in winter than in summer.

3.2. Oceanographical Conditions

3.2.1. Large scale features

South Atlantic Circulation: The surface currents in the South Atlantic Ocean take the general form of a large anticyclonic gyre. The eastern boundary of this system is generally taken as the Benguela Current and the South-east Trade Wind Drift.

The primary driving forces responsible for this circulation are classically considered to be the Tropical Easterlies and the high latitude Westerlies. The South American and African land masses provide the boundaries for the circulation but meridional winds along these boundaries were not considered to be major driving mechanisms. Recently however, Bang (1973) has found that an equatorward jet at the edge of the continental shelf off Cape Peninsula may account for as much as one third of the total northward transport in surface to intermediate waters in the Southern Atlantic Ocean. He concluded that the strength of this jet is largely due to the local wind structure and hence that the local winds may have a profound effect on the circulation of the whole ocean system. The validity of this somewhat startling conjecture as yet awaits confirmation!

The Benguela Current Regime: Forming the eastern boundary of the South Atlantic Gyre the Benguela Region is a region of upwelling resulting from the strong south-easterly winds. The Benguela Current carries cold, low salinity water northwards between 34° S. and 15° S. keeping within 200 kilometres off the coastline (Shannon, 1970).

Shannon (1966) considered the Benguela Region to be divided into two regions with slightly different characteristics. The Northern Region was considered to be the area north of 29°S. whilst the Southern Region comprised the area between Cape Point and Cape Columbine. Although most "classical" Benguela concepts have been formulated for the Northern Region, only the Southern Region will now be considered.

As an upwelling region, the Southern Benguela Region is characterised by low temperatures and salinities, with surface temperatures as low as 9° C and salinities below 34.6 ‰ having been recorded near the coast (Shannon, 1970). The source of the upwelled water is the South Atlantic Central Water. Figure 3.1 shows a surface temperature chart of the Cape upwelling region. Upwelling occurs close to the shore and is strongest near Cape Town and Cape Columbine. Bang (1973) considers that the uplifting of water may occur in two stages, the first a dynamic uplifting onto the continental shelf and the second when the water is brought to the surface as a result of local wind/Ekman transport mechanisms. The presence of cold water on the shelf results in rapid manifestation of upwelling during a south-east wind as cold water need only be displaced from this level. Figure 3.2 shows schematically the dominant features of the Cape upwelling system as depicted by Bang (1976).

Close to the shore the topographic control of the wind has consequences for upwelling. Upwelling almost always appears strongest in the lee of mountain chains rather than exposed bays. In particular, the position of wind gaps in the Cape Peninsula mountains have been related to positions of preferred initiation of upwelling (Andrews and Cram, 1969). Consequently most active upwelling occurs close to shore.

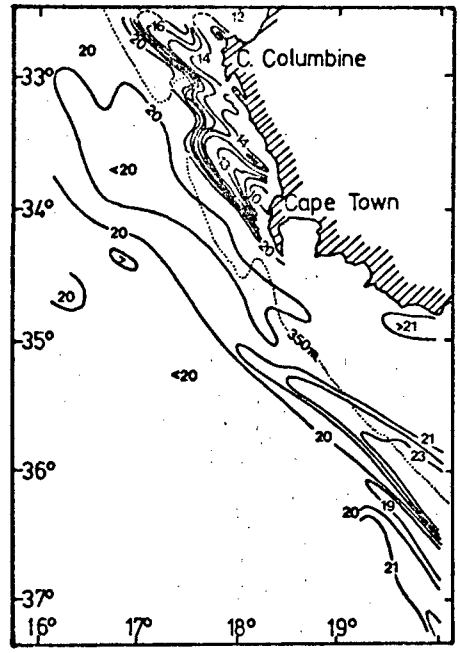

Fig. 3.1 Surface temperature chart indicating the main surface features of the Cape upwelling system. (after Bang, 1972)

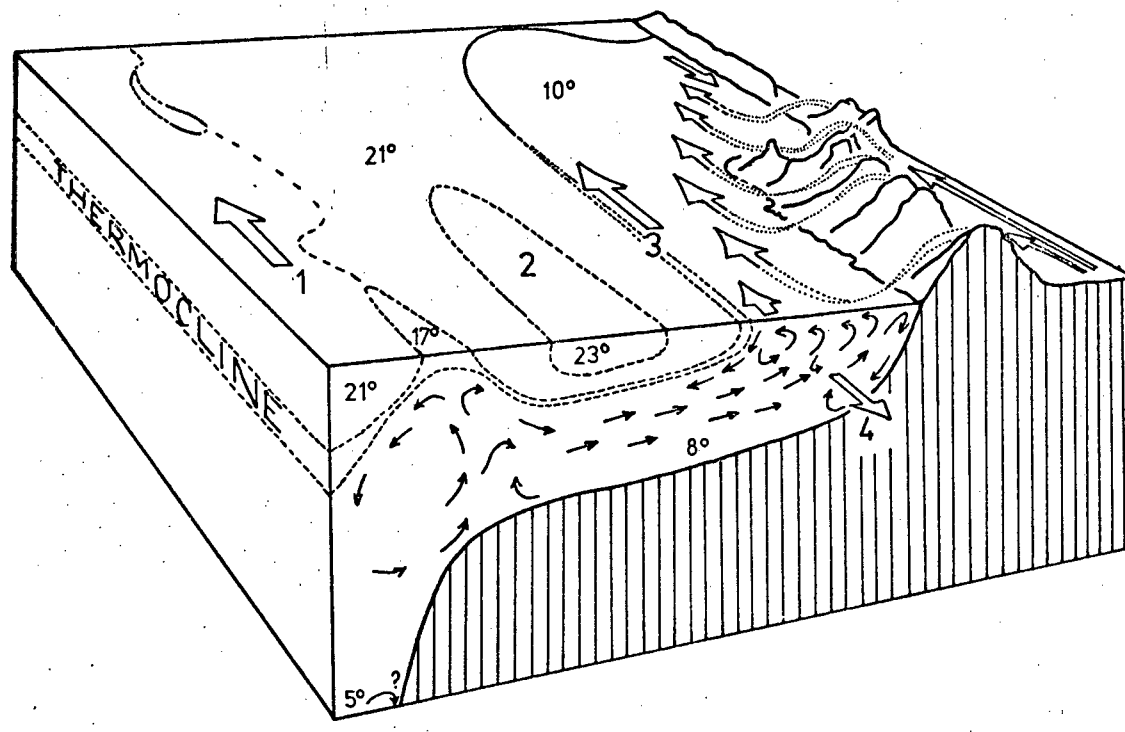

Fig. 3.2 A three-dimensional impression of the Cape upwelling system showing

1. the Jet
2. shallow patches of Agulhas Current water
3. the Benguela Front
4. the De Decker Undercurrent. (after Bang, 1976)

3.2.2. Local oceanographic features

Upwelling Centres: The topographic influence of the Cape Peninsula mountains on upwelling has been mentioned. In the vicinity of Melkbosstrand and Matroos Bay, however, the topography is fairly flat with no hills rising much above 40 metres within several kilometres of Matroos Bay. Figure 3.3 illustrates the sea surface temperatures on the 23rd January, 1971 at which time strong southerly winds were being experienced. The tongue of cool water to the south-west of Cape Town represents the topographically influenced upwelling centre. Another region of active upwelling also occurs off Melkbosstrand with a tongue of cool water extending past Matroos Bay. Harris and Bain (1976) have confirmed the location of this upwelling centre on many occasions. As no major topographic features occur near Melkbosstrand it is likely that the change in orientation of the coastline may influence the positioning of this upwelling centre. Although not a primary goal of the research, the investigations may reveal whether Matroos Bay, which has a similar although somewhat smaller deflection of the coastline than that at Melkbosstrand, presents a favourable circumstance for upwelling.

Local Current Systems: Although the basic characteristics of the upwelling system are known, few direct current measurements have been made in the region, particularly close to the shore. From 1953 to 1965 several drift card studies were performed off the western Cape coast (Duncan, 1967; Duncan and Nell, 1969). As a result of these investigations Duncan (1967) stated that "there is always a southerly inshore current in the region, and except occasionally in winter, there is always a northerly current offshore". The evidence from this study does not confirm this result and will be dealt with more fully in Section 5.2.

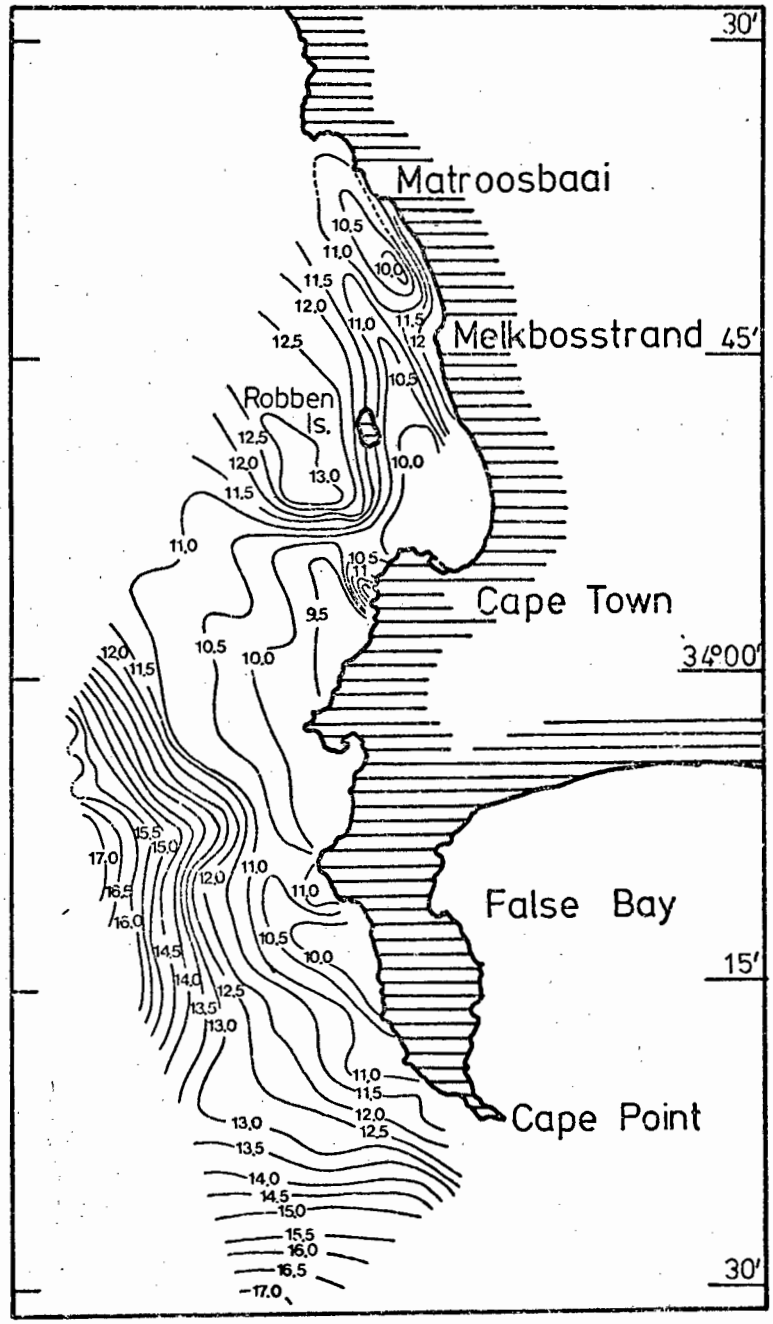

Fig. 3.3 Sea surface temperatures in the Cape upwelling region, 23 January, 1971. (courtesy of Div. of Sea Fisheries)

Between 1966 and 1970 hydrological stations were manned on a monthly basis within Table Bay (van Ieperen, 1971). In this study a northward movement predominated in the bay. This was attributed to the dominance of the winds on the circulation. The results of this investigation may not however be applicable to Matroos Bay region due to the coastal changes in the region.

In order to obtain adequate design data for the construction of a nuclear power station, ESCOM (Electricity Supply Commission) have maintained, since 1969, a monitoring unit at Melkbosstrand, 15 kilometres to the south of Matroos Bay. The data obtained from this location has in part been presented in a series of progress reports (Mallory, 1970 to 1977) and in part by the National Research Institute for Oceanology, NRIO (CSIR, 1976a) and also, it appears by Summers (1975) although he does not state the source of his information. Some of the ESCOM data have been reanalysed by Harris and Bain (1976). Further studies in this region are in progress.

Current roses presented in the first six ESCOM Progress Reports (Mallory, 1970 to 1974c) generally indicate that, near Melkbosstrand, surface currents between .5 and 9 kilometres from shore are polarized, flowing either north or south. This agrees with the northern-most data obtained by van Ieperen (1971). Further north, toward Matroos Bay, the currents were found again to be well polarized but in a north-west–south-east direction, presumably in response to the change of orientation of the coastline. The currents nearest the shoreline showed the greatest degree of polarization and subsurface currents were more polarized than surface currents.

The strongest currents were generally found to be along the polarization axis and surface currents were generally greater than subsurface current.

Wind - Current Relationships: In a region of strong upwelling it is to be expected that a relationship between the local winds and currents will exist. Van Ieperen (1971) found a correlation to exist between the wind and current direction but not between the speeds of the wind and current. He explained this by the fact, that, although winds may change rapidly, inertia may prevent the current from doing so. 80 kilometres to the north of Matroos Bay, off Saldanha, both surface and subsurface currents between 5 and 50 kilometres from shore were found to agree closely in both direction and magnitude with the wind velocity. Currents generally lay in the range .1 to .3 $m.sec^{-1}$. (CSIR, 1976b).

That the wind was the main factor in surface current generation off Melkbosstrand was also found by Summers (1975). Figure 3.4 illustrates the relationships observed between winds from the four principle directions and the surface currents off Melkbosstrand. A good correspondence is noted, especially for the northerly and southerly wind directions. Harris and Bain (1976) have also found good correlation to exist between the winds and the currents. Examples of such agreement are illustrated by figure 3.5.

With the good correlation between the wind and the current that has been observed both to the north and immediately to the south of Matroos Bay, a correlation between the wind and the coastal current observed near Matroos Bay may be expected. But, a note of warning is needed. Harris and Bain (1976) have reported instances where the surface current, derived from surface temperature measurements, appears on occasions to be deflected from the coast by the changing coastal morphology just to the south of Matroos Bay.

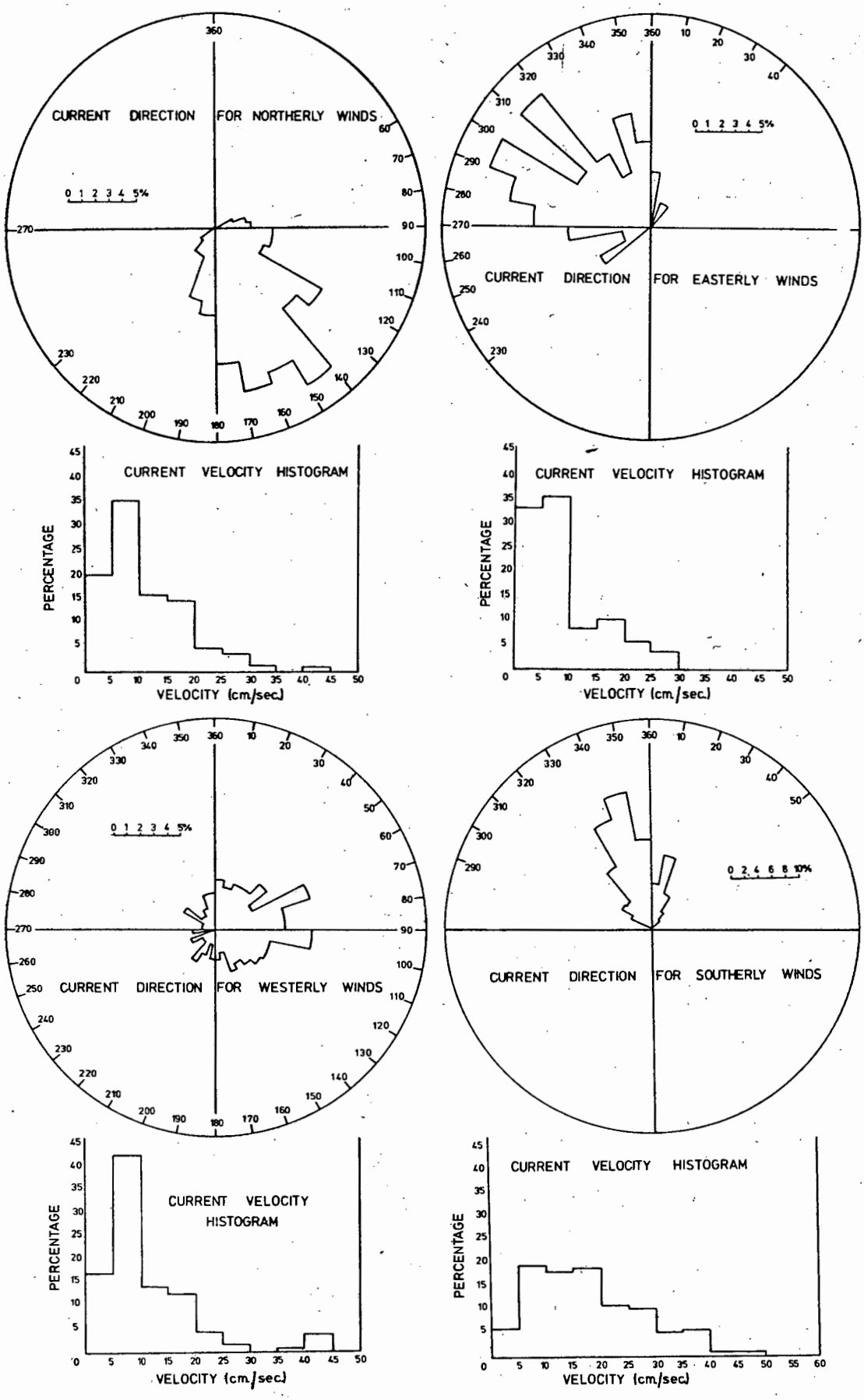

Fig. 3.4 Wind – Current Relationships, Duynefontein. (after ESCOM, 1975.)

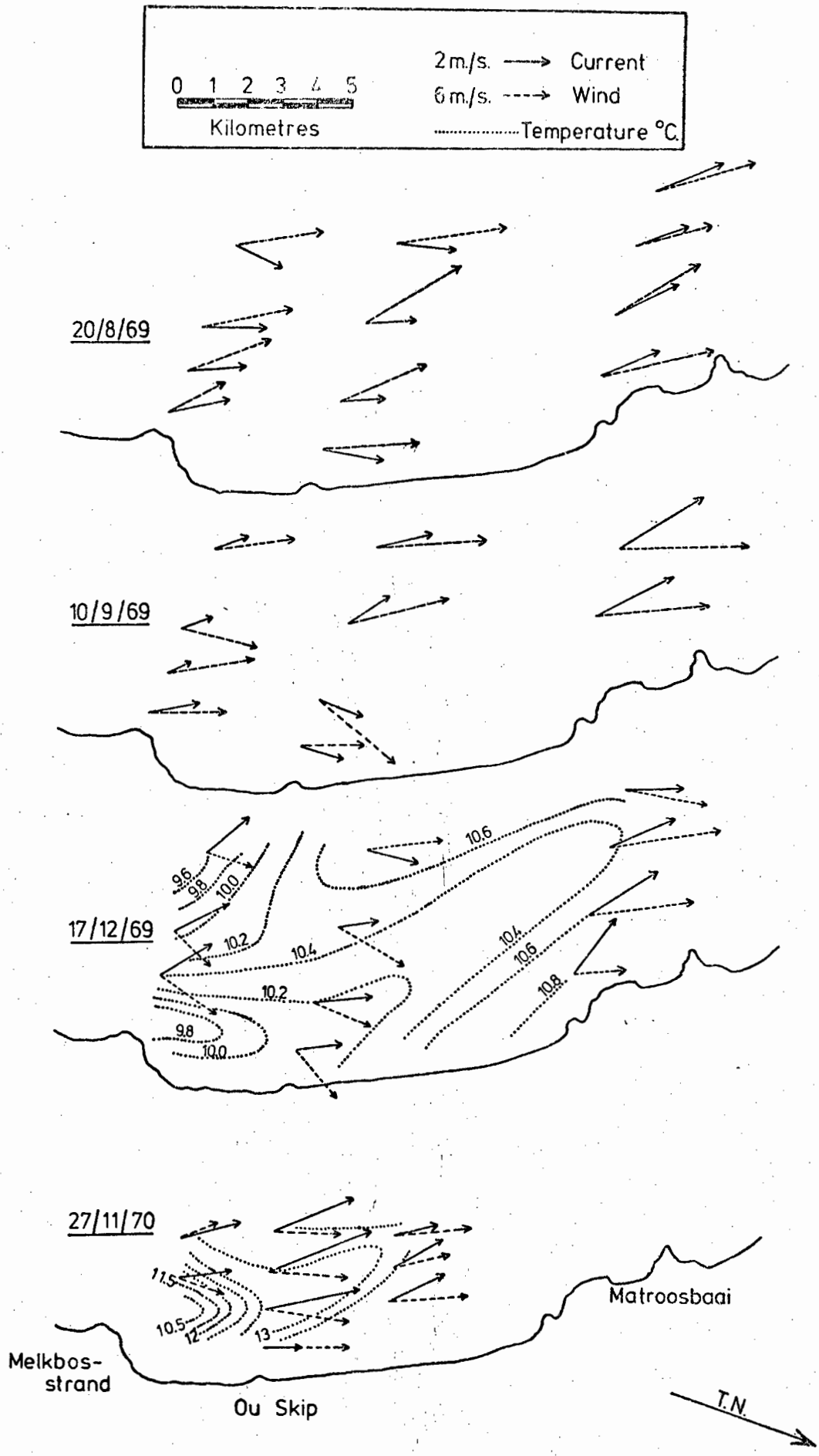

Fig. 3.5 Relationship between winds and surface currents near Melkbosstrand (after Harris & Bain, 1976).

An example of this situation is illustrated by the currents observed on the 17th December, 1969 of figure 3.5. The nearshore surface current is deflected offshore in the vicinity of Matroos Bay (see also Frontispiece). Under such conditions it is possible that an eddy may develop giving rise to an apparent counter-current off Matroos Bay. On other occasions, for example the 20th August, 1969 (figure 3.5), the offshore deflection of the current is not so prominent.

Temperature and Salinity Measurements: With the response of the water to the winds taking the form of upwelling of deep, cooler and less saline water, both isotherms and isohalines are expected to slope upward towards the coast. The result of this is that a plan view of the sea surface distribution of temperature or salinity would show contours oriented parallel to the coast with coolest, least saline water nearest the shore. An overall response of this nature has been observed (Bang, 1972; van Ieperen, 1971; CSIR, 1976b) but local effects cause inhomogeneities.

Within Table Bay van Ieperen (1971) found surface temperature generally lay within the range 10°C to 15°C with the highest temperaaures being reported during winter. He also found that salinities lay in the range 34.7 to 35.0 ‰ with the highest values being observed in the winter months. This range of salinities is consistent with the range observed at Melkbosstrand between February 1970 and January 1971. During this period 60% of the salinity measurements at a depth of 5 metres lay in the range mentioned (Mallory, 1971).

Harris and Bain (1976) have shown that there is good correlation between the wind and the sea water temperatures off Melkbosstrand. Their observations confirm the preference of upwelling to be initiated near Melkbosstrand as mentioned earlier, with cooler water then advected northwards and offshore, see figure 3.5.

Tides and Tidal Currents: Corange lines for the South-eastern Atlantic Ocean are almost parallel to the coast of Africa. Cotidal lines in this region show a change of one hour in over 20° of latitude (Doodson, 1958).

According to the South African Tide Tables for 1976 (S.A.N., 1976), the Mean High Water Spring (MHWS) Tide in Table Bay is 1.69 metres, the Mean Low Water Spring (MLWS) .27 metres, a range of 1.42 metres.

The Mean High Water Neap (MHWN) tidal elevation for Table Bay is 1.26 metres and the Mean Low Water Neap (MLWN) elevation is .71 metres (relative to Chart Datum), a resultant range of .55 metres.

Summers (1975) reported maximum values of the onshore-offshore component of the tidal current off Melkbosstrand ranging upto .15 metres sec^{-1} at Spring Tide. Radar tracked buoys deployed in the same position by Bain (pers. comm.) during calm wind conditions have failed to show any tidal velocities of the strength reported above and the tidal currents reported by Summers (1975) are to be treated with caution.

Off Saldanha Bay, under similar calm conditions existing on the 28th and 29th November, 1975, only weak tidal currents were observed 3 kilometres from shore in 45 metres of water. The tidal range at the time of observation was 1.14 metres, approximately mid-way between the Spring and Neap ranges for the area, 1.5 and .6 metres respectively. Similarly, two moored Aanderaa current recorders did not show strong tidal influences even at the mouth of Saldanha Bay (CSIR, 1976b).

As a result of the low tidal elevations and currents expected no attempt has been made to correct any velocity readings for tidal currents. No evidence of tidal currents was observed.

4. DATA COLLECTION AND PROCESSING

4.1. Current Determination

It is perhaps anomalous that in this age of satellites, computers and instrument packages that no simple device for determining nearshore water movements has come into standard use. Rather, the trend has been for each researcher to modify existing methods or to develop his own to suit his requirements. Perhaps this reflects upon the wide range of conditions, scales and goals that may be encountered, or perhaps on the infancy of nearshore and coastal research in general and the exacting conditions encountered in this environment.

For this study the desired system had to be readily available and/or cheap to construct and hence disposable. It was necessary that the system used be accurately able to be positioned upto a range of approximately two kilometres; rigorous, and hence able to be employed within the surf zone; subject to minimal wind drag, and producing minimal handling problems both in the field and with data processing.

Although aerial photographic methods may be employed to satisfy such conditions, the method adopted was theodolite tracking of floats deployed from a boat. The advantage of this system was that temperature and salinity samples could also be obtained from the boat.

The floats used consisted of a sealed tin, .10 m. high and .10 m. diameter (figure 4.1). Through the tin a 1 m. wire was bronzed with .55 m. projecting from the top. On the top of the wire a brightly painted and numbered stiff calico flag was supported by dowels. At the lower end of the wire a lead weight (300gm) was attached to keep the flag upright. From this weight a cord led to a "blind" drogue of one square metre. At each end of the drogue a dowel was placed to keep

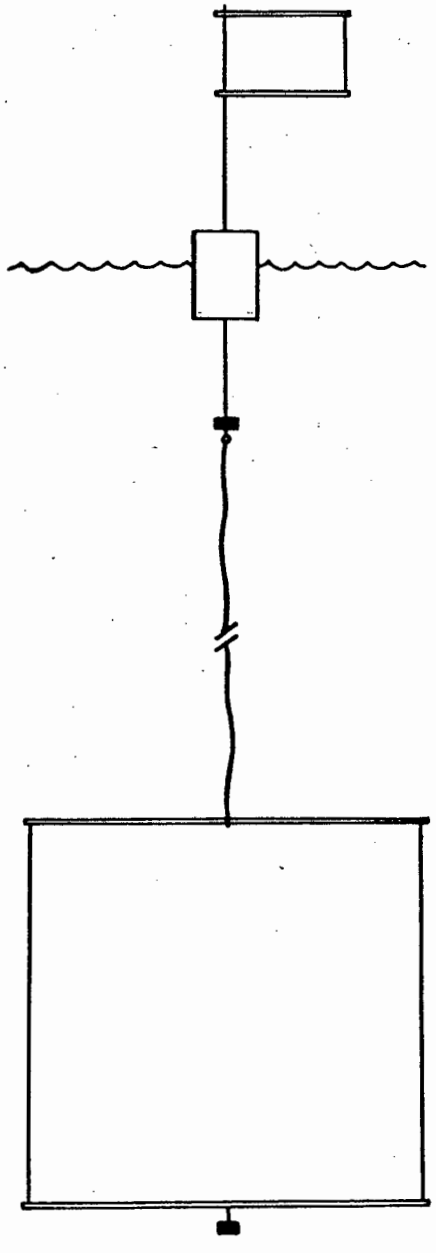

Fig. 4.1 Design of floats used for current measurements.

the drogue rigid and a sand ballast helped the drogue to maintain its depth. The length of the cord between the float and the drogue was adjusted so that the centre of the drogue was either one metre or five metres below the water surface. The size of the flag was selected to be .2 x .3 metres as this gave a compromise between visibility and wind drag. Calibration of the system in a wind-wave flume indicated that the wind induced velocity on the float was only .4% of the wind velocity at a height of 10 metres. Consequently, for most applications, the wind drag was found to be negligible compared with the current velocity. Details of the calibration procedure are found in Appendix A.

Floats were tracked by shore-based theodolites read to the nearest minute of arc. The positions of the theodolites was determined by the Land Survey Department of the University of Cape Town. Synchronous readings were made on floats by theodolite operators maintaining continuous radio contact. The time of reading on a float was recorded and is within 5 seconds of the time of observation, but, as the shortest time between successive readings was only a minute and a half, errors in velocity so produced were generally small.

During the course of the Matroos Bay study, floats were often placed outside the bay in order to determine the direction and speed of the coastal current. Further information on the direction of the current could often be determined by observations on a system of buoys moored approximately 800 metres off the northern headland (as station 1 of figure 4.2).

All times referred to in this report are South African Standard Time (S.A.S.T. = G.M.T. + 2 hours).

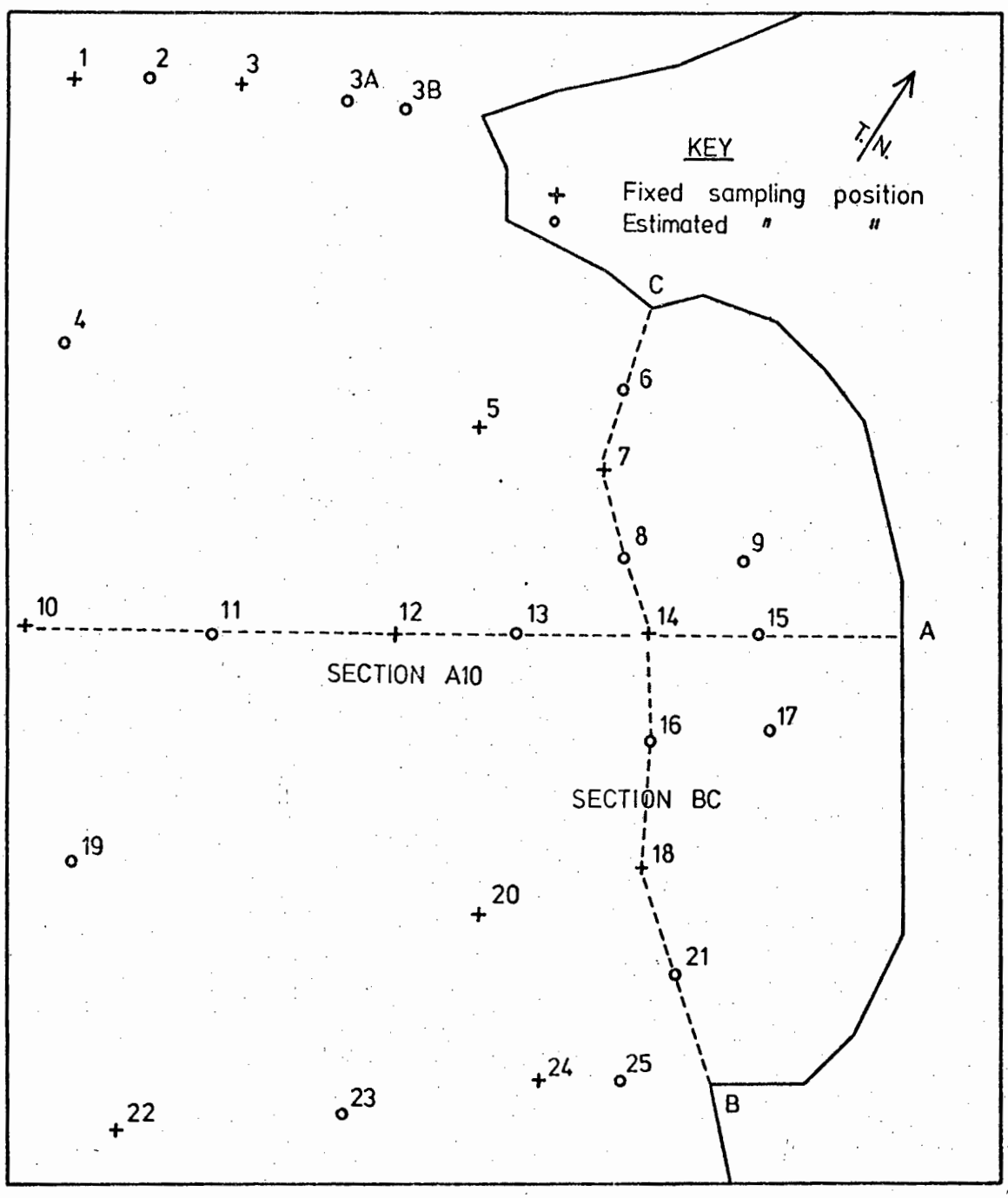

Fig. 4.2 Matroosbaai temperature & salinity sampling stations.

4.2. Temperature and Salinity Determination

With the prevalent upwelling conditions of the region, temperature and salinity seemed to provide ideal natural tracers for the study of water movements. The measurement of water temperature and salinity also gave a possible method for assessing whether upwelling was induced within Matroos Bay.

Field trips were planned to last for approximately a week at a time in order to observe the changes within the system with varying meteorological conditions. During each trip it was desired to sample both temperature and salinity on a regular basis, if possible, twice a day. A network of twenty seven sampling stations was employed at which surface readings were taken (figure 4.3). Approximately half of these stations were marked by a small moored buoy positioned by theodolite, the remainder were estimated between the fixed positions by the boat operator. The relative position of the unmarked stations is known but their absolute position may differ slightly.

In addition to the surface readings, profiles were obtained along two lines; one between the headlands, points marked B and C on figure 4.2; the other, perpendicular to this line and running through the centre of the bay from station 10 to position A of figure 4.2. Initially both temperature and salinity samples were taken at 5 metre vertical intervals to the bottom but later a shallow water bathy-thermograph replaced the individual temperature readings. Salinity profiling was discontinued after three trips as it was found to be insufficiently valuable to warrant the time consumed in obtaining the samples.

Typically it took from one to two hours to collect all the samples and the results may be considered as reasonably synoptic in most cases.

Accuracy and Calibration of Equipment: Surface temperature readings were obtained using a "Zeatron G.P.E. Remote Reading Electronic Thermometer", a thermistor based instrument with a range of -10° C to 50° C. The uncalibrated accuracy of the instrument is ± .6°C but on calibration the reliability was improved to ± .2° C. Whilst this was not ideal, it was sufficient to give an overall picture of the gross features of the water temperature. The accuracy of the shallow water bathythermograph was also ± .2° C.

Water samples were collected in glass bottles which were sealed and returned to the laboratory for salinity analysis on a "Plessy Laboratory Salinometer Model 6230N". This is an inductive coupling salinometer with an accuracy of .003 ‰ after corrections for drift and temperature have been made.

4.3 Wind Records

Wind records were obtained from the ESCOM Research Unit who maintain a Lambrecht Recording Anemometer at Ou Skip (figure 2.2), a low, rocky outcrop 4 kilometres north of Melbosstrand. The anemometer is located 10 metres above the ground. Because of the lack of prominent topographic features between Melkbosstrand and Matroos Bay the wind records were assumed to give a good indication of the winds experienced at Matroos Bay. This was confirmed by field notes made during periods of observation. Only during light, variable wind conditions were differences noted but under these conditions the effect of the wind on the circulation was expected to be small.

4.4. Wave Records

For several years wave records have been obtained off the coast, 6 kilometres north of Melkbosstrand (Shillington, 1974, 1976; Mallory, 1970-1977; CSIR, 1976a). The CSIR

maintain at least one Waverider Buoy in the vicinity and the ESCOM Unit maintain a Wemelsfelder Wave Recorder on a Sea Tower located approximately 1 kilometre offshore. The water depth at the Sea Tower and Waverider "C" was about 13 metres. The location of the Sea Tower and two Waverider Buoys is shown in figure 4.3. When available the characteristic wave height, H_{mo}, and period, T_p, obtained from spectral analysis of the record from Waverider "C" was used in the analysis of the data. The Waverider, after having been washed away from site "C" on several occasions, was relocated at site "E", a position close to that formerly occupied by Waverider "A". Therefore the statistical comparison available between Waveriders "A" and "C" may be used to determine whether significant differences exist between the data obtained at the two sites.

If the spectral results from the Waverider were not available then the Wemelsfelder data was used although only hand analysed using the methods of Draper (1966). To determine whether or not the Wemelsfelder data could be used with confidence if the Waverider data was not available, a comparison was made between the data obtained between January and June, 1976 by each recorder. The ratio of the significant wave height, H_s, obtained from the Wemelsfelder measurements to the characteristic wave height, H_{mo}, obtained from the Waverider records was found to be $H_s/H_{mo} = 0.94$. For the same records the relationship between the zero-crossing period, T_z, and the spectrally obtained peak period, T_p, was found to vary but remained generally within the limits $\frac{1}{2} \leq T_z/T_p \leq 1$. Thus, although the heights obtained by the different methods showed good correlation, no consistent relationship was observed between the periods.

A comparison between the Waverider wave height data obtained at the locations "A" and "C" and the Sea Tower data between 1st April, 1974 and 31st May, 1976 led to the following

ratios; A: Sea Tower = 1: 0.92, A: C = 1: 0.92 (CSIR, 1976a). Thus, as the ratios of the wave heights are within the accuracy tolerance of the instruments, the wave heights obtained at the various positions were considered as equal.

The bathymetric contours offshore of Matroos Bay and Melkbosstrand are almost parallel to the coast (see Section 2). Wave refraction diagrams for the area were prepared by the CSIR (1976a) for waves from the south-south-west to the north-west and of periods varying from 6 to 18 seconds. A selection of these diagrams is presented as figures 4.3 to 4.9 showing only the 6 and 16 second refraction patterns of the wave orthogonals. These diagrams illustrate that, in general, little divergence or convergence of the orthogonals occurs between Matroos Bay and Melkbosstrand, particularly for waves approaching the coast from the west-south-west.

Wave direction data are available on only 20 of the 36 occasions when observations of the nearshore circulation were made. On the occasions when data were available the waves approached from the south-west. On those occasions, the wave records obtained some 9 kilometres to the south were almost definitely representative of the waves at Matroos Bay.

The CSIR (1976a) found that over the 12 month period, June 1974 to May 1975, approximately 89% of waves at Melkbosstrand approached from between the south-west to the west. It is likely, therefore, that, even on the days when information on the wave direction is not available, the waves did approach the coast from the south-west. Although there is no direct evidence that the waves recorded were of similar height and period as those experienced at Matroos Bay, it was most likely that any differences were not significant. Indeed, no occasions were noted when the observations of wave height made visually at Matroos Bay conflicted with the metered value subsequently obtained from Melkbosstrand.

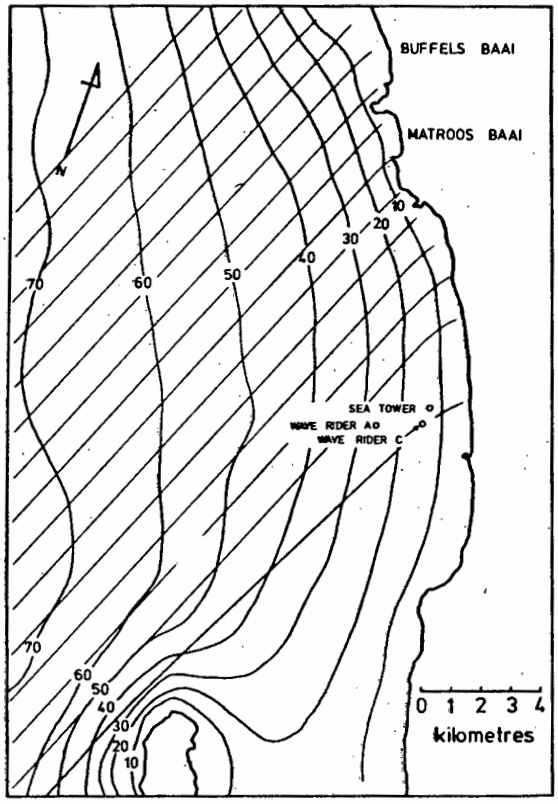

Fig.4.3a Wave Refraction Diagram, SSW, 6sec

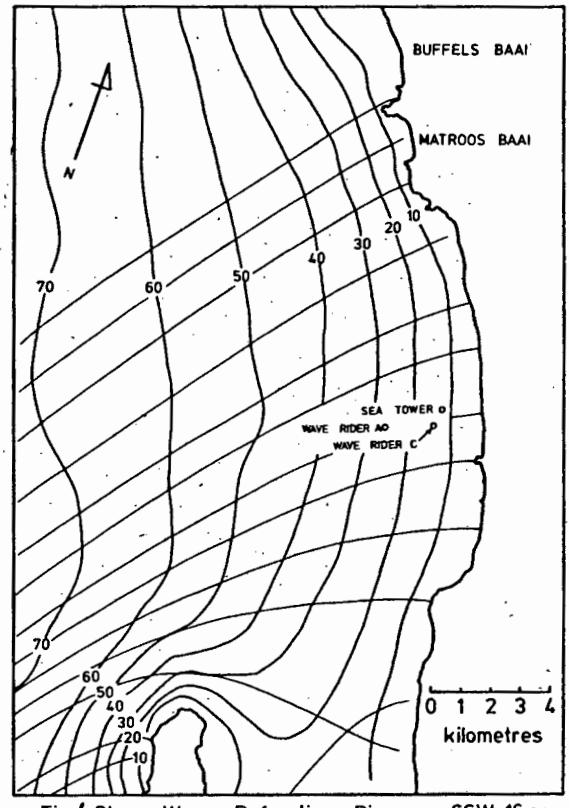

Fig.4.3b Wave Refraction Diagram, SSW, 16 sec.

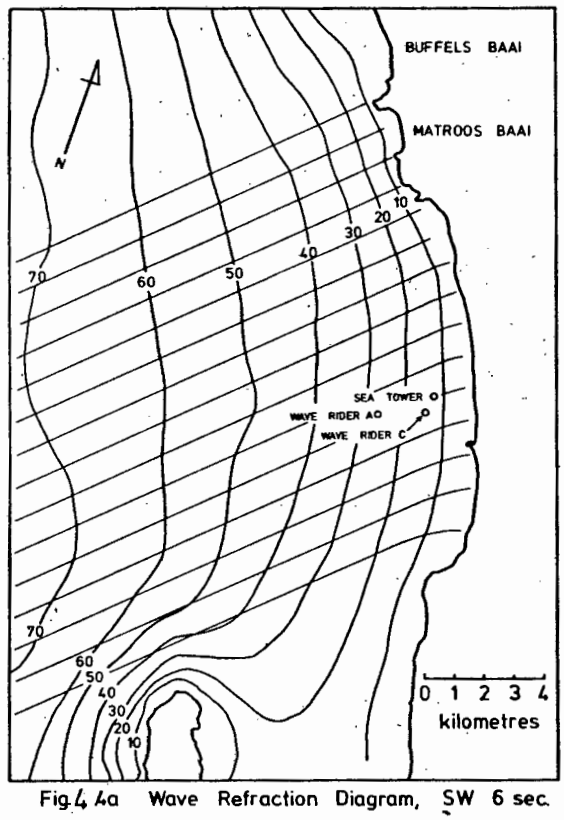

Fig.4.4a Wave Refraction Diagram, SW 6 sec.

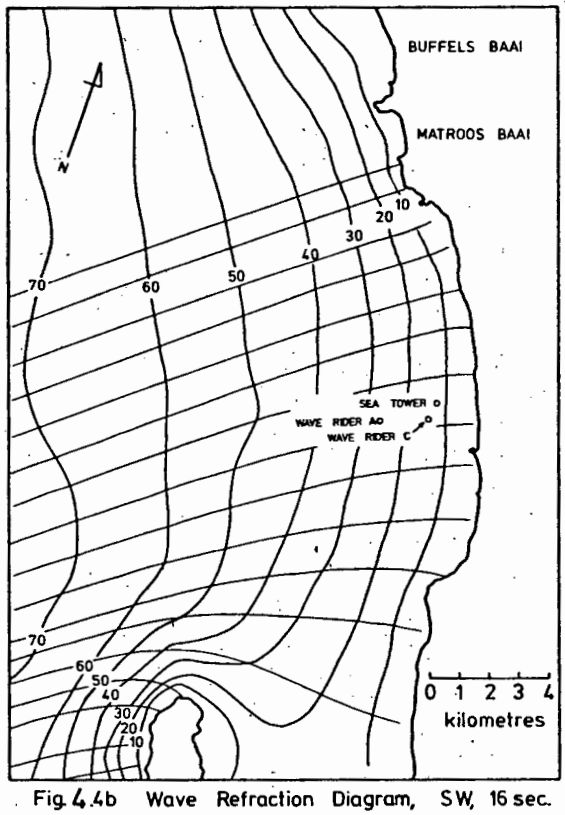

Fig.4.4b Wave Refraction Diagram, SW, 16 sec.

All figures after C.S.I.R. C/SEA 7608, 1976

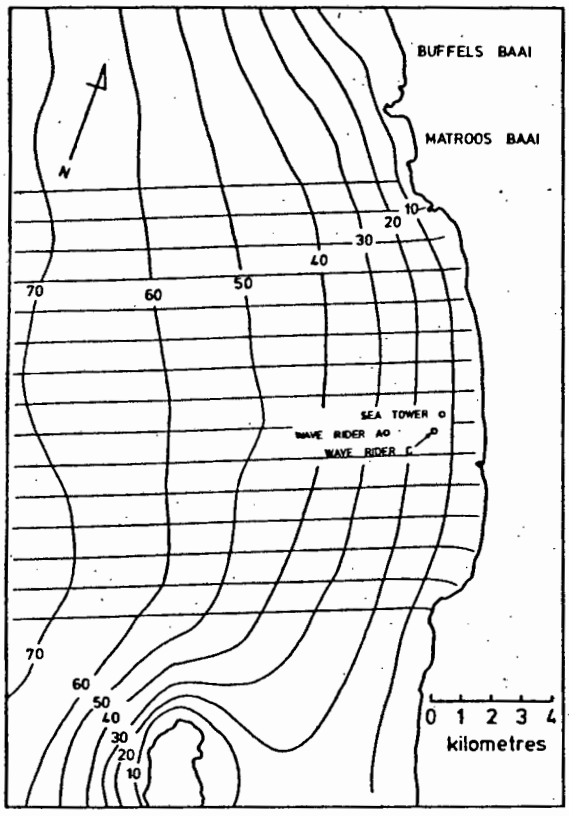

Fig. 4.5a Wave Refraction Diagram, WSW, 6 sec.

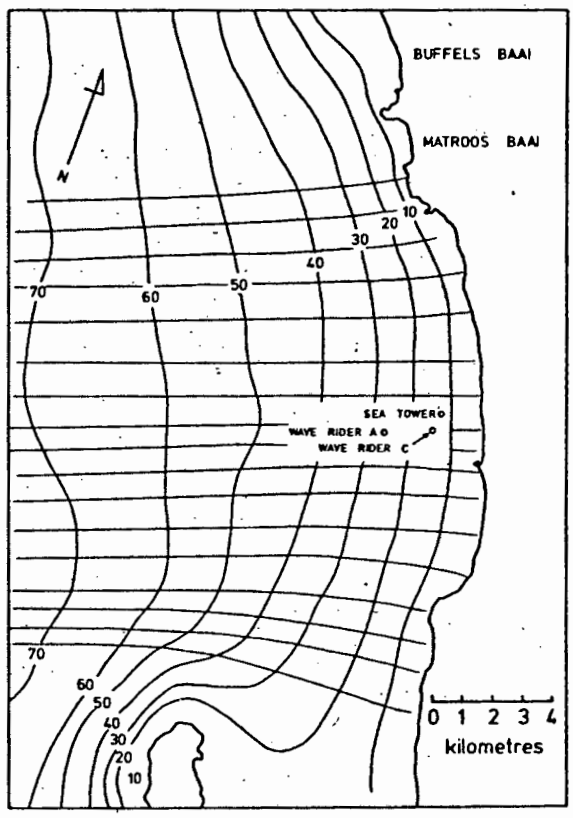

Fig. 4.5b Wave Refraction Diagram, WSW, 16 sec.

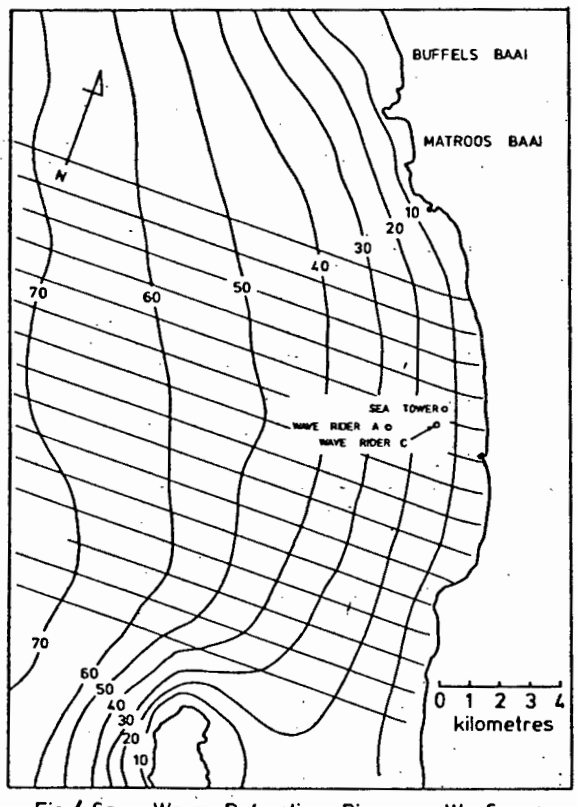

Fig. 4.6a Wave Refraction Diagram, W, 6 sec.

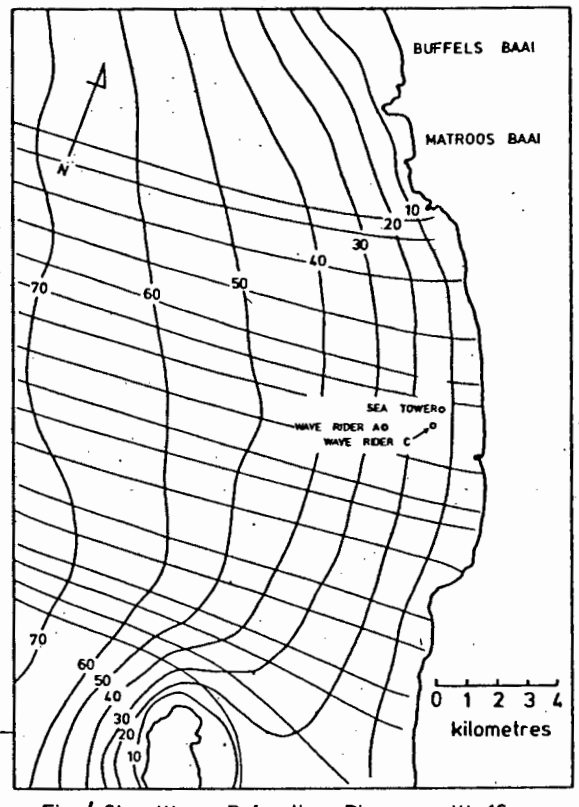

Fig. 4.6b Wave Refraction Diagram, W, 16 sec.

All figures after C.S.I.R. C/SEA 7608, 1976

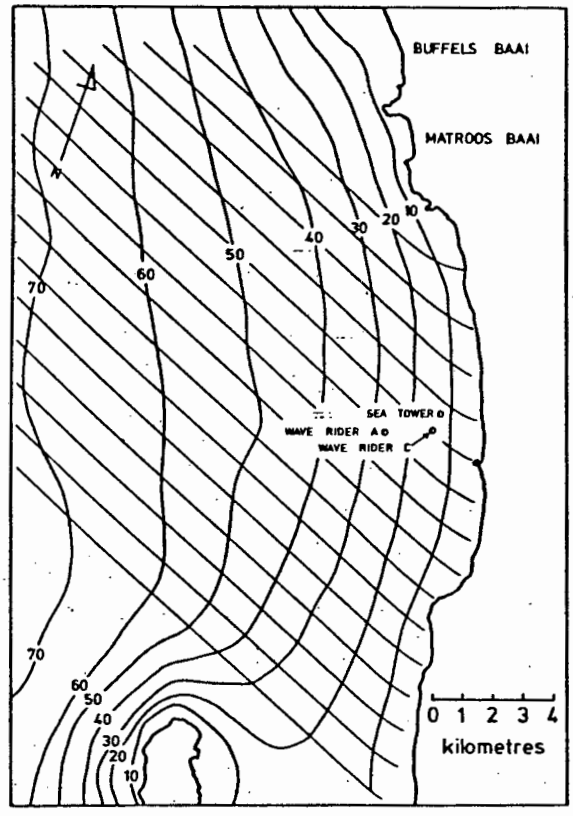

Fig. 4.7a Wave Refraction Diagram, WNW, 6 sec.

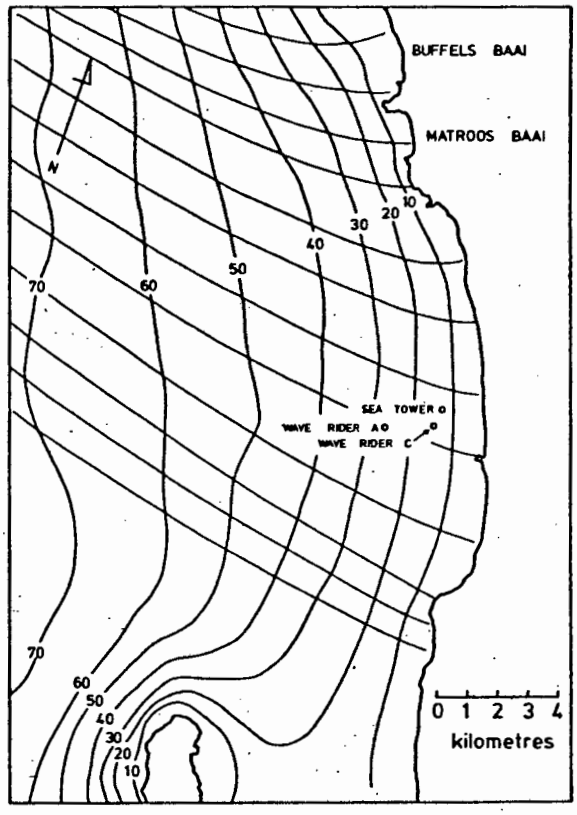

Fig. 4.7b Wave Refraction Diagram, WNW, 16 sec.

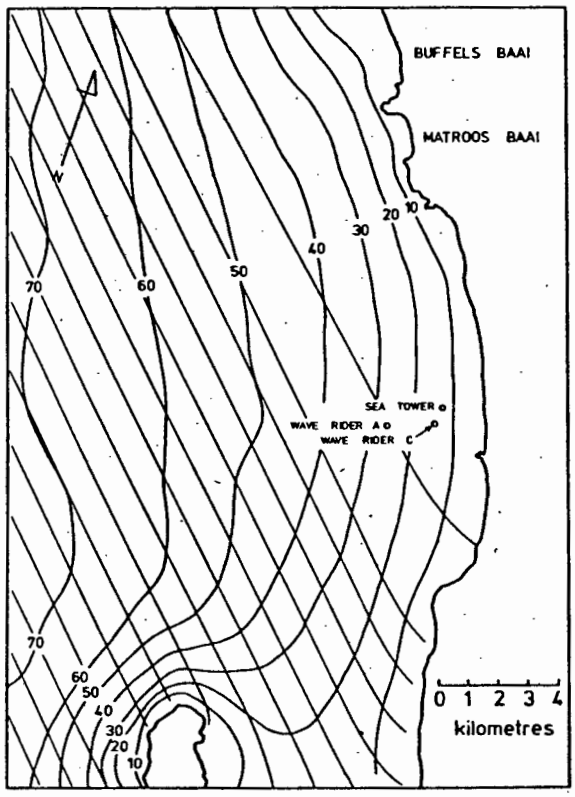

Fig. 4.8a Wave Refraction Diagram, NW, 6 sec.

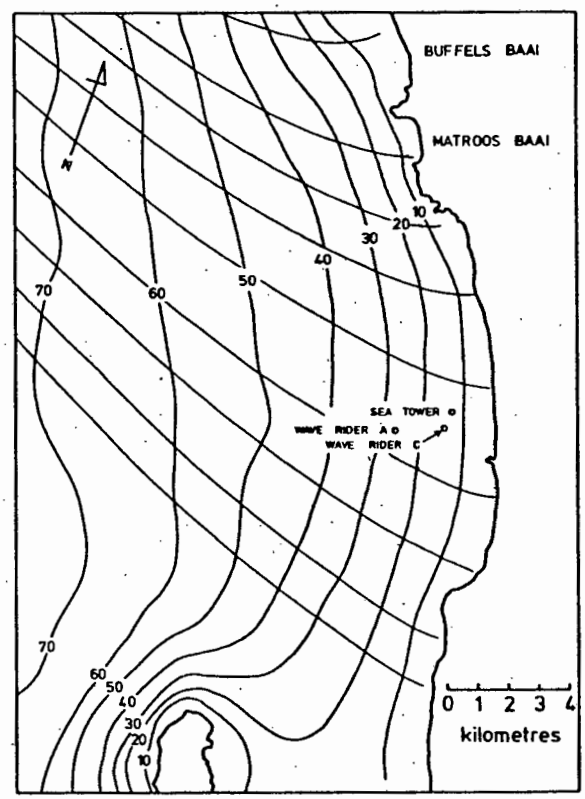

Fig. 4.8b Wave Refraction Diagram, NW, 16 sec.

All figures after C.S.I.R. C/SEA 7608, 1976

Wave direction records were also obtained from the ESCOM Unit. Wave directions were obtained from radar photographs of the wave field. Directions were measured at two positions, approximately 500 m. apart, located near the sea tower in 13 metres of water. No significant difference was detected between the two locations and they will be considered as one. For a period, records of wave direction were available for the same area from the Fisheries Development Corporation of South Africa Limited. These records were made using the Direction of Swell Orientation (D.O.S.O.) recorder (Retief and Vonk, 1974). Recording with this instrument was discontinued after 29th April, 1976.

Records obtained by both methods are incomplete due to the shortcomings of each method. Both techniques require that waves be reasonably high before a recording can be registered. The radar photographic method also requires that some wind be present to provide a reflective surface on the water.

No attempt has been made to extrapolate the wave data to give deep water values as the refraction and shoaling processes encountered at Melkbosstrand would also be encountered by waves entering Matroos Bay.

Wave data tabulated were determined at 1400 hours.

5. RESULTS AND DISCUSSION

5.1. Physical Properties - Temperature and Salinity

Measurements made on a scale of tens of kilometres have revealed considerable gradients of temperature and salinity resulting from upwelling. It was not known, however, whether the changes observed over a horizontal scale of approximately one and a half kilometres and vertical scale of upto 25 metres would be revealing but it was found that they certainly were, both on a seasonal time scale and, on occasions, on a daily time scale. Seasonal changes were in response to the seasonal wind patterns but the daily changes were more often in response to the circulation than to the local winds.

The maxima and minima of each set of synoptic surface temperature and salinity records and the range of values are presented in table 5.1. Surface temperatures recorded ranged from a maximum of 17.5°C to a minimum of 8.4°C, a range of 9.1°C. The maximum range measured during one set of observations was 3.5°C whilst the minimum was 0.3°C. The average surface temperature range was 1.9°C with a standard deviation of 0.5°C.

Surface salinities ranged from a maximum of 35.137 ‰ to a minimum of 34.536 ‰ , a range of .601 ‰ . The maximum range of the salinity record in one set of observations was .244 ‰, the minimum only .005 ‰. The average surface salinity range was not large, only .08 ‰ with a standard deviation of .07 ‰.

Figure 5.1 shows eight typical surface temperature - salinity relationships that were observed. The diagram illustrates that the significant density, σ_t , differences observed were generally the result of temperature changes, not of salinity

TABLE 5.1 : Matroos Bay Surface Temperature and Salinity Maxima and Minima

DATE	TIME	TEMPERATURE (°C)			SALINITY (‰)		
		Maximum	Minimum	Range	Maximum	Minimum	Range
28-01-76	PM	11.5	10.5	1.0	-	-	-
29-01-76	NOON	13.5	11.0	2.5	34.710	34.657	.053
	PM	14.0	11.0	3.0	34.681	34.664	.017
30-01-76	AM	14.0	10.5	3.5	34.794	34.670	.124
	PM	14.0	11.0	3.0	34.683	34.670	.013
31-01-76	AM	12.2	10.0	2.2	34.685	34.669	.016
	PM	(*)16.5	(*)13.2	(*)3.3	34.691	34.663	.028
01-02-76	AM	-	-	-	34.702	34.697	.005
14-02-76	PM	12.5	11.5	1.0	-	-	-
15-02-76	PM	-	-	-	34.691	34.662	.029
16-02-76	AM	(x)13.0	10.5	1.5	34.725	34.676	.049
	PM	14.5	11.0	3.5	34.755	34.627	.128
19-02-76	AM	14.8	12.7	2.1	34.780	34.682	.098
12-04-76	PM	16.0	13.0	3.0	-	-	-
14-04-76	AM	15.0	13.1	1.9	34.736	34.709	.027
	PM	17.5	16.0	1.5	-	-	-
15-04-76	AM	17.0	14.5	2.5	34.723	34.699	.024
	PM	15.0	14.0	1.0	34.711	34.584	.127
17-04-76	AM	16.3	14.1	2.2	34.643	34.536	.107
18-04-76	AM	15.5	13.8	1.7	34.649	34.612	.037
	PM	16.2	13.8	2.4	34.666	34.621	.045
19-04-76	NOON	15.2	14.5	0.7	34.650	34.572	.078
22-05-76	AM	14.5	12.0	2.5	34.805	34.786	.019
	PM	14.6	13.1	1.5	-	-	-
23-05-76	AM	14.5	12.3	2.2	34.791	34.781	.010
	PM	13.5	11.6	1.9	34.792	34.785	.007
25-05-76	PM	16.2	14.0	2.2	34.812	34.786	.026
10-07-76	AM	13.6	13.0	0.6	35.115	35.070	.045
	PM	14.0	13.0	1.0	35.125	35.039	.086
16-07-76	PM	12.1	11.8	0.3	34.995	34.953	.042
18-07-76	PM	13.3	(x)11.6	1.7	35.137	34.944	.193
02-09-76	PM	10.7	8.4	2.3	-	-	-
03-09-76	AM	11.8	9.7	2.1	34.851	34.610	.241
	PM	12.4	10.6	1.8	34.863	34.619	.244
04-09-76	AM	12.0	10.3	1.7	34.845	34.637	.208
	PM	12.1	10.3	1.8	34.859	34.669	.190
07-09-76	AM	13.0	12.2	0.8	34.952	34.881	.071
	PM	13.3	11.1	2.2	34.994	34.860	.134
		Mean 1.9 sd .8 of 37			Mean .079 sd .070 of 33		

(*) Dubious value due to instrument malfunction.

(x) Second highest or lowest value used as highest or lowest spurious.

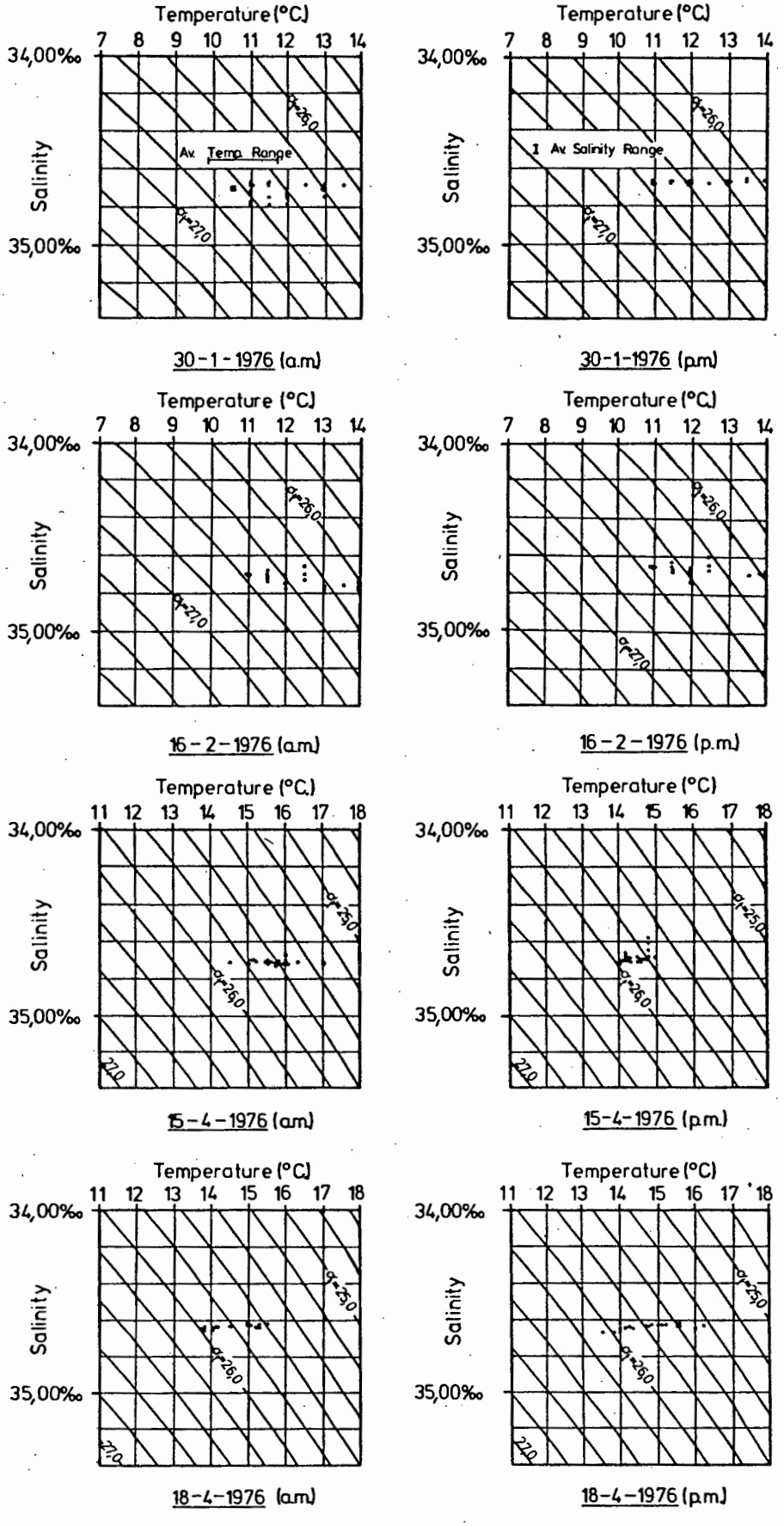

Fig. 5.1 Typical surface temperature – salinity relationships observed in Matroosbaai.

changes. On occasions when both temperature and salinity readings were made at subsurface levels this relationship was also found to hold. It was on the basis of this evidence that the time consuming subsurface salinity readings were discontinued.

The density of the water, expressed in terms of σ_t lay between 25 and 27.

Correlation of Temperatures and Salinities with the Winds: Figure 5.2 shows the variation with time of the temperature and salinity extrema listed in table 5.1. Also illustrated are the vectors of the wind velocity recorded at Ou Skip. For clarity only six hourly wind vectors are shown. Attempts were made to correlate changes in the physical properties with the local wind behaviour but with little success. Attempts were also made to relate changes in temperature and salinity with the direction of the coastal current but again with little success.

Bain (pers. comm.) has suggested that the response time of the isotherms at Melkbosstrand to the wind is of the order of twelve to twenty four hours. The current response there may occur within hours (Mallory, 1975a). The response of the isotherms near Matroos Bay appears to be slower than at Melkbosstrand. It is suggested, that, as temperature and salinity changes are an indication of upwelling, that Matroos Bay is not a preferential area for upwelling as is Melkbosstrand.

The temperature and salinity at an offshore station, station 10, was generally higher than the temperature and salinity at the nearshore station, station 14. Temperature records are available from both stations on 37 occasions. On 29 of these, the nearshore value was lower than the offshore

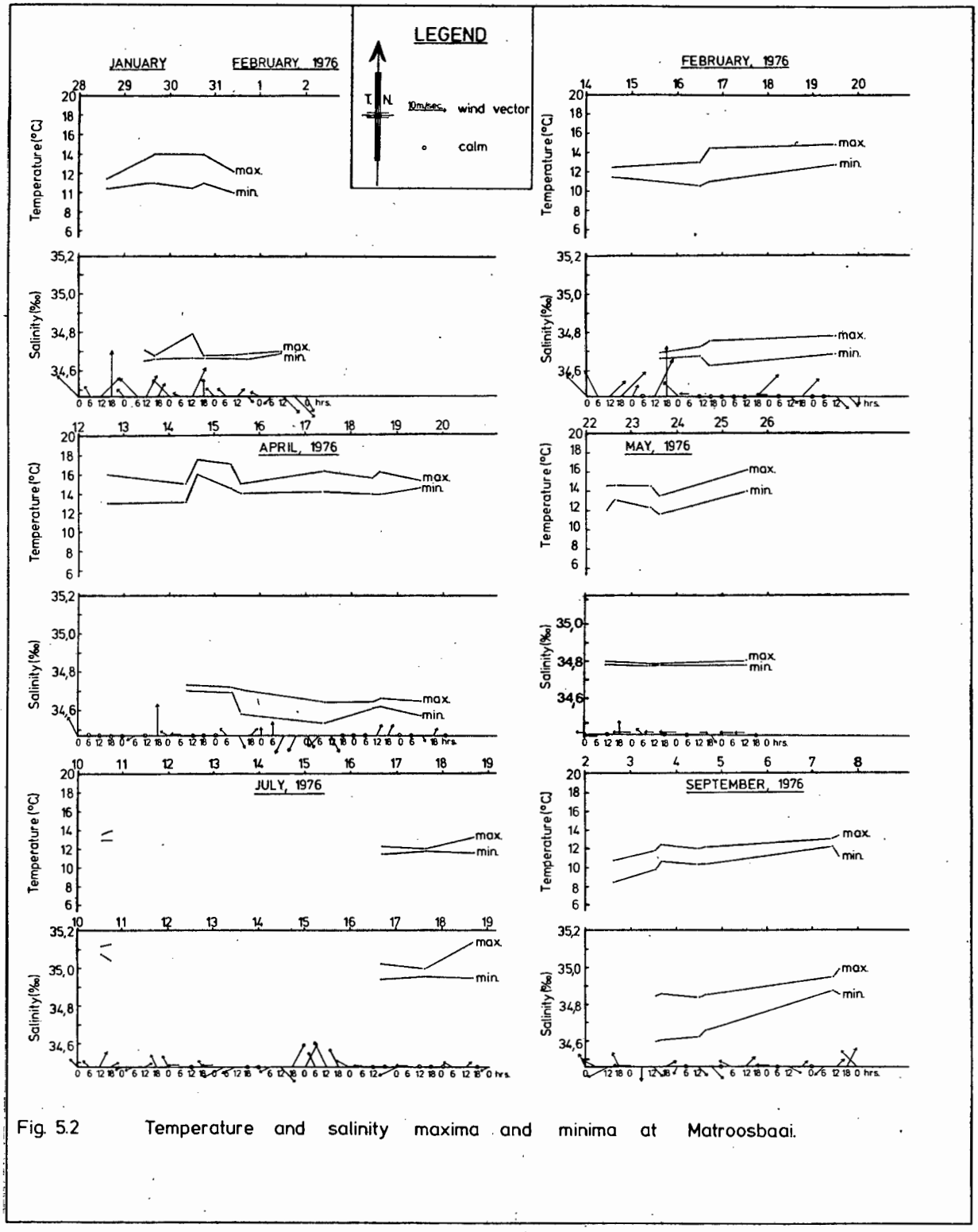

Fig. 5.2 Temperature and salinity maxima and minima at Matroosbaai.

value. With the salinity data, out of 31 occasions that were observed, the nearshore salinity was lower than the offshore salinity on 22 occasions. This seems to indicate that some upwelling may have been occuring close to shore, within 20 metres depth of water. The possibility of advection from the Melkbosstrand region, however, cannot be excluded.

Of the five occasions when the offshore temperature was less than the nearshore temperature, three occured during the field trip of April, 1976. Light, variable winds were very frequent at this time, thus, solar heating and nearshore circulations may have had more influence on the temperature distribution than did upwelling.

On a time scale of several days to a week, correlation could be seen between the wind and the temperature or salinity more readily than on the daily time scale. This correlation took the form of a gradual warming, or salinity increase after the cessation of a period of intense southerly winds. Prior to all the field excursions except that of April 1976, moderate or strong southerly winds were recorded. The gradual warming and salinity increase that followed such events may be seen on figure 5.2, particularly in the case of the September 1976 values.

Figure 5.3. illustrates several of the seasonal characteristics of the upwelling system. The rectangles shown indicate the range of surface temperature and salinity values observed during each trip. The T-S curve for the South Atlantic Ocean has been superimposed.

The rectangles of figure 5.3 have been parametarised in the manner shown by figure 5.4. The line (a,b) represents the portion of the T-S curve for the South Atlantic Ocean that corresponds to the South Atlantic Central Water (SACW)

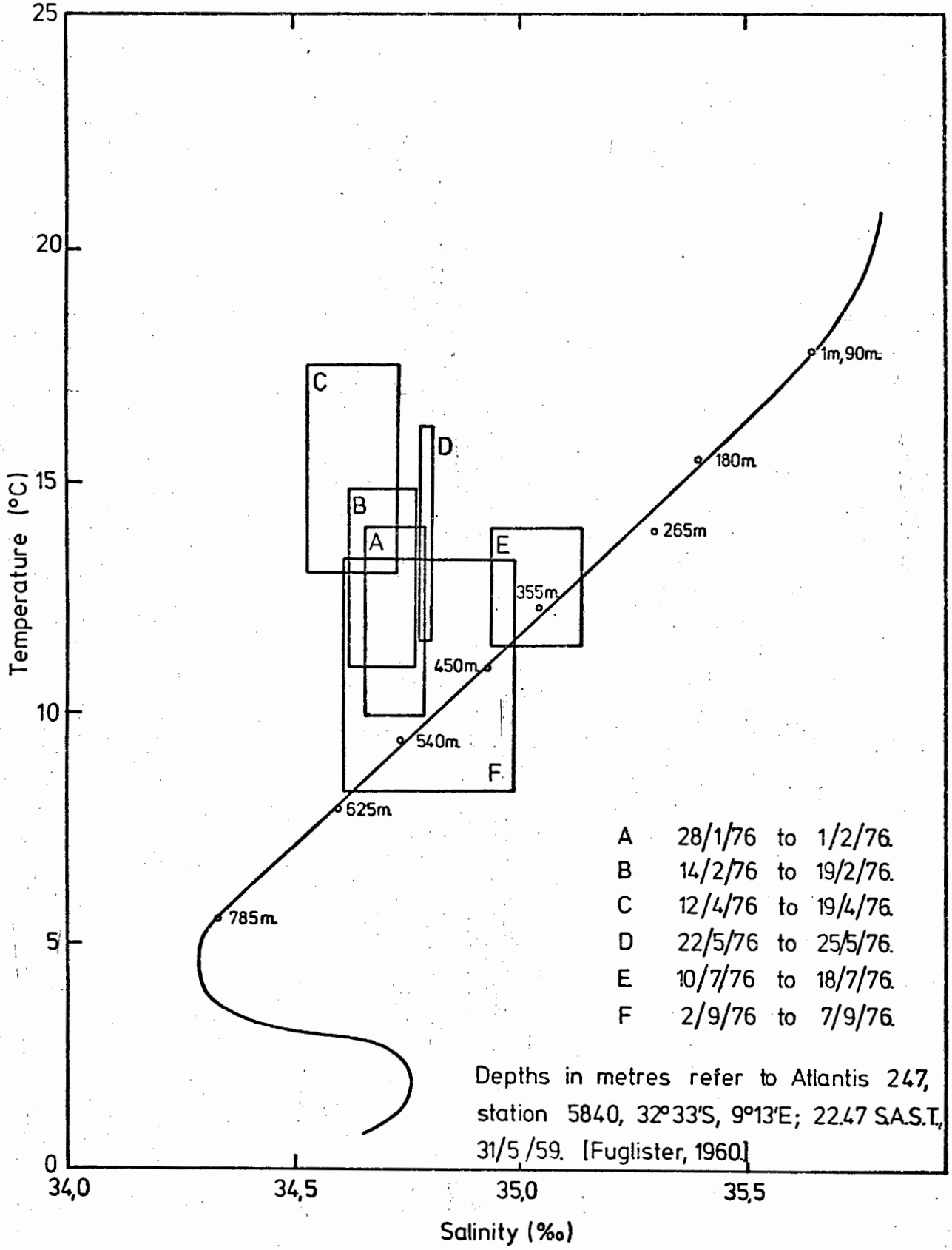

Fig. 5.3 T-S diagram for the South Atlantic Ocean showing the range of values observed.

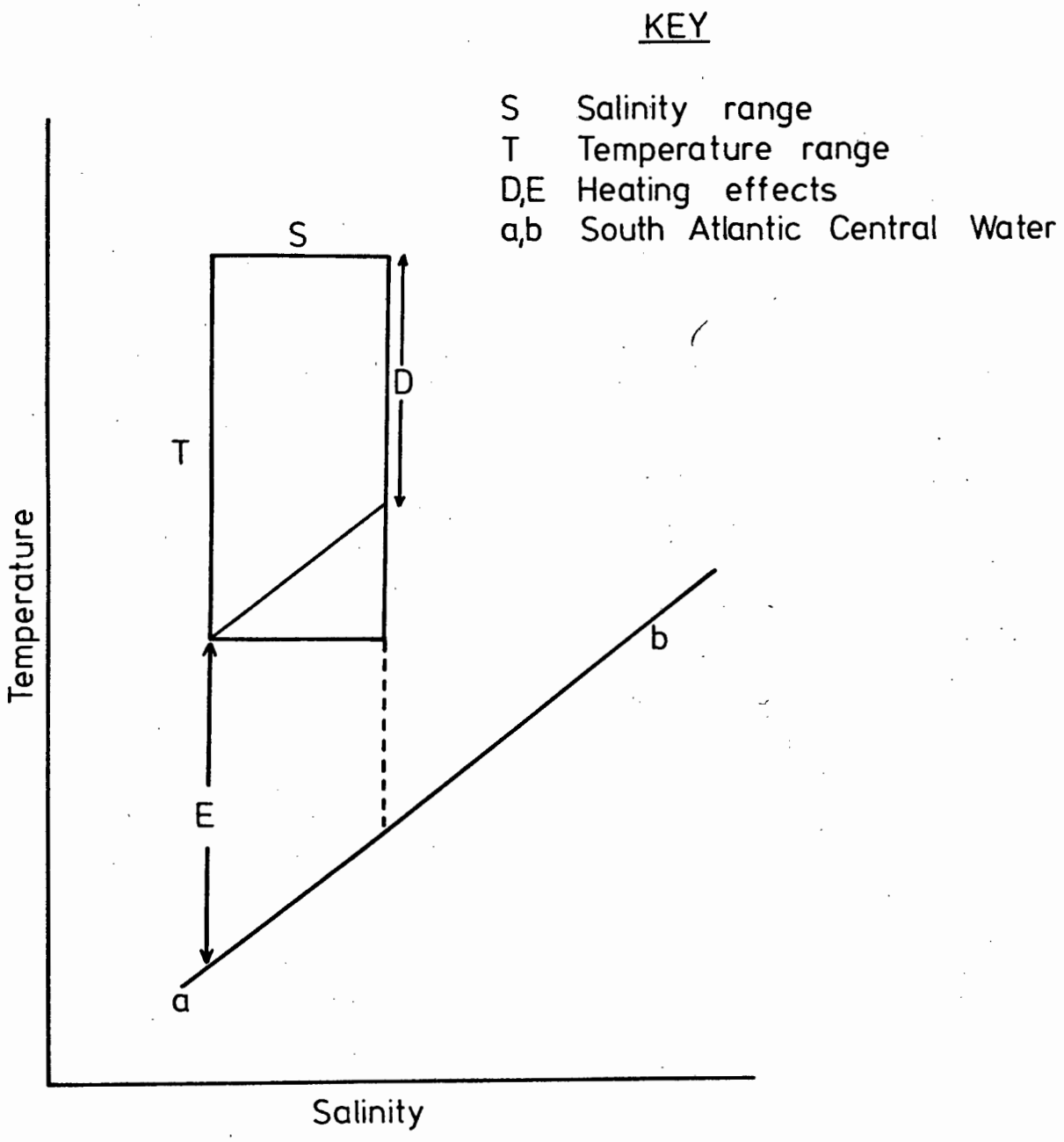

Fig. 5.4 Parameters describing the temperature–salinity observations.

from where upwelled water is believed to originate. (Hart and Currie, 1960; Stander, 1964; Shannon, 1966). If it may be considered that in the process of upwelling salinity is a conservative property, but due to mixing and solar heating, temperature is not, then the elevation, E, of the observed surface temperature above the point on the SACW curve with the same salinity is a measure of the temperature rise that has occured. As each point on the SACW curve corresponds to a particular depth, the depth from which the water has been upwelled may be determined. During winter the value of E may represent the dilution of the water due to precipitation and runoff. If the temperature range and salinity range measured are denoted T and S respectively, then the difference, D, (ignoring units) is also a measure of the heating of the water. In fact, if upwelling has taken place with little mixing or heating occuring until the water reaches the surface, D will represent the solar heating. Due to the small spatial scale of this study and the two-stage upwelling in the region, calculations of the rate of solar heating are not warranted from the data presented.

The values of the parameters described above are listed in table 5.2. The parameters relating to the three summer recordings (A,B,C) show that the depth from which water was upwelled increased from mid to late summer. The heating also increased during this time. The average summer heating was approximately 2.8°C. In the intermediate season, May, the depth of upwelling had decreased but it appears that the effect of surface heating, indicated by parameter D, was quite large. By winter the effects of heating, characterised by either parameter D or E was small, approximately 0.5°C, whilst the depth of upwelling was at a minimum for the observations. The dilution of the water resulting from precipitation and runoff in winter amounted to .03 ‰. This justifies the assumption that negligible dilution of water occurs.

TABLE 5.2 : Parameters relating to the temperature and salinity values observed

Date	Temperature Range, T (°C)	Salinity Range, S (‰)	Temperature Increase		Approximate Depth of Upwelling (metres)
			E (°C)	D (°C)	
A, 28-01-76 to 01-02-76	4.0	.14	1.3	2.6	585
B, 14-02-76 to 19-02-76	3.8	.15	2.7	2.3	615
C, 12-04-76 to 19-04-76	4.4	.20	5.6	2.4	645
D, 22-05-76 to 25-05-76	4.6	.03	1.9	4.3	520
E, 10-07-76 to 18-07-76	2.5	.20	0.3	0.5	450
F, 02-09-76 to 07-09-76	5.0	.38	0.2	1.2	620

The observations made in September 1976, F, were made soon after the first strong south-easter of the summer 1976-1977 season. It is interesting to note the characteristics recorded in this period. The depth from which the water had been upwelled was quite large, but, as was expected, the heating was minimal. The values for this period share both summer and winter characteristics, thus completing the cycle of seasonal characteristics.

Temperature records made to the west of Robben Island and within Table Bay between 1967 and 1969 (van Ieperen, 1971) generally show that, below a depth of 40 metres, highest temperatures occurred during winter. By early to mid spring temperatures had decreased nearly to their summer values. The rapid response of the temperatures to the strong south-easterly winds may be explained by either of two processes. One, that the water upwelled onto the shelf is maintained on the shelf throughout the winter primarily by the dynamic upwelling. The rapid response being a consequence of the proximity of the water to the surface. The other, suggested by Bang (1976), is the possible existence of "springs of upwelling" where upwelling rates of the order of 30 metres per hour are envisaged. In either case the dominance, as early as September, of the southerly winds seems to have an important bearing on the upwelling process and the temperature distribution recorded.

The depth from which water was upwelled was determined by considering a "typical" T-S diagram for the South Atlantic Ocean. The profile selected was located 9° of longitude west of Cape Town and showed no upwelling characteristics (Fuglister, 1970). The depth from which water was upwelled was greater during summer than in winter. The maximum depth from which upwelling was recorded was 645 metres, the minimum depth, 450 metres. These depths are in excess of the 200 to 300 metres usually quoted as the depth from which

water is upwelled (Shannon, 1970). Most values quoted, however, refer to the northern Benguela Region (see Section 3.2.). In the Southern Benguela Region a two-stage upwelling process occurs (Bang, 1973). The first stage is a dynamic upwelling of water onto the continental shelf, the second, a wind induced upwelling to the surface. The depth of 600 metres from which water was upwelled therefore represented the combined effect of two upwelling processes.

At times, the temperature and salinity distributions observed could be explained after a consideration of the currents. An understanding of this interrelationship relies on a knowledge of the currents, hence, this discussion will be postponed until the currents have been discussed (Section 5.3.7.).

Review: The response of the thermal and haline characteristics to the winds occured on a time scale which was seasonal and to a lesser extent, weekly. No response to the winds was noted on a daily time scale. Thus, the variation of the temperature and salinity characteristics was a response of the overall system of which Matroos Bay forms only a small part. With a large spatial scale, the longer time scale of the response is to be expected. An understanding of the more rapid fluctuations requires an appreciation of the larger scale features in conjunction with the smaller scale variability.

5.2. Coastal Currents off Matroos Bay

Qualitative descriptions of the "coastal" current direction and strength are listed in table 5.3. The description primarily indicates whether the flow was up the coast, "northerly", or down the coast, "southerly". On occasions no nett flow parallel to the coast was detected. On other

TABLE 5.3 : Relationship between coastal currents and wind conditions - Matroos Bay

DATE	COASTAL CURRENT		WIND CONDITIONS	
	Direction	Strength	PRESENT Direction/Strength	PAST Direction/Strength
27-01-76	Northerly-offshore	unknown	Southerly/moderate	Southerly/strong
29-01-76	Confused	light	Southerly/moderate	Southerly/strong
30-01-76	Southerly	light	Southerly/light	Southerly/moderate
31-01-76	Southerly-onshore	moderate	Variable /light	Southerly/light
01-02-76	Southerly	very strong	Northerly/moderate	Variable /light
15-02-76	Northerly-offshore	moderate	Southerly/strong	Southerly/strong
16-02-76	Northerly	moderate	- /calm	Southerly/strong
19-02-76	No Flow-onshore	light	Northerly/light	Variable /light
20-02-76	Northerly	strong	Southerly/light	Northerly/light
12-04-76	Northerly	moderate	Variable /light	Variable /light
13-04-76	Southerly	unknown	Variable /light	Variable /light
14-04-76	Northerly	light	Variable /light	Variable /light
15-04-76	Southerly-onshore	light	Variable /light	Variable /light
17-04-76	Southerly-onshore	moderate	Northerly/light	Variable /light
18-04-76	Northerly-offshore	moderate	Southerly/light	Northerly/light
19-04-76	Northerly	light	Variable /light	Southerly/light
22-05-76	Confused	light	Variable /light	Southerly/light
23-05-76	Confused-offshore	light	Variable /light	Variable /light
25-05-76	No Flow	light	Variable /light	Variable /light
10-07-76	Northerly	moderate	Southerly/light	Southerly/moderate
16-07-76	Northerly	moderate	Variable /light	Southerly/moderate
02-09-76	Northerly-onshore	moderate	Variable /light	Southerly/strong
03-09-76	Northerly-onshore	light	Northerly/light	Variable /light
04-09-76	Southerly	light	Northerly/light	Northerly/light
07-09-76	No Flow	light	Variable /light	Variable /light

Current Direction Occurences	
Southerly	7
Northerly	12
Other	6

Current Range (approx)	
light	0-.05 $m.sec^{-1}$
moderate	.05-.15 $m.sec^{-1}$
strong	.15-.25 $m.sec^{-1}$
very strong	> .25 $m.sec^{-1}$

occasions currents could not be described as "northerly" or "southerly" and have been recorded as "confused". If onshore or offshore motion was detected then this has also been recorded. Qualitative wind conditions are also given in table 5.3. The winds have been divided into "present" conditions, referring to the winds observed on the day of observation, and "past" conditions, which take into account the previous day or two.

Of the 25 days data for which observations of the "coastal" current were available, 7 indicated a southerly flow, 12 a northerly flow and 6 indicated confused or no flow conditions.

In table 5.4 the winds have been correlated with the "coastal" currents observed. The main diagonal of the matrices indicate occasions when there was correlation between the wind and the "coastal" current. A correlation was observed on 12 occasions out of 25 with both the "present" and the "past" wind conditions. The majority of the non-correlated occasions were recorded during periods of light, variable winds. Of seven occasions when a southerly wind was recorded, 5 had northerly currents whilst of 5 occasions when the northerly wind was recorded, 3 had southerly currents. If "past" winds are considered, a good correlation was found at times when a southerly wind had been blowing but not when a northerly wind had been blowing.

Thus, in general, a fair degree of correlation between the winds and the currents was found if a dominant wind direction existed. Variable winds resulted in no definite current flow. The poor agreement between the northerly "past" winds and the currents may be a result of the relative weakness and short duration of such winds, compared to the dominant southerly winds of the region.

TABLE 5.4 : Occurence of coastal currents during differing wind conditions

Coastal Current Direction	Wind Direction					
	Present			Past		
	Northerly	Southerly	Other	Northerly	Southerly	Other
Southerly	3	1	3	1	2	4
Northerly	1	5	6	2	7	3
Other (No flow or confused)	1	1	4		2	4

Number of observations: 25
Correlation wind: current (main diagonal): 12
Non-correlation (off diagonal): 13

Number of observations: 25
Correlation past wind: current (main diagonal): 12
Non-correlation (off diagonal): 13

The agreement between the "coastal" current direction and the wind direction is improved if moderate or strong wind conditions are considered. Only four occasions were observed with moderate or strong winds as the "present" wind. On three of these, the wind and current directions coincided. Three out of the four occasions were conditions of southerly wind. Eight occasions were observed with moderate or strong winds as the "past" wind. On six of these, the wind and current directions coincided. Seven out of the eight occasions were conditions of southerly winds.

The small number of occasions when offshore/onshore motion was detectable, prohibits firm statements being made in this context. Three of the four offshore flowing current components were recorded during northerly flow and three of the five onshore flowing current components during southerly flow. This movement is in accord with the principles of upwelling.

The primary surface water movement of the Benguela Region is in a northerly direction and away from the coast, the water near the coast being replaced by water upwelled from greater depth. The existence of surface currents flowing southwards near the western Cape coast has been mentioned in several reports. The evidence for such counter-currents is based primarily on drift card studies made between March 1953 and July 1965, reported by Duncan (1967) and Duncan and Nell (1969). Shannon (1966, 1970) mentions the existence of southward flowing counter-currents close inshore in this region in all seasons but being most marked in winter. The basis of this statement were the drift card studies mentioned above and ships drift measurements. The schematic flow pattern of Duncan and Nell (1969) is illustrated by figure 5.5.

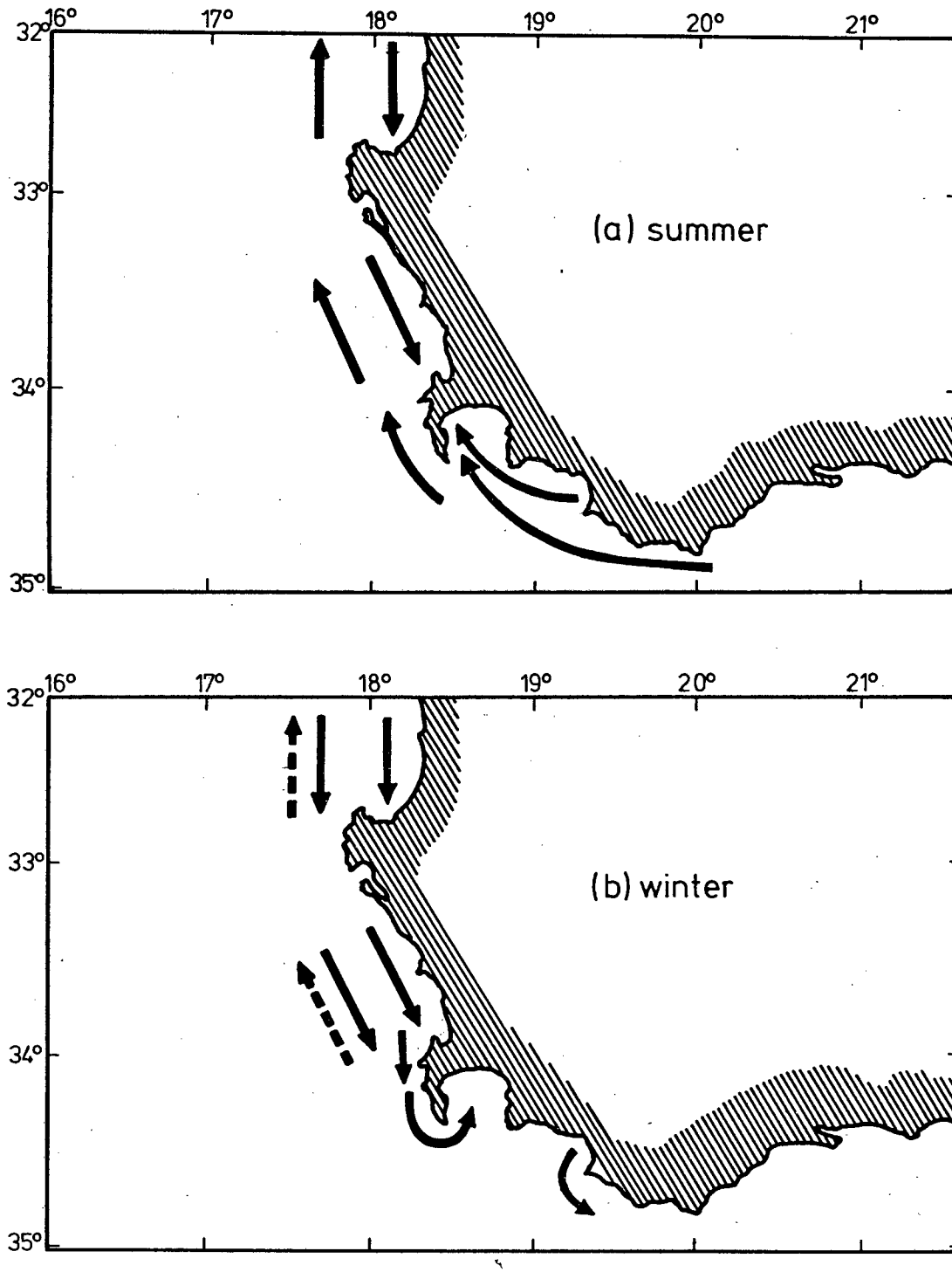

Fig. 5.5 Seasonal pattern of surface flow during (a) summer and (b) winter [after Duncan and Nell, 1969].

FRONTISPIECE

South flowing currents were recorded on only seven occasions. A south-flowing current counter to the wind direction occured only once if "present" winds are considered, twice with "past" winds. Several reasons may exist for the inconsistency between the data obtained off Matroos Bay and that obtained by the drift card studies, but one major reason may be the bias of the drift card study towards a particular result. The use of drift cards to study ocean circulation relies on the existence of currents that will move the cards shorewards. Consequently only during down-welling events, when a southerly and onshore flow exists, will cards placed off the western Cape coast be recovered. The higher frequency of such events during the winter months and the bias of the drift card studies may have led Shannon (1970) to report the counter-current as being most marked in winter.

Another possible reason for the lack of agreement between the present study and that with the drift cards may lie in the scale of the motion observed. Duncan and Nell (1969) do not define specifically their coastal region but their diagram (figure 5.5) suggests that it may occupy the region within 25 kilometres off the coast. The data used for the extraction of "coastal" currents in this study was taken within a kilometre of the shoreline. Thus the "coastal" currents described by the two models may in fact be different phenomena and not comparable at all. No evidence to deny the possible existence of counter-currents existing further than one kilometre offshore was provided by this study.

Review: The "coastal" current direction observed off Matroos Bay appeared to respond in sympathy with the wind direction, particularly if the winds are moderate or strong. This conclusion is in accord with other studies made in this region (Mallory, 1975a; Summers, 1975; Harris and Bain, 1976;

CSIR, 1976a). No agreement was found between the strength of the wind and of the current. Little evidence was found to support the presence of a permanent counter-current existing near the shore.

5.3. The Nearshore Circulation of Matroos Bay

5.3.1. The circulation types observed

This study was an attempt to determine the overall picture of the circulation within Matroos Bay. Two dominant circulation types were recognised within the bay at different times. One was characterised by the existence of a strong rip current flowing diagonally from the northern headland towards the centre of the mouth of the bay, inducing an anticlockwise flow in the northern region of the bay. Figure 5.6a illustrates two examples of this "anticlockwise" circulation type. The other circulation type was dominated by a rip current at the centre of the bay inducing a clockwise circulation in the northern end of the bay. Two examples of this "clockwise" circulation type are illustrated by figure 5.6b. Appendices B, C and D illustrate three further examples of the circulation types observed. With experience, the two patterns were often distinguishable from the shore and visual observations have been included in the analysis when float paths have not been available. On occasions the circulation observed did not fit either of the above, having characteristics of both or neither type. Such circulations were described as "undefined". In an attempt to find the forcing mechanisms of the circulation, winds, coastal currents and wave characteristics were considered. Interactions between these mechanisms may make the individual effect of one difficult to distinguish. For example, the interrelationship of the winds and the coastal currents may make the effects of these parameters difficult to separate. The relevant wave data are listed in table 5.5 whilst the wind and coastal current data are listed in table 5.3.

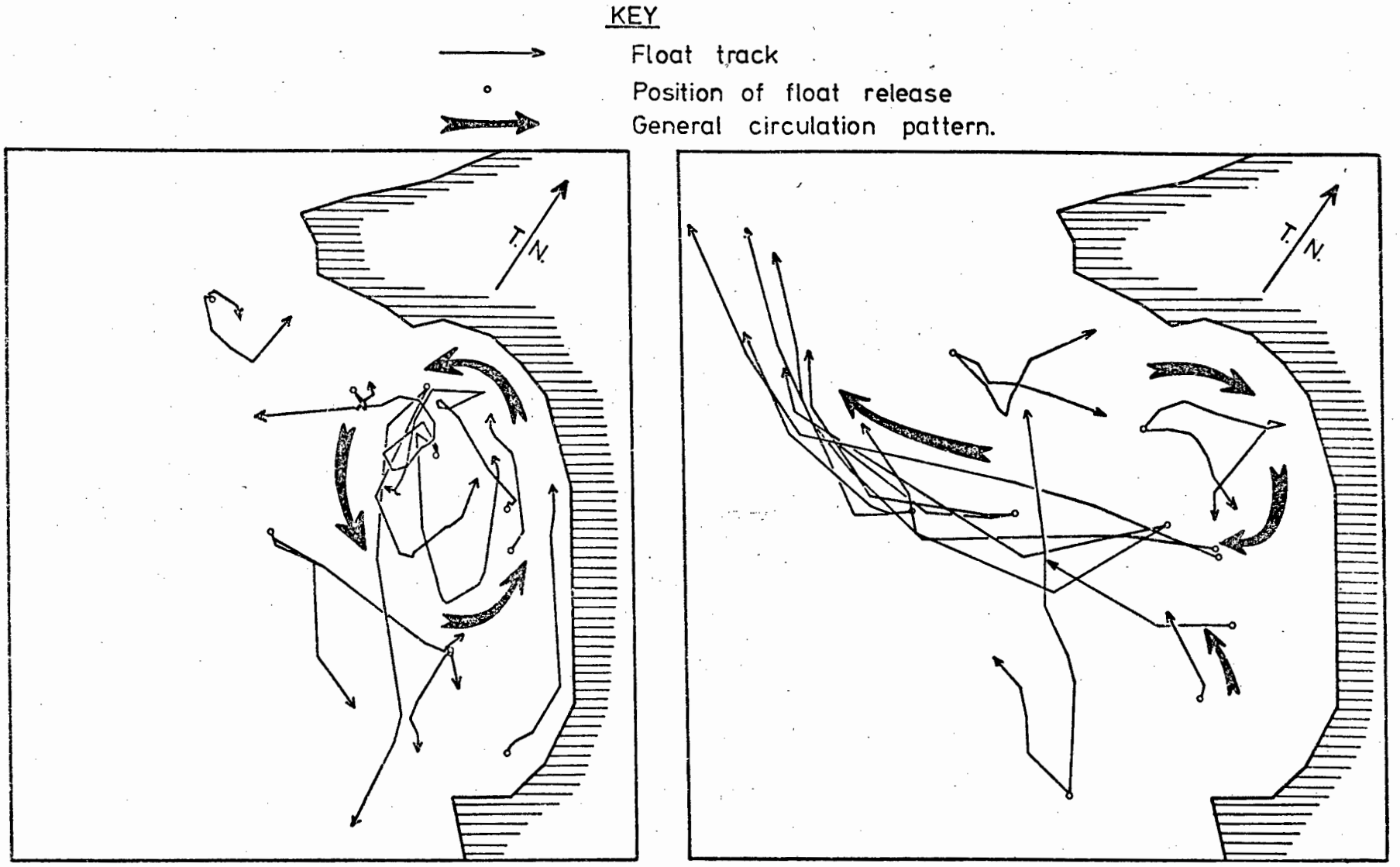

(a) Anticlockwise circulation pattern observed on 15TH. April, 1976.

(b) Clockwise circulation pattern observed on 16TH. February, 1976.

Fig. 5.6 Typical circulation patterns observed in Matroosbaai (a) Anticlockwise Circulation, (b) Clockwise Circulation.

KEY

——— Float track

o Position of float release

➡ General circulation pattern

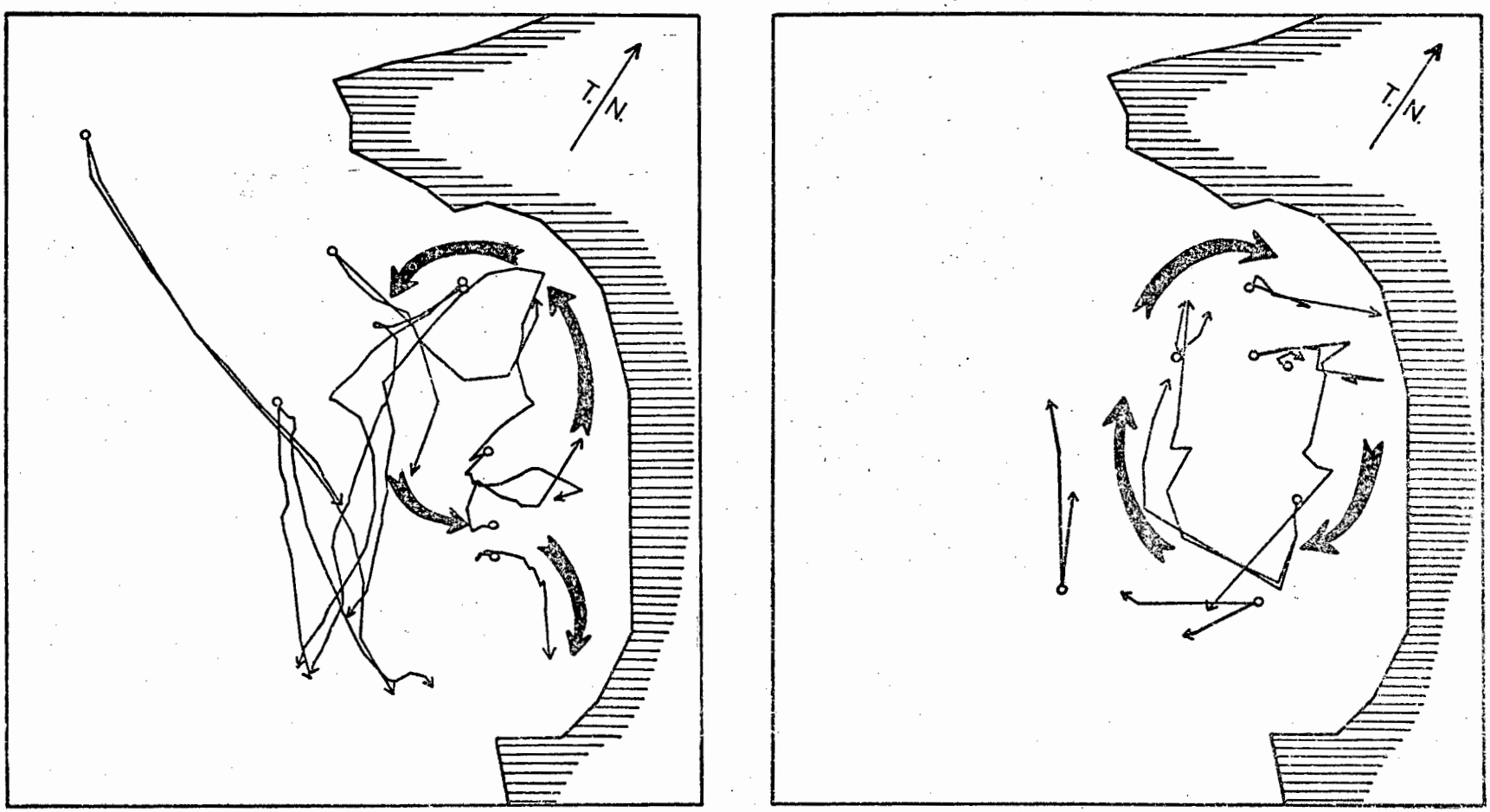

(a) Anti-clockwise circulation pattern observed on 17TH April, 1976.

(b) Clockwise circulation pattern observed on 16TH July, 1976.

Fig. 5.6 (cont.) Typical circulation patterns observed in Matroosbaai; (a) Anti-clockwise Circulation, (b) Clockwise Circulation.

TABLE 5.5 : Wave parameters possibly influencing the circulation types observed in Matroos Bay.

DATE	CIRCULATION TYPE	CHARACTERISTIC WAVE HEIGHT H_{mo} (m)	PEAK WAVE PERIOD Tp (sec)	WAVE DIRECTION D.O.S.O.	RADAR	WIND CONDITIONS
17-10-75	A	0.73	6.6	-	-	Northerly/light
23-10-75	U	0.46	5.9	-	-	Variable/light
30-01-76	A	0.88	9.9	210°	244° M	Southerly/light
31-01-76	U	0.89	8.4	206°	-	Variable/light
01-02-76	U	0.88	8.4	262°	245° M	Northerly/moderate
14-02-76	C(*)	0.94	5.2	-	253° I	Southerly/moderate
15-02-76	C(*)	2.54	8.1	-	246° M	Southerly/strong
16-02-76	C	1.66	9.4	204°	-	Calm
18-02-76	C(*)	1.52	9.6	210°	-	Variable/light
19-02-76	C	1.35	8.0	210°	-	Northerly/light
20-02-76	C	2.66	7.7	220°	-	Southerly/light
12-04-76	C	1.75	9.2	220°	-	Variable/light
13-04-76	A(*)	0.72	7.6	-	-	Variable/light
14-04-76	A	0.69	7.3	-	-	Variable/light
15-04-76	A	0.58	8.0	204°	-	Variable/light
17-04-76	A	1.40	7.3	192°	241° I	Northerly/light
18-04-76	C	2.43	9.8	192°	-	Southerly/light
19-04-76	C	1.51	9.0	202°	258° I	Variable/light
20-05-76	C(*)	2.04	10.6	-	237° M	Southerly/moderate
21-05-76	C(*)	1.66(Ø)	12.7(Ø)	-	-	Southerly/light
22-05-76	A	1.24(Ø)	10.8(Ø)	-	-	Variable/light
23-05-76	A	1.12(Ø)	12.4(Ø)	-	-	Variable/light
24-05-76	A(*)	1.14	9.1	-	-	Northerly/light
25-05-76	U	1.32	9.8	-	-	Variable/light
10-07-76(Ø)	C	1.22	8.0	-	243° I	Southerly/light
16-07-76	C	1.54	9.9	-	-	Variable/light
18-07-76	C	1.34	9.9	-	-	Variable/light
25-08-76	C(*)	3.11	10.0	-	-	Southerly/moderate
01-09-76	C(*)	2.79	9.1	-	241° M	Southerly/strong
02-09-76	C	1.39	10.0	-	-	Variable/light
03-09-76	A	0.55	6.0	-	-	Northerly/light
04-09-76	A	1.25	7.7	-	248° M	Northerly/light
05-09-76	C(*)	3.83	9.8	-	243° M	Variable/light
06-09-76	C(*)	1.71	7.8	-	-	Variable/light
07-09-76	C	2.21	8.7	-	238° M	Variable/light
07-10-76	A(*)	0.80(Ø)	12.5(Ø)	-	-	Southerly/light

Wave characteristics recorded at 1400 hours
(*) Visual observation
(Ø) Wave height and periods obtained on and after 10-07-76 from station E
(Ø) Values computed from Wemelsfelder data
M Middle position
I Inshore position

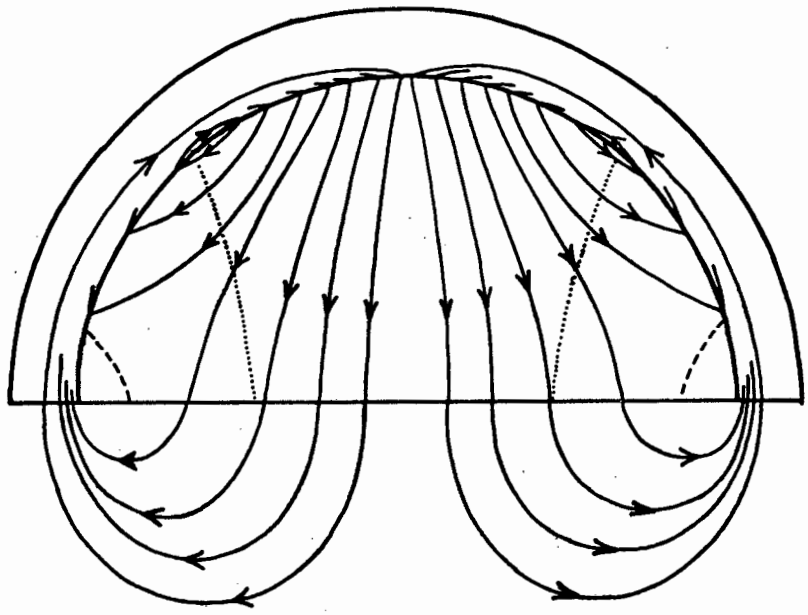

Fig. 5.7 Streamline pattern resulting from obliquity of wave incidence.
(after O'Rourke & LeBlond, 1972.)

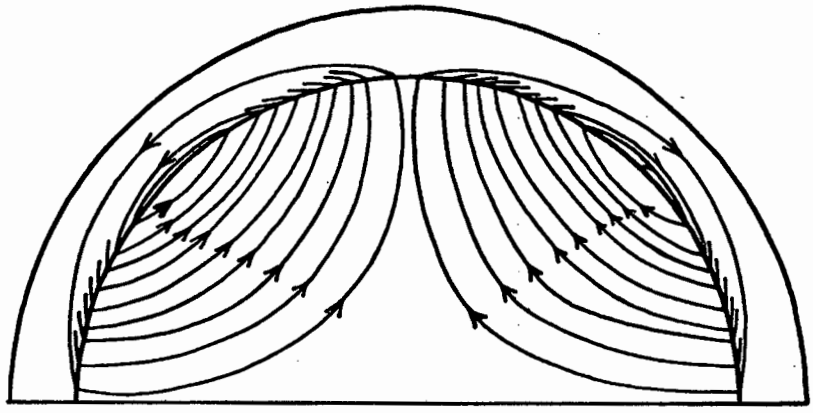

Fig. 5.8 Streamline pattern resulting from non-uniform wave amplitude.
(after O'Rourke & LeBlond, 1972.)

zone and the net direction of the longshore flow and the position of the rip currents or inflow will depend on which mechanism is dominant.

Refraction reduces the wave obliquity and increases wave height differences. The effects of refraction may therefore determine which mechanism will dominate.

If a bay is exposed to short period waves (high frequency), little refraction will be expected. The non-uniformity of the wave heights will therefore not be great and the obliquity will be significant irrespective of the wave height. The oblique incidence of the waves will be expected to dominate the wave height differences in generating longshore currents.

If, however, waves of high period,(low frequency) are incident on the bay, and, if the bay is of sufficient size, then refractive effects will be great. As the wave progresses towards shore its obliquity will steadily decrease and the wave height differences will increase. Thus, the lower the wave height, the longer time the wave will remain unbroken, and the more likely it is that the non-uniform wave height term will become dominant. Short period waves are therefore expected to produce clockwise circulation patterns, even at a fairly small wave height. High period waves are expected to produce an anticlockwise circulation type if the wave height is low and a clockwise circulation at higher wave heights.

To determine the effect of the wave height and period on the circulation types it is desirable to consider the data that was obtained when other mechanisms influencing the circulation were weak. Ideally, only those results obtained when no coastal currents were flowing and only light, variable winds were blowing would be used. Only on two occasions were samples collected during such conditions.

Seven data are available however, from occasions during which light, variable winds and only light coastal currents were recorded. On these occasions four anticlockwise and two clockwise circulations were recorded. One undefined circulation was also noted. These seven data have been plotted on figure 5.9a. The axes represent the wave height and period, different symbols represent the circulation types. Anticlockwise circulation was observed during periods of low waves and clockwise circulation during periods of high waves. This distribution agrees with the distribution predicted by the physical discussion given above. This graph, however, presents too few data to draw firm conclusions concerning the effect of wave height and period on the circulation type.

All the data relating to wave heights and periods from table 5.5 have been plotted on figure 5.9b, irrespective of the wind and coastal currents. The two circulation types occupy distinct regions on this diagram. Two possible divisions may be drawn separating these regions. The first division is taken somewhat arbitrarily through the origin and indicates that both wave height and period were important in determining the circulation type. This is in accord with the qualitative description given above. Of the 36 data available, only two do not fall within the appropriate regions delimited by this curve. The other possible division is the characteristic wave height of 1.25 metres. Only three points are found outside their respective regions marked by this division.

The division depending on both the wave height and period is to be preferred on the basis of the physical argument given above. The division marked only by the wave height was made possible by the restricted range of wave periods observed in the field situation, 5.2 to 10.6 seconds

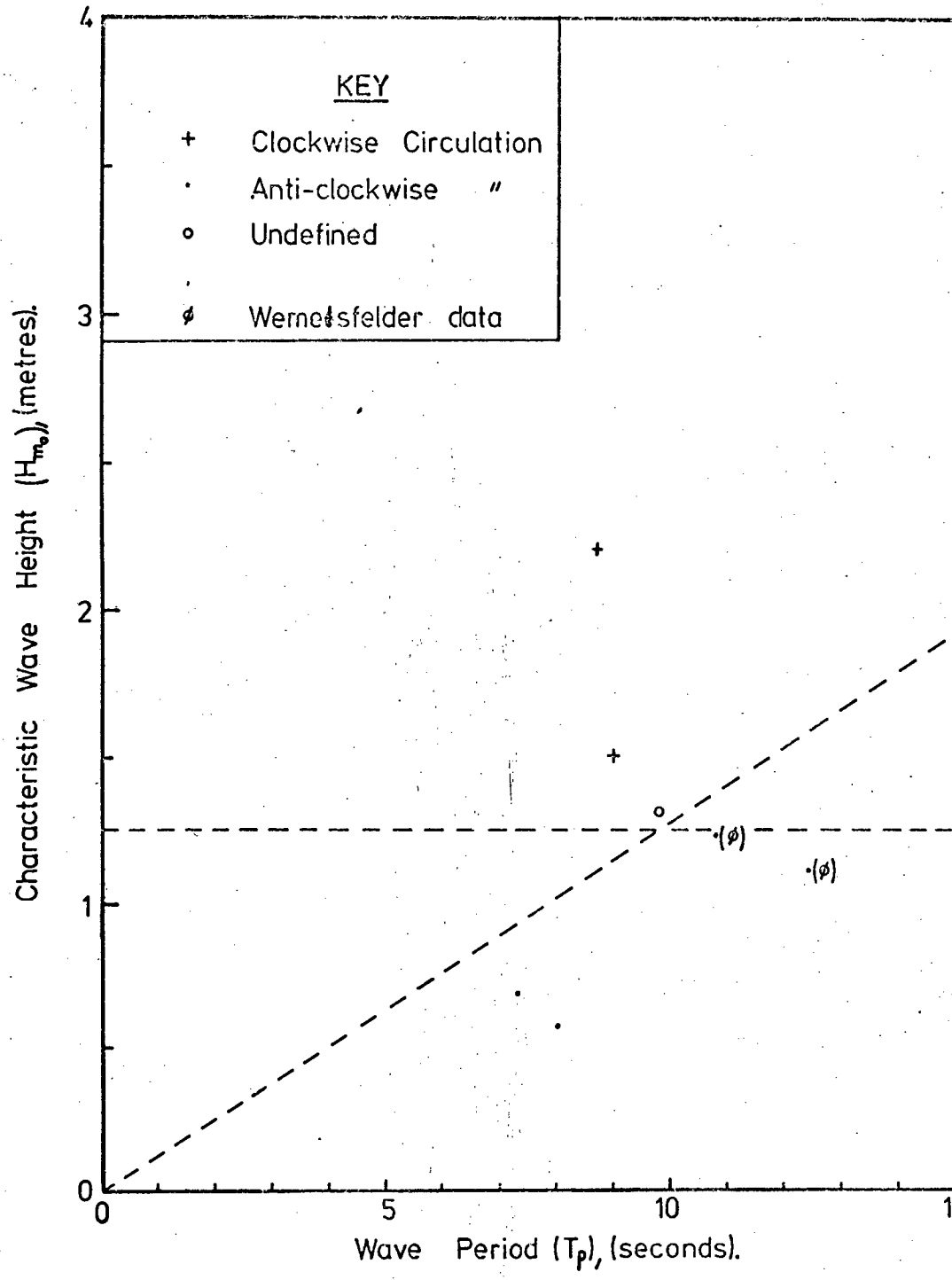

Fig. 5.9a Observed distribution of circulation types in Matroosbaai during periods of light variable winds and weak coastal currents.

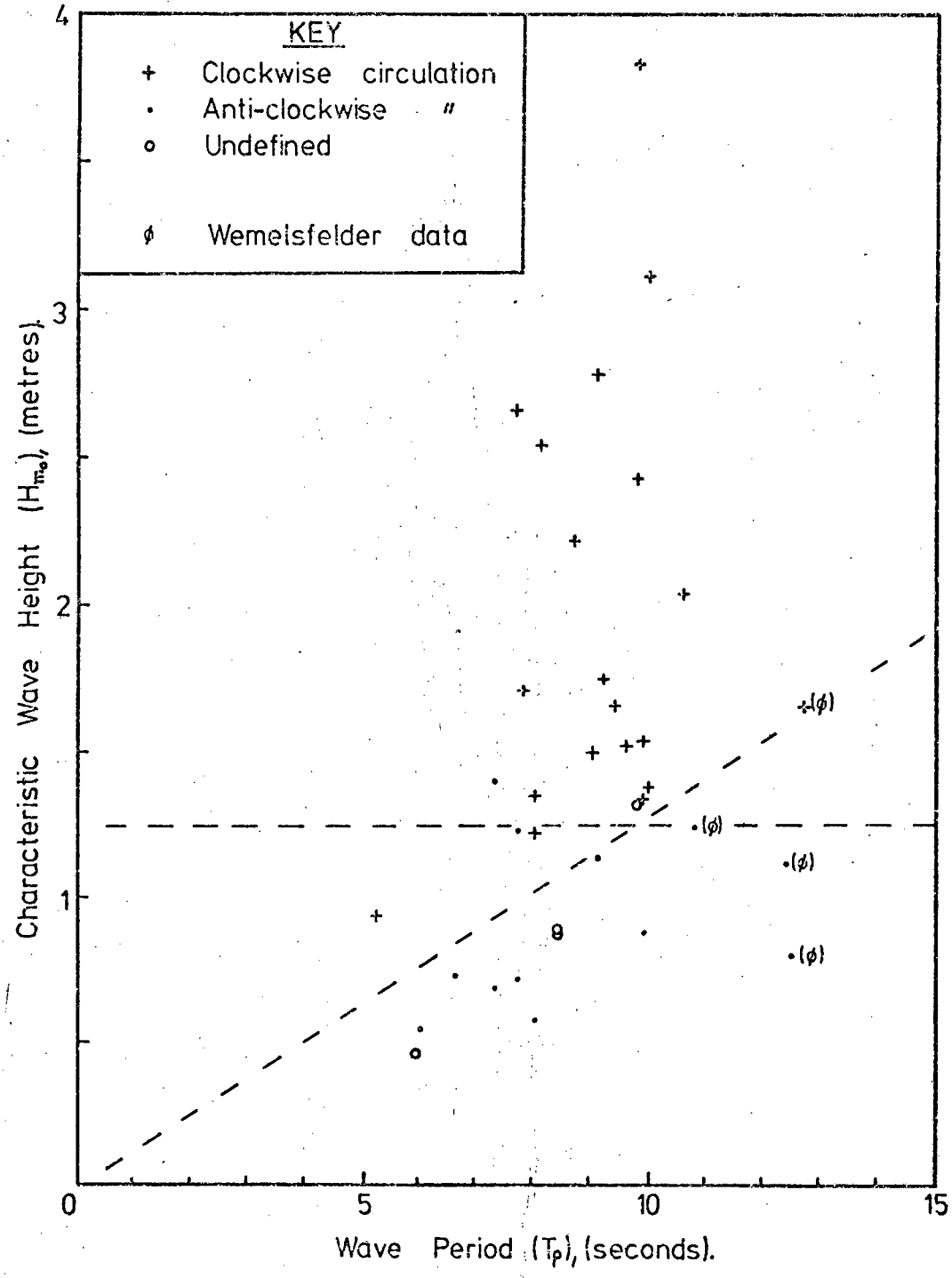

Fig. 5.9b Observed distribution of circulation types in Matroosbaai as a function of wave height and period (all data).

(excluding Wemelsfelder data, see Section 4.4). This division is not in strict accord with the physical principles described above but does make for a somewhat easier descriptive, theoretical and statistical treatment.

The undefined circulation types appear to lie close to the boundary based on both height and period considerations. Such circulations may have been transitional.

Two occasions were recorded for which the circulation type was not in agreement with the division based on both the wave height and period. These occasions were recorded on the 17th April, 1976 and the 4th September, 1976. On both occasions the wave height was increasing rapidly during the field measurements. The range on the 17th April was from a height of 1.15 metres at 0200 hours to 1.11 metres at 0800 hours, 1.40 metres at 1400 hours and 1.62 metres at 2000 hours, the periods ranged between 7.3 and 7.9 seconds. At the same times on the 4th September, the wave heights were 0.70 metres, 0.96 metres, 1.25 metres and 2.36 metres with periods ranging from 6.5 to 8.9 seconds. Hence, it is possible that the system was in fact undergoing a change from anticlockwise to clockwise circulation, but, either the effects of the wind and coastal currents or the inertia of the system had prevented the change in circulation from occurring.

A very good correlation was found between the circulation types and the wave height and period, irrespective of the wind and coastal currents. This suggests that the wind and coastal current conditions were less important than the wave height and period in determining the circulation within the bay.

It is possible that the winds or coastal current may have had some effect on the circulation, particularly when the effect

of the waves was small. It was desirable to consider the situation when no waves were present, but such a situation was not observed. To take into account only data recorded when small wave heights were observed would bias the results towards the anticlockwise circulation. Therefore, in the investigation of the possible effects of the winds and coastal currents all data have been used.

Wind Effects: Ekman (1905) showed that a stationary wind field over an infinite homogeneous ocean would result in a current distribution within the ocean in which velocity decreased with depth and the direction of the current rotated to the left (in the Southern Hemisphere). In a finite depth ocean the situation becomes more complex but the results remain analytic and may be found in many texts (e.g. Krauss, 1973). The angle which the wind makes to the coast will also influence the velocity of the wind driven currents (Ekman, 1905). Thus, in a region of changing topography the effect of the wind on the circulation may not be simply evaluated.

In shallow water the wind induced current is closely aligned with the wind direction. The speed of the surface current increases with the water depth. A south-easterly wind blowing over Matroos Bay may therefore induce a vorticity into the water velocity. Sheltering by the headlands may introduce a curl in the wind stress and thus accentuate the vorticity. On the basis of this very simple model it may be expected that south-easterly winds would lead to a clockwise circulation in Matroos Bay. North-westerly winds may be expected to induce an anticlockwise circulation in the bay.

The number of occasions for which the various circulation types were observed under different wind conditions is represented by table 5.6. On nine of the eleven occasions

TABLE 5.6 : Distribution of circulation types with the "present" and "past" wind conditions

Circulation Type	Wind Conditions					
	Present			Past		
	South	North	Other	South	North	Other
Clockwise	9	1	11	10	3	8
Anticlockwise	2	5	5	4	1	7
Undefined		1	2	1		2

Number of observations: 36
Correlation: 16
Non-correlation: 20

Number of observations: 36
Correlation: 13
Non-correlation: 23

during which southerly winds were blowing, a clockwise circulation pattern was recorded. On five out of seven occasions when northerly winds were blowing, an anticlockwise circulation was recorded. Thus, at first sight there appears to be fairly good correlation between the wind direction and the circulation type. If, however, the wind was the dominant forcing mechanism of the circulation within the bay then light, variable winds would not be expected to produce strong circulations, yet, of the 18 occasions of light, variable winds, 16 were found to have well defined circulation patterns. More cases of clockwise circulation types were recorded under variable wind conditions than under southerly winds and an equal number of anticlockwise patterns were observed under variable winds as under northerly winds. The existence of such well defined circulations under variable wind conditions confirms the suggestion that the wind was not the dominant factor influencing the circulation.

All points not indicating a correlation between the winds and the circulation could be explained by the wave height and period.

The "past" wind conditions showed a similar distribution to the "present" wind conditions. Interpretation however, must be treated with care, for, as indicated by the discussion of coastal currents, the response of the water to the winds may have been rapid. The similarity of the response of the "past" and "present" wind conditions may have been due to the persistence of the winds.

Coastal Currents: If the current flowing past the mouth of the bay induces an eddy within the bay similar to the separation eddy observed in small scale hydraulic flows, then, a northerly flowing current may be expected to produce a clockwise eddy in the bay; a southerly flow, an anticlockwise eddy. The results of small scale hydraulic studies are

not, of course directly applicable to the larger scale but serve simply as an analogy to indicate what may be expected. Bain (pers. comm.) has observed eddies with a diameter of several hundred metres near Melkbosstrand under north-westerly current conditions, but not under south-easterly current conditions.

The occurrence of the different circulation types for the different coastal current directions is given by table 5.7. Of the 23 data available 15, approximately 65%, infer a correlation. The effect of the coastal current was expected to be greatest when the currents were strongest, but, the very strong south-flowing currents of the 1st February, 1976, failed to produce the expected anticlockwise circulation. All the occasions when the circulation types do not correlate with the coastal current direction may be explained by the wave height and period.

Wave Direction: That the angle at which waves approach a coast can affect the nearshore circulation is well known and has been the subject of much analytical and observational research (Galvin, 1967; Longuet-Higgins, 1972; Miller and Barcilon, 1976). If a headland exists on a beach the situation becomes more complex. Gourlay (1974) gives several field examples and a laboratory study of such situations and indicates that a rip current can often develop in the lee of a headland or breakwater. On the exposed side of the headland the angle of incidence may tend to generate longshore currents flowing towards the junction of the headland with the beach. A rip current may form at this position. Thus, in an embayment formed by two headlands the effects of a change of the angle of incidence may be difficult to distinguish.

Due to the limitations of the systems used for collection of wave direction data (see Section 4.4), few data are

TABLE 5.7 : Distribution of circulation types with "coastal" current direction

Circulation Type	Coastal current		
	Northerly	Southerly	Other
Clockwise Circulation	9		2
Anticlockwise Circulation	2	5	2
Undefined Circulation		2	1

Number of observations: 23
Correlation: 15
Non-correlation: 8

available with which to determine whether or not the circulation responded to changes in the direction of wave approach.

Only seven records were available from the D.O.S.O. during conditions of clockwise circulatin type. The peak of the direction histogram on such occasions lay between 192° and 220°. Three readings were available from the same instrument during anticlockwise circulation, all lay between 192° and 210°. The wave directions determined by radar when clockwise circulations were observed lie in the range 237° to 258° (8 readings). Wave directions determined at times of anti-clockwise circulations lie in the range, 241° to 248° (3 readings) (table 5.8). Thus, the circulation types indicate no preferred directional range. Both methods indicate that the waves affecting the region of study were mainly from the south-west octant. Thus, they approach the coast almost normally. This is in agreement with the findings of Shillington and Harris (1974) that the origin of the swell incident on the beaches of the western Cape lies in the low pressure region to the south-west of Cape Town. Neither the directions obtained from the D.O.S.O. nor the radar show any marked directional difference.

The consistent difference of 40° to 50° between the two methods is puzzling. It is not known why such a difference should exist. It is not due to refractive effects as both methods evaluate the direction at approximately the same position. Operators of each system maintain that the directions quoted are relative to True North, thus the difference does not appear to be due to a magnetic declination ($\sim$ 24°W) correction being omitted from one set of data. As changes in the wave direction produced no effects on the circulation type, the reason for difference between the two methods was not investigated further.

TABLE 5.8 : Distribution of wave directions and circulation types. (Number of readings in brackets).

Circulation Type	D.O.S.O. record	Radar record
Clockwise Circulation	192° - 220° (7)	237° - 258° (8)
Anticlockwise Circulation	192° - 210° (3)	241° - 248° (3)

Review: An investigation of the meteorological and oceanographic conditions that may influence the circulation within Matroos Bay was performed. The wave height and period were found to be the most important factors affecting the circulation type. A reasonable correlation was found between both the wind and coastal current direction and the circulation type. Only for the wave direction could no influence on the circulation types be detected.

As a correlation was found between wind and coastal current direction and the circulation types, the effect of these two mechanisms cannot be ignored. It is, however, interesting to speculate on whether the correlation found, did in fact, depend on a relationship between the winds and the waves.

5.3.3. On the correlation between the winds and coastal currents with the wave heights

A possible explanation for the correlation found on many occasions between the wind and coastal current direction and the circulation may be found by considering the surface air pressure distribution over the South Atlantic Ocean. Shillington and Harris (1974) have shown that waves reaching the Cape's shores may often be traced to low atmospheric pressure distributions in the vicinity of Gough Island. Taljaard (1967) indicates that this is an area of high occurence of cyclone centres in all seasons (figure 5.10). The pressure distribution is also responsible for the winds experienced at Cape Town (see Section 3.1). Thus, the pressure distribution over the South Atlantic is responsible both for the waves and the winds experienced.

Figure 5.11 illustrates the synoptic pressure distributions over the South-east Atlantic Ocean from the 11th to the 20th February, 1976 and the resultant wave height variations experienced at Melkbosstrand. On the 11th February a "low" was located to the south of Gough Island. Its presence is

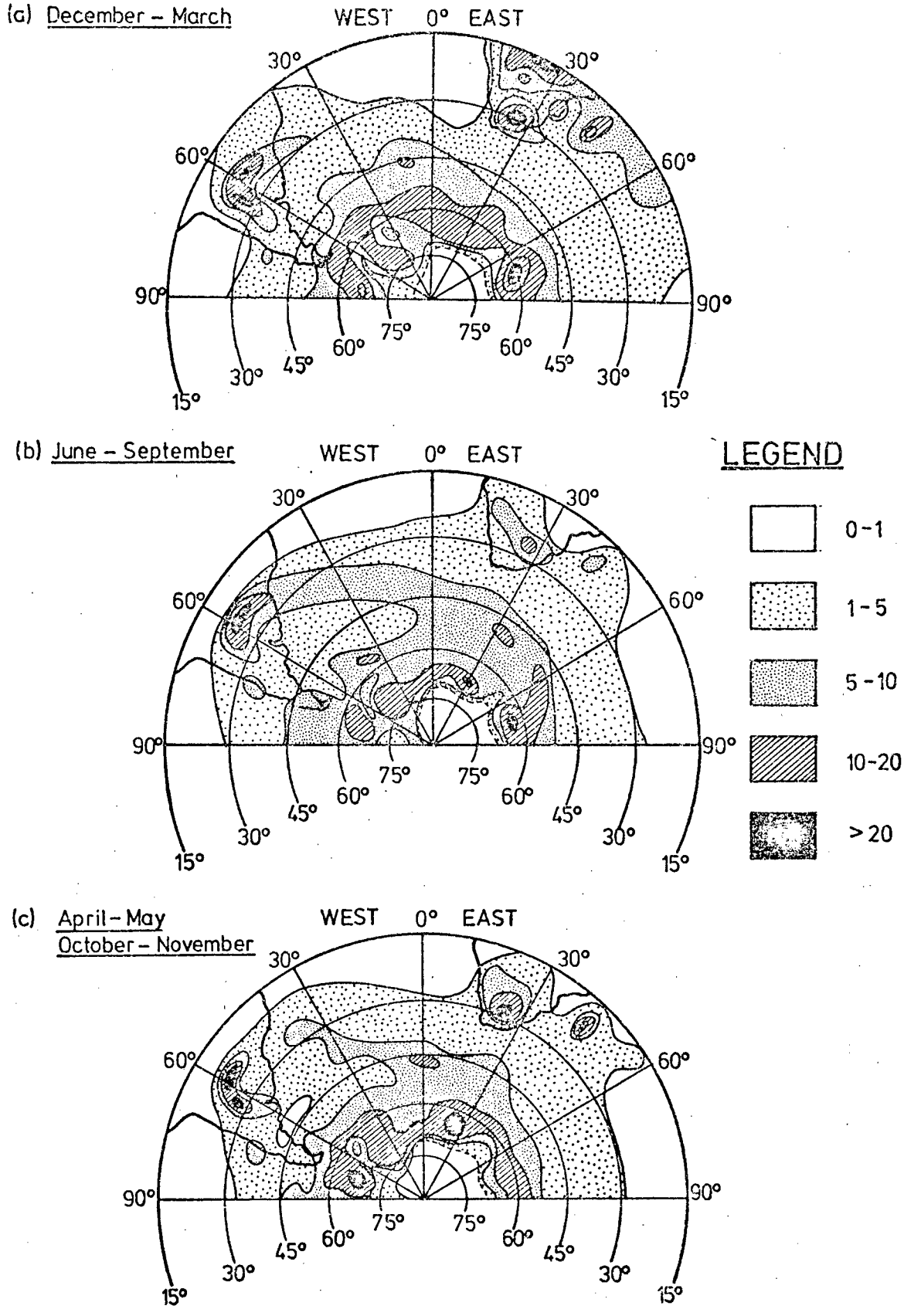

Fig. 5.10 Distribution of cyclone centres per unit area (438,000 km²) per 4-month season of the I.G.Y. (from Taljaard, 1967.)

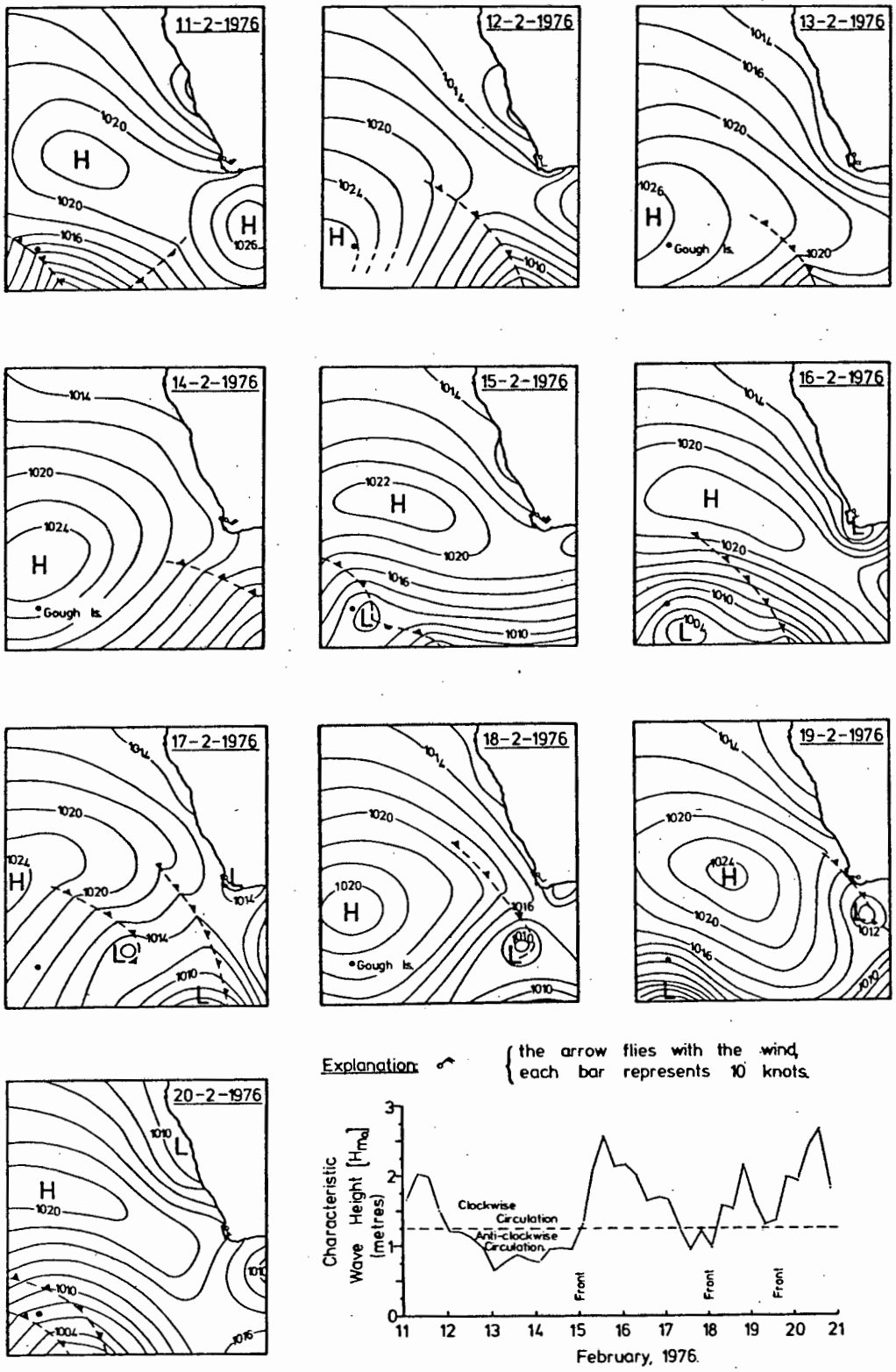

Fig. 5.11 Synoptic pressure distribution over the south-east Atlantic Ocean showing the influence of the resulting winds on the waves recorded at Melkbosstrand.

indicated by the two fronts coming from this region. Further to the north, the South Atlantic Anticyclone may be seen ridging to the south of Africa, producing strong south-easterly winds at Cape Town. This is a typical summer distribution of the pressure system and is responsible for favourable upwelling conditions off the western coast.

On the 12th and 13th February, 1976 the low pressure region moved to the east passing well to the south of Cape Town. Another low developed to the west. This low also moved to the east and had a trough extending almost to Cape Town on the 14th February. Wave heights had fallen since the 11th February and on the 14th were low, only .94 metres. The wave period was also low, 5.2 seconds, indicating the local nature of the waves. Moderate south-easterly winds were being experienced. After the passage of the front, wave heights increased rapidly as the waves generated to the south-west of Cape Town arrived concurrently. The anticyclone, after the passage of the front had ridged to the south of Africa and again produced strong south-easterly winds. Another low pressure region had developed near Gough Island.

During the following few days a coastal low pressure region developed over the Cape, suppressing the south-easterly winds and producing variable winds. In this period, from the 16th to 18th February, wave heights fell sufficiently to permit the development of the anticlockwise circulation on the 17th February. Unfortunately coastal fog prevented observations to confirm this. During this time the lows continued their eastward movement and by the 19th February another front was situated off Cape Town. After the passage of this front on the 20th February waves increased rapidly in height and the wind swung to the south-east.

The cycle of events may be simplified as follows: Wave heights decrease prior to the passage of a front. North-westerly winds are experienced before a front. After the passage of the front, winds swing to the south-west or south-east. Soon after the arrival of the front wave heights increase and are therefore likely to occur concurrently with southerly winds. Wave heights begin to decrease again before the arrival of the next front.

Hence, although a relationship between the wind and the circulation types exists, an examination of the atmospheric pressure distribution reveals that this relationship may be coincidental, not causative. As the coastal currents may be driven by the winds, a similar interrelationship may be expected between the coastal currents and the circulation types.

5.3.4. Theoretical concepts relating to the origin of the driving forces of the circulation

An understanding of the concepts pertaining to the observed circulation system may be gained by considering the vertically integrated and averaged equations of motion and continuity,

$$\frac{\partial \rho u}{\partial t} + \left[u \frac{\partial \rho u}{\partial x} + v \frac{\partial \rho u}{\partial y} \right] = -\rho g \frac{\partial \eta}{\partial x} - \frac{1}{\eta + h} \left[\frac{\partial S_{xx}}{\partial x} + \frac{\partial S_{xy}}{\partial y} \right] + \frac{\tau_x}{\eta + h} \qquad 5.1$$

$$\frac{\partial \rho v}{\partial t} + \left[u \frac{\partial \rho v}{\partial x} + v \frac{\partial \rho v}{\partial y} \right] = -\rho g \frac{\partial \eta}{\partial y} - \frac{1}{\eta + h} \left[\frac{\partial S_{yx}}{\partial x} + \frac{\partial S_{yy}}{\partial y} \right] + \frac{\tau_y}{\eta + h} \qquad 5.2$$

$$\frac{\partial}{\partial x} \left[u (\eta + h) \right] + \frac{\partial}{\partial y} \left[v (\eta + h) \right] = 0 \qquad 5.2$$

where u (x,y), v (x,y) are the depth mean velocities, τ_x, τ_y the frictional resistances, h, is the still water depth and η the displacement of the mean water level from the still water level due to the presence of the waves. ρ is the mean water density, g, the gravitational acceleration and S_{ij} is the Radiation Stress Tensor.

The simplest solution to these equations may be derived by considering a steady state situation where no longshore variation exists, i.e. $\frac{\partial}{\partial y} \equiv 0$. In this case the equations of motion yield

$$\rho g (\eta+h) \frac{\partial \eta}{\partial x} = - \frac{\partial S_{xx}}{\partial x} + \tau_x \qquad 5.4$$

$$\tau_y = \frac{\partial S_{xy}}{\partial x} \qquad 5.5$$

and, if the frictional term, τ_x, is zero, equation 5.4 may be evaluated to yield the familiar results for the wave setup for small amplitude waves outside the surf zone (Longuet-Higgins and Stewart, 1962).

$$\eta = - \frac{1}{8} \frac{H^2 k}{\sinh 2kh} \qquad 5.6$$

Solution of equation 5.5 yields an expression for the longshore current, $\langle v \rangle$. The form of the solution is dependent on the assumptions made concerning the wave characteristics after breaking and the form of the dissipation term, τ_y . Longuet-Higgins (1970a), for example, balanced the thrust by a quadratic bottom friction of the form

$$\tau = \rho C |\underline{u}| \underline{u} \qquad 5.7$$

i.e. $$\tau_y = \frac{2}{\pi} C \rho u_m \langle v \rangle$$

and derived the expression for the longshore current, $\langle v \rangle$

$$\langle v \rangle = \left(\frac{h}{h_b}\right) \begin{cases} v_o & ; h < h_b \\ 0 & ; h > h_b \end{cases} \qquad 5.8$$

where

$$v_o = \frac{5\pi}{8} \frac{u_m}{C} s \sin \phi_b \qquad 5.9$$

and

$$u_m = \frac{\gamma}{2} (g h_b)^{1/2}$$

is the maximum orbital velocity of the waves, C is the frictional coefficient ($\simeq 10^{-2}$); s is the slope of the sea floor; γ, the ratio of the wave height, H, to the water depth; and ϕ_b the angle of incidence of the waves to the shore. Subscript, b , denotes that the parameter is to be evaluated at the breaker line. This formulation clearly

leads to a velocity discontinuity at the breaker line. To obtain a continuous flow distribution both Bowen (1969a) and Longuet-Higgins (1970b) introduced a horizontal diffusion term. The derivation of Longuet-Higgins (1970b) assumes that the horizontal diffusion term has the form

$$\frac{\partial}{\partial x}\left(\mu_e h \frac{\partial v}{\partial x}\right)$$

where, by simple physical arguments, a possible form of the horizontal eddy viscosity, μ_e, is

$$\mu_e = N \rho \alpha (gh)^{1/2} \qquad 5.10$$

N is a dimensionless constant with probable limits

$$0 < N < 0.016 \qquad 5.11$$

Using this formulation the normalised velocity, $V = \frac{\langle v \rangle}{v_0}$, of the longshore current is shown to be

$$V = \begin{cases} B_1 X^{p_1} + A X & ; 0 < X < 1 \\ B_2 X^{p_2} & ; 1 < X < \infty \end{cases}$$

where

$$B_1 = \frac{p_2 - 1}{p_1 - p_2} A \qquad B_2 = \frac{p_1 - 1}{p_1 - p_2} A$$

$$p_1 = -\frac{3}{4} + \left[\frac{9}{16} - \frac{1}{P}\right]^{1/2} \qquad p_2 = -\frac{3}{4} - \left[\frac{9}{16} - \frac{1}{P}\right]^{1/2}$$

$$A = 1 / \left(1 - \frac{5}{2} P\right) \; ; \; P \neq \frac{2}{5} \qquad 5.12$$

for a non-dimensionalized distance offshore, $X = \frac{x}{x_b}$.

The parameter, P, represents the relative importance of mixing and friction and is defined

$$P = \pi \left(\frac{s N}{\gamma C}\right) \qquad 5.13$$

where C is a frictional coefficient.

Bowen (1969a) made the assumption that the horizontal eddy viscosity, μ_e, was constant and hence the horizontal diffusion term became

$$\mu_e \frac{d^2 v}{d x^2}$$

whereupon a solution was obtained for the longshore current in terms of Modified Bessel Functions. The differences between the velocity distributions predicted by these two derivations are not of great importance here. Rather, it is

noted that each achieves a smooth transition of velocities across the breaker line, the position of maximum longshore current velocity moving to a position inshore of the breaker line. Both analyses rely solely on the obliquity of the wave incidence to provide the driving mechanism for the longshore current and each treats the change of obliquity across the surf zone in a different manner.

If, as is often the case in both laboratory and field studies, there is a longshore variation in the wave forcing then the terms

$$-\rho g \frac{\partial \eta}{\partial y} \quad - \quad \frac{1}{\eta+h} \frac{\partial S_{yy}}{\partial y}$$

of the equation of longshore motion (equation 5.5) cannot be neglected. The inclusion of these terms in the equation of motion, equation 5.5, is equivalent to a linearization of the steady state version of equation 5.2. As a consequence of ignoring the non-linear terms, rapidly varying flow that may occur near rip currents cannot be satisfactorily treated.

Several authors have dealt with the generation of longshore currents in this situation (Bowen, 1969b; O'Rourke and Le Blond, 1972; Komar, 1975). A treatment similar to that given by Komar (1975) for a straight beach, in which only the frictional term of Longuet-Higgins (1970a) is considered, gives the clearest insight as to the origin of the forcing terms. The linearized steady state equation of motion is

$$\tau_y = \rho g (\eta+h) \frac{\partial \eta}{\partial y} + \frac{\partial S_{xy}}{\partial x} + \frac{\partial S_{yy}}{\partial y} \qquad 5.14$$

and in shallow water the Radiation Stress Tensor takes the form

$$S_{ij} = E \begin{bmatrix} \cos^2\phi + \frac{1}{2} & \cos\phi \sin\phi \\ \cos\phi \sin\phi & \sin^2\phi + \frac{1}{2} \end{bmatrix} \qquad 5.15$$

where E is the wave energy, $E = \frac{1}{8} \rho g H^2$, and ϕ is the angle of incidence of the waves as defined by the definition sketch, figure 5.12. The first term of equation 5.14 may

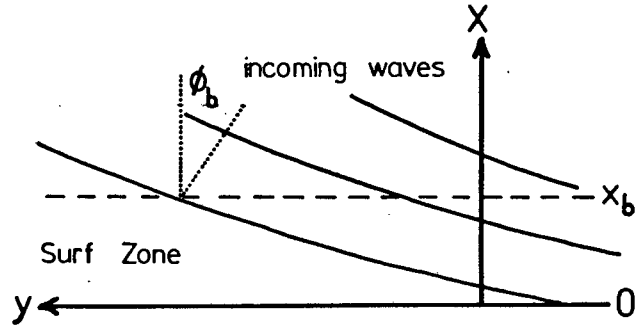

(a) Plane Beach

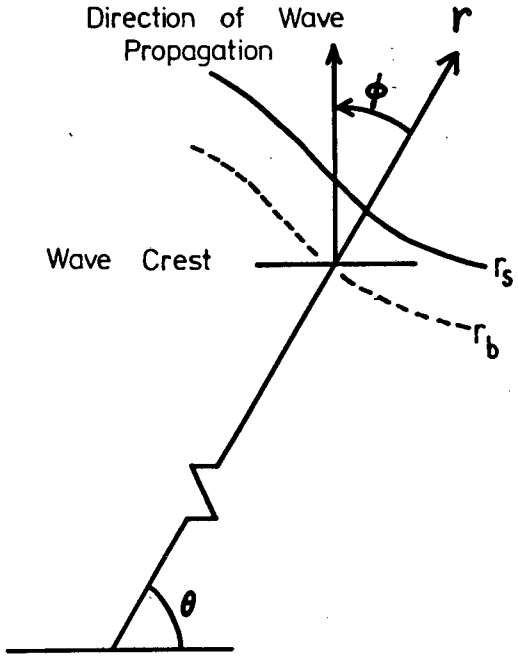

(b) Definition of the angle of incidence, ϕ made by the direction of wave propagation and the radial vector, r at the breaker line for a semi-circular beach.

Fig. 5.12 Definition sketches for longshore currents.

be evaluated at the breaker line using the shallow water approximation of equation 5.6 to obtain

$$\eta = -\frac{H^2}{16h} \qquad 5.16$$

where, H is the wave height and h the depth of water. Thus, if a plane beach is considered, $\frac{\partial h}{\partial y} = 0$ and $\frac{\eta+h}{h} \simeq 1$, the contribution to the longshore current arising from differences in the setup is

$$\langle v \rangle = -\frac{\pi}{c}\ \frac{u_m}{4\gamma}\ \frac{\partial H}{\partial y} \qquad 5.17$$

when the retarding force is taken as the bottom friction, equation 5.7. To evaluate the contribution of the setup gradient within the surf zone where $\frac{\eta+h}{h} \not\simeq 1$ the expression

$$\eta = K(h_b - h) + \eta_b \qquad 5.18$$

where $K = \left(1 + \frac{8}{3\gamma^2}\right)^{-1}$ must be used, with a more complex expression replacing equation 5.17.

The contribution to the longshore current arising from the second term of equation 5.14 is simply the longshore current due to oblique incidence given by equations 5.8 and 5.9.

The third term of equation 5.14, results from longshore gradients of the flux of longshore momentum of the waves parallel to the coast, $\frac{\partial S_{yy}}{\partial y}$, which in shallow water may be expressed as

$$\frac{\partial}{\partial y} E\left(\frac{3}{2} - \cos^2\phi\right)$$

In differentiating this term, the angle of incidence of the waves, ϕ, may, for most considerations of a plane beach be considered independent of the longshore direction, y. However, in considering a curved coast, changes in the angle of incidence of the waves will be expected and so $\phi = \phi(y)$ will be considered. The contribution to the longshore currents of the third term becomes

$$\langle v \rangle = \frac{\pi}{c}\ \frac{u_m}{2\gamma}\left\{ H \cos\phi \sin\phi \frac{\partial \phi}{\partial y} + \left(\frac{3}{2} - \cos^2\phi\right)\frac{\partial H}{\partial y} \right\} \qquad 5.19$$

and is thus dependent not only on the change of the wave height along the breaker line, $\frac{\partial H}{\partial y}$, but also on the change of direction of the waves, $\frac{\partial \phi}{\partial y}$.

Thus, if the characteristics of the wave approaching the shore show variations in the longshore direction, then, not only the wave obliquity but also the longshore changes of the wave height and of the angle of incidence will have an effect in the generation of longshore currents. Bowen (1969b) showed that, even if waves were normally incident on a beach, longshore variations in the wave height could lead to the development of a nearshore circulation system.

The system of equations with both longshore variations and horizontal mixing has been solved analytically for a plane beach by Le Blond (1972) and Komar (1975). Le Blond (1972) maintains the change of the breaker angle term whilst Komar (1975) omits this term as it is small, in general, for plane beaches.

A theoretical solution of the wave driven circulation within a semi-circular bay was developed by O'Rourke and Le Blond (1972). By considering the linearized equations of motion and the shallow water approximations for the radiation stress they obtained, to $0(\delta)$, the following expression for the transport stream function, Ψ,

$$-\frac{2}{g\alpha^2}\left\{\left(\frac{\partial}{\partial s}-\delta\right)\frac{f}{d^2}\frac{\partial \psi}{\partial s}\right\} = \frac{\partial}{\partial s}\left\{\sin 2\phi\left(\frac{\partial}{\partial s}-2\delta\right)d + 2\delta\cos 2\phi\frac{\partial d}{\partial \theta} - 3\delta d\sin 2\phi\frac{\partial \phi}{\partial \theta}\right\} \qquad 5.20$$

where $f = \frac{2}{\pi}\rho C u_m$ is a friction coefficient, and is a function of the total depth, $d = \eta + h$; α is the ratio of the wave amplitude and the depth, a/d; and s, is a radial co-ordinate defined by

$$s = \frac{r - r_s}{r_b - r_s} \qquad 5.21$$

where r is the radial distance. Subscripts b, s refer to

the breaker - and shore-lines respectively (figure 5.12). δ is defined by

$$(r_s - r_b)^2 / r_s^2 = \delta^2 \ll 1 \qquad 5.22$$

Angles ϕ, θ refer to the angle of incidence of the wave and the azimuthal co-ordinate respectively (figure 5.12b). The headland of the bay has azimuthal co-ordinate $\theta = 0$, the centre of the bay, $\theta = \frac{\pi}{2}$.

The authors give the following discussion of the driving forces of the right-hand side of equation 5.20, " .... There are three types of forcing terms ... for a beach in the shape of an arc of a circle where ϕ is everywhere the angle made by the wave number vector to the shore normal. ... The second term, which is proportional to $\cos 2\phi \frac{\partial d}{\partial \theta}$ is the only one that does not vanish when $\phi = 0$ everywhere, i.e. when the waves are normally incident on the shore. It is intuitively obvious, and confirmed by the presence of the $\frac{\partial d}{\partial \theta}$ factor, that longshore currents will occur in this situation only because of longshore inhomogenities in topography or in the incoming wave field ... The terms proportional to $\sin 2\phi$ lead to longshore currents because of the oblique angle of incidence of the waves. The first such term, $\sin 2\phi \left(\frac{\partial}{\partial s} - 2\delta\right) d$, involves only uniform oblique incidence... The term $\sin 2\phi \frac{\partial \phi}{\partial \theta}$ brings in the variations in angle of incidence along the beach". The similarity of these terms with those previously discussed for the plane beach is clear and the origin of such terms is the same, whether for a plane or curved beach, as the physical processes participating are the same although the strength of the effects may differ.

They go on to develop the equation describing the form of the transport stream function within the surf zone of a semi-circular beach,

$$\psi = -\frac{\gamma \pi m^{3/2} g^{1/2}}{c d_b^{1/2}} \left[\frac{-m^{3/2} \cos\phi \sin\phi (1 - \delta s}{6} + \frac{\delta \cos 2\phi}{5} \frac{\partial m}{\partial s} s^{1/2} + \frac{\delta m^{3/2} \cos\phi \sin\phi}{4} s \frac{\partial \phi}{\partial \theta} \right] s^3 \qquad 5.23$$

where $d = m(\theta)\, s = \eta + h$

and the longshore velocity is given by

$$v_\theta = \frac{1}{r_s \delta d} \frac{\partial \psi}{\partial s} \qquad 5.24$$

By considering the simple case of laterally uniform wave field normally incident on the bay, with refraction occuring, and, assuming that the functions, $\phi_b(\theta)$, $m(\theta)$ had the following simplified forms

$$\phi_b(\theta) = \phi_o \cos\theta \qquad 5.25$$

$$m(\theta) = m_o(1 - p\cos 2\theta) \qquad 5.26$$

O'Rourke and Le Blond (1972) were able to show that the transport stream function within the surf zone became

$$\psi = k s^3 \left\{ \frac{-\phi_o(1-\delta s)}{6} \left[(1-p)\cos\theta - p\cos 3\theta \right] + \frac{2}{5} p \delta s^{1/2} \sin 2\theta - \phi_o^2 \frac{\delta s}{8} \sin 2\theta \right\} \qquad 5.27$$

where $k = \gamma \frac{\pi}{2} g^{1/2} m_o^{5/2}/C$. The assumptions used in this derivation were, that the angle of incidence of the wave, ϕ, changes little through the surf zone, i.e. $\cos\phi = \cos\phi_o$; the refraction in the bay is sufficiently fast that ϕ_o is small i.e. $\sin\phi_o \simeq 1$ (sic) and, that wave heights are not quite uniform i.e. $p^2 \ll 1$.

The order of the terms is the same as that in equation 5.20. Thus, the first term is derived from consideration of uniform oblique incidence. Figure 5.7 illustrates the streamlines of the circulation generated by this oblique incidence term. The wave number vectors have everywhere a component away from the mouth of the bay, consequently, the longshore current is forced away from the headlands and converges at the back of the bay.

The second and third terms of the equation arise from changes of amplitude of normally incident waves and from the

non-uniformity of wave incidence. Figure 5.8 (after O'Rourke and Le Blond, 1972) presents the streamline patterns completed from considerations of only the second term. Longshore currents within the surf zone are forced from the centre of the bay towards the ends of the headlands. The streamline pattern for the third term have not been calculated but have a similar form to that of the second term but reversed in direction and smaller in magnitude. O'Rourke and Le Blond (1972) give examples in which the third term has a magnitude approximately 10% of the second term.

In the situation described, the longshore current generated by the oblique incidence term dominated the non-uniform wave height term with the result that longshore currents would flow towards the back of the bay. The authors recognise, however, that this need not be the case at all times: "one need only to consider a bay where the wave refraction is complete by the breaker line so that the wave crests are very nearly parallel to the shore". Further, they go on to state that "... the simplicity of the analysis and the physical insight it provides into the phenomena, have been achieved at the price of a number of assumptions, the worst of which is patently the overall neglect of lateral momentum diffusion and the linearization of the equations". These assumptions will not be discussed here nor will the applicability to a real situation of the simplified forms describing the breaker angle, $\phi_b(\theta)$, and the water depth parameter, $m(\theta)$. Clearly, the formulation of these functions given by equations 5.25 and 5.26 is realistic. The exact solution may be considered as a result of the offshore refraction problem.

5.3.5. Theoretically predicted circulation characteristics

The nature of the longshore currents predicted by the model of the semi-circular bay will now be examined. In this

section consideration will primarily be given to the direction of flow of the longshore current. The direction of flow will depend on the relative strength of the two primary forcing mechanisms. The velocities predicted may not be accurate due to the neglect of horizontal diffusion and the linearization of the equations.

In order to apply the results of such analysis to Matroos Bay one must assume that Matroos Bay can be envisaged as being formed by two headlands, making the arcs of a circle, with a straight beach in between. The beach will be assumed to be sufficiently small that circulation patterns do not form on this section of the beach but, that the circulation generated along the headlands is the dominant circulation in the bay.

From equations 5.23 and 5.24 the longshore current velocity at the mid-surf position, $s = \frac{1}{2}$, is obtained as

$$v_{\frac{1}{2}} = \frac{\gamma \pi m^{3/2} g^{\frac{1}{2}}}{r_s \delta d_b^{\frac{1}{2}} C} \left\{ m^{3/2} \sin 2\phi_b \left[\frac{2\delta - 3}{24} \right] + \frac{7}{20\sqrt{2}} \delta \cos 2\phi_b \frac{\partial m}{\partial \theta} + \frac{\delta}{8} m^{3/2} \sin 2\phi_b \frac{\partial \phi}{\partial \theta} \right\} \quad 5.28$$

and, if the variation of the angle of incidence of the waves, $\phi_b(\theta)$, and the water depth, $m(\theta)$, around the bay have the form described by equations 5.25 and 5.26 and the parameters $C = 10^{-2}$, $\gamma = .8$, $r_s = 500$ metres, $\delta = .05$ are taken as typical for Matroos Bay then

$$v_{\frac{1}{2}} = m_o^{3/2}(1 - p\cos 2\theta)^{3/2}(-1.971 - 1.590\,\phi_o \sin\theta)\sin 2\phi_b + 0.382 \cos 2\phi_b\, m_o\, p \sin 2\theta \quad 5.29$$

The effect of the three variables, m_o, p and ϕ_o may now be investigated. In practice the width of the surf zone relative to the radius of curvature of the bay depends on m, but it will be considered as constant, for simplicity. Consideration of equation 5.22 shows this to be a reasonable assumption if $p^2 \ll 1$, and the range of m_o is small.

The obliquity of the wave incidence at the headland, $\theta = o$, is denoted by the variable, ϕ_o. This variable is clearly dependent on the refraction of the waves outside the bay, and, therefore, on the bottom topography and the wave period. On a real coastline the region immediately offshore of the headland of the bay may be an area of rapidly changing obliquity as the wave must, over this short region, change its angle of incidence from zero along the plane region of beach outside the bay to the value ϕ_o at $\theta = o$. This region does not receive treatment in the model explicitly but the expected dominance of the oblique incidence term in this region is found in the model as indicated by the streamlines of figure 5.7.

The terms m_o and p relate to the water depth and the water depth changes around the bay. m_o is the water depth at the breaker line mid way between the headland and the centre of the bay, $\theta = \pi/4$, p is an index of the rate of change of the water depth with angular distance, θ. Thus, both m_o and p will be dependent on the refraction of the waves. As the breaker height is assumed to be related to the water depth by the proportionately constant, γ, these two variables may also be treated as being related to the wave height. m_o may also vary independently due to changes of the deep water wave height.

Figure 5.13 illustrates the effects of changing the variables m_o, p and ϕ_o in equation 5.29. Each set of curves is centred around the case $p = 1/3$, $m_o = .7$ and $\phi_o = .05$. For the case $\phi_o = 0$, that is, a case of complete refraction so that no net obliquity remains, the resultant longshore current is positive for $o < \theta < \frac{\pi}{2}$. The current is directed towards the headlands and reaches a maxima at $\pi/4$ (compare with figure 5.8). For the case $p = o$, no resultant wave height gradient exists and the current is negative for $o \leq \theta < \frac{\pi}{2}$ and, thus, directed towards the centre of the bay (compare with figure 5.7).

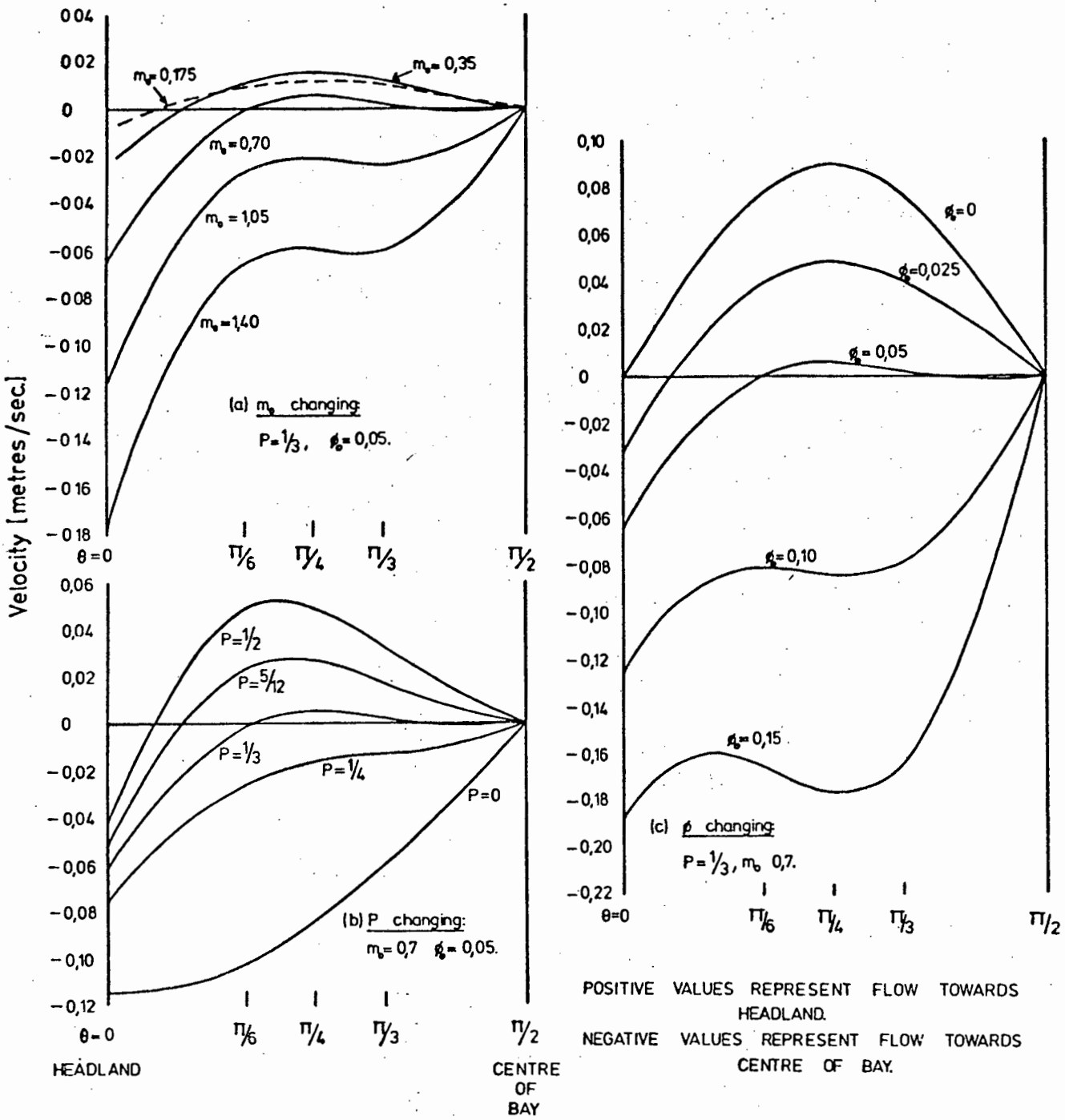

Fig. 5.13 Predicted longshore currents along a headland showing the effect of the variables m_b, P and ϕ_b.

As the circulation is symmetric about $\theta = \frac{\pi}{2}$, a flow towards the centre of the bay (curve negative) at a point near $\theta = \frac{\pi}{2}$ will result in a central rip current developing. Conversely, if the flow is away from the centre of the bay (curve positive) close to $\theta = \frac{\pi}{2}$ then a central inflow will occur and a rip current may develop elsewhere. A rip current will occur where the curve of the predicted longshore current changes from negative to positive values with increasing angle θ, as a convergence of flow will occur at such a point. The assumption that has been made here is that the longshore current evaluated at the mid-surf position is representative of the entire surf width. This may not always be valid (Komar, 1975).

It may be seen on figure 5.13 that on some curves the entire flow is negative (away from the headlands) and for other curves, regions occur where the flow is negative near $\theta = 0$ and positive at greater angles. The cases that lead to entirely negative flow are characterised by m_o large, (i.e. high waves), ϕ_o large, (i.e. a large angle of incidence) and p small, (i.e. small wave height gradient). The last two of these cases are self-explanatory but the first is not. It, as a consequence of the $3/2$ power dependence of water depth occurring in the oblique incidence term with only a unitary power in the wave height gradient term of equation 5.29.

The longshore current distribution may alter from flow towards the centre of the bay to a flow towards the headland if one of three changes occur; one, a decrease of the angle of incidence of the waves; two, a decrease of the water depth or three, an increase of the wave height gradient. The position at which the rip occurs does not appear to migrate slowly from the centre of the bay, $\theta = \frac{\pi}{2}$, towards the headlands, $\theta = 0$, as any of these factors are altered. Instead, with only a small change of parameters m_o, p and ϕ_o the position of the rip affects a rapid change from $\theta = \frac{\pi}{2}$ to approximately $\theta = \frac{\pi}{6}$, after which gradual changes occur

as the rip current migrates towards the headland. Sufficient change in any of the three variables may therefore change the circulation type observed.

All three parameters, m_o, ρ and ϕ_o, will be affected by refraction. m_o has the additional degree of freedom afforded by the wave height variations that may exist. As a wave approaches a shoreline at an oblique angle it is refracted with the result that the angle of incidence decreases (ϕ_o decreases), and the wave orthogonals diverge (ρ increases). Consequently, the effect of changing the wave height will be to produce effects on m_o, ρ and ϕ_o that will be reinforcing. As a result, increasing or decreasing wave height may be all that is required to effect a change in the circulation types observed.

Review: The circulation predicted using equation 5.29 is in agreement with that observed in the northern regions of Matroos Bay. High waves will lead to a central rip current and low waves, a rip current from the side of the headland.

5.3.6. Edge wave influences

It was observed, although seldom confirmed by float tracking that, even when one rip was dominating the flow, a relic of the other rip was usually visible. Three rip currents were usually observed near the shore. The strong central rip that dominated the clockwise circulation resulted from the combination of two rips moving diagonally offshore to meet in the centre of the bay, just outside the surf zone. When the northern rip was dominating the flow in the bay these rips were weaker and remained distinct.

With the uniform beach bounded by headlands and exposed to the open ocean an ideal situation exists for establishing a system of standing edge waves. Bowen (1972) gives the

resonant period, T, for a standing edge wave between two headlands a distance, b , apart as

$$T^2 = \frac{4\pi}{g} \frac{b}{m \sin(2n+1)s} \qquad 5.30$$

where s is the beach slope, m and n the longshore and offshore modal numbers, respectively.

Due to the range of periods observed, 5 to 10 seconds, the Iribarren Number, ζ, for Matroos Bay will lie in the range $0.13 \leq \zeta \leq .25$. In this range, edge waves are predicted to respond to a forcing mechanism with a range of the order of several minutes (Sasaki and Horikawa, 1975). Amplitude modulation observed on the wave records of the 21st to 25th July, 1975 had a period of approximately 125 seconds. The determination of such a period from the 10 minute, six-hourly records was, however, a subjective procedure, and the range of values obtained was quite large.

Table 5.9 gives the resonant periods for standing edge of modes (m, n) less than 5. It is seen that a forcing mechanism with a period of approximately 125 seconds (± 10%) could lead to resonance at modal numbers (m,n) equal to (1,2), (1,3), (2,1) and (5,0). The corresponding rip current spacing would be 1500, 1500, 750 and 300 metres.

Guza and Inman (1975) have shown that for a beach of slope s, for a distance, $x < x_o$, and of constant depth, h_o for distances $x > x_o$, there exists a minimum width of the beach below which waves of offshore mode, n, cannot be trapped. If the nondimensional beach width, χ, suggested by Bowen and Inman (1969) is defined

$$\chi = (2\pi)^2 x / T^2 g s \qquad 5.31$$

then the minimum beach width, χ_{min}, may be calculated. For mode n = 1, the minimum beach width is $\chi_{min} = 6.5$,

TABLE 5.9 : Standing edge wave resonant periods for m, n less than 5, for a bay of length 1500 metres

		Longshore modal number, m				
		1	2	3	4	5
Offshore modal number, n	0	307.0	217.1	177.3	153.5	137.3
	1	177.3	125.4	102.4	88.7	79.3
	2	137.4	97.2	79.3	68.7	61.5
	3	116.2	82.2	67.1	58.1	51.2
	4	102.6	72.6	59.2	51.3	45.9
	5	92.9	65.7	53.7	46.5	41.6
Wavelength, L (metres)		3000	1500	1000	750	600

Units : seconds.

for mode n = 2 is χ_{min} = 21.0, and for mode n = 3 is χ_{min} = 43.5. There is no minimum beach width for mode n = 0. Guza and Inman (1975) show that the minimum width corresponds closely to the postion of the last offshore maxima of the edge wave of the mode considered. It is suggested here, that, for a beach bounded by headlands there may be a minimum headland length below which edge waves of mode n cannot be trapped. No theoretical justification for this suggestion is offered, however, it seems reasonable that the reflection of the waves from the headland will only be satisfactory if the full offshore distance of the edge wave, as defined by the last offshore maxima, is reflected. Thus, the mimimum beach width defined for the slope truncation and that for the headland length may be expected to be similar.

If this is so, the modal numbers that may be supported are (5,0) and possibly (2,1). The modal number combination (5,0) would be expected to result in 6 rip currents being produced. This was not observed. The combination (2,1) would result in 3 rip currents, one at each end of the bay and one in the middle. This modal combination would not result in the two rip currents observed near the centre of the bay.

Four possible longshore modal numbers, m, were found to have periods that may respond to a forcing mechanism having a period of about 125 seconds. Of these, only standing edge waves with a modal number, m, equal to 2, would predict a central rip current. Not one of the modes would predict only two rip currents near the centre of the bay. All would predict rip currents along the headlands.

The response described in which the edge waves have the same period as the forcing mechanism is a sychronous response. It is possible, however, that a response that is subharmonic

to the period of the forcing mechanism may occur. A sub-harmonic response would have a period of the order of 250 seconds. No possible standing edge waves have a period of this length. The response times closest are 217 seconds and 307 seconds, and correspond to modal numbers (1,0) and (2,0) respectively. Again, neither would result in the observed rip current spacing.

The possible modes of the trapped edge waves that may exist within Matroos Bay have been considered. None of the possible modes explains the observed distribution of rip currents. In particular, no explanation for the joining of the two rip currents occuring near the centre of the bay was provided.

The position of the rip currents may be explained by the balance of the forces acting along the headlands (see Section 5.3.5.). The joining of the two rip currents near the centre of the bay may simply be due to the physical dimensions of the bay preventing the coexistence of two strong rip currents, separated by only a small distance.

The presence of remnants of the rip currents may be a topographically induced flow resulting from scouring of the bed on previous occasions (for example, see Appendix D), or may be due to an incomplete balance of the forcing terms.

5.3.7. Relationships between the temperature - salinity distribution and the circulation

Having considered the circulation characteristics of Matroos Bay region, the interrelationship between the temperature and salinity distribution and the circulation patterns will be considered. As the distribution of these properties is determined by the physical processes acting, it should be possible to explain the property distribution after a consideration of these processes.

It was, in general, not possible to deduce the temperature or salinity distribution knowing the circulation patterns, nor was it possible to determine the circulation patterns from the temperature and salinity distributions.

Three case histories in which the temperature and salinity distributions assisted the interpretation of the float paths are presented as Appendices B, C and D. Appendix B deals with the observations made on the 14th April, 1976, and illustrates good agreement of the temperature and salinity distribution with an anticlockwise circulation. Appendix C presents the observations of 18th April, 1976 when clockwise circulation was observed. Appendix D illustrates an example of a small scale oceanic front and shows how the circulation, temperature and salinity characteristics differed on either side of the front.

Consideration of the data available led to the following tentative conclusions. In general, the temperature distribution may be more readily explained by the current movements than may the salinity distribution. The clockwise circulation type showed better agreement between currents and surface temperature distributions than did the anticlockwise circulation type. The section taken across the mouth of the bay generally showed a region of uniform temperature at the position of the dominant rip current. This was interpreted as being the result of the mixing in the surf zone.

In trying to determine whether a relationship existed between the currents and the temperature and salinity distributions several interpretations may arise or agreement may be found in some regions but not others. For this reason, interpretation should rely on the analysis of each case on its merits rather than trying to generalize.

5.3.8. Residence times and frequency of occurence of the circulation types

The residence time of a substance in a particular environment is of interest to those concerned with the dispersal and diffusion of some property from that environment. With the development of the industrial township of Atlantis, it may not be long before Matroos Bay comes under consideration for waste disposal purposes. Hence, a few comments on this topic are warranted.

The residence time, τ , for a reservoir may be defined as the average lifetime of a molecule within the reservoir. It may be shown that the residence time is equal to the number of molecules in the reservoir, N, divided by the flux into the reservoir, $^{dN}/_{dt}$, (Craig, 1957)

$$\tau = {}^{N}/_{\frac{dN}{dt}} \qquad 5.32$$

To arrive at this expression, instantaneous complete mixing of the influx molecules is assumed. This is a situation that may not be approximated in a real situation. The effect of incomplete mixing and of recirculation of outflow will be to increase the effective residence time of water in the reservoir. The residence time calculated by exchange, equation 5.32, is thus, in fact, a lower limit of the time that water may remain in a particular reservoir.

The residence times, computed by exchange, for Matroos Bay are listed in table 5.10. For this calculation the line between the headlands, B-C of figure 4.2, was taken as the boundary of the bay. Typically, the residence time for the bay was between 0.8 and 1.7 x 10^4 seconds (2.5 to 4.5 hours). 75% of the residence times fell within this range.

The clockwise circulations had a mean residence time of 1.27 x 10^4 seconds (3.5 hours) with a standard deviation of .33 x 10^4 seconds. This relatively short residence time

TABLE 5.10 : Residence times in Matroos Bay calculated by exchange

DATE	CIRCULATION TYPE	RESIDENCE TIMES x 10^4 sec	(approx. hours)
30-01-76	A	.83	(2.5)
31-01-76	U	3.6	(10)
01-02-76	U	2.6	(7)
16-02-76	C	.78	(2)
19-02-76	C	1.3	(3.5)
12-04-76	C	.71	(2)
14-04-76	A	1.5	(4)
15-04-76	A	1.1	(3)
17-04-76	A	1.6	(4)
19-04-76	C	1.4	(4)
22-05-76	A	1.0	(3)
23-05-76	A	1.1	(3)
25-05-76	U	1.5	(4)
10-07-76	C	1.3	(3.5)
16-07-76	C	1.2	(3.5)
18-07-76	C	1.7	(4.5)
02-09-76	C	1.4	(4)
03-09-76	A	5.6	(16)
04-09-76	A	1.5	(4)
07-09-76	C	1.6	(4.5)
Means	Total	1.7	(4.5)
	C Only	1.3	(3.5)
	A Only	1.8	(5)
	U Only	2.6	(7)

Legend:
- A = Anticlockwise circulation
- C = Clockwise circulation
- U = Undefined, neither anticlockwise or clockwise circulation types dominant.

may be attributed to the strong central rip current that, at times, flowed well beyond the line between the headlands and almost perpendicularly to it.

The mean residence time for the anticlockwise circulation types was 1.78^{4} x 10 seconds (5 hours) with a standard deviation of 1.57×10^{4} seconds. The variability of the residence time for this circulation type results from the variable angle at which the rip current from the northern end crosses between the headlands. Very often recirculation was prominent during periods of anticlockwise circulation, suggesting that the effective residence time could be considerably greater than that calculated. For example, a float deployed at 0853 hours on the 14th April 1976 was still circulating in the northern gyre of the bay at 1407 hours on the 15th April. This represents an effective residence time of 29 hours. The residence time calculated by exchange for these days was 4 and 3 hours respectively. Recirculation may thus increase the residence time by an order of magnitude.

Days on which the circulation characteristics were poorly defined tended to have long residence times, mean 2.57×10^{4} seconds (7 hours), with a standard deviation of 1.05×10^{4} seconds.

The times least favourable for waste disposal are therefore likely to occur during anticlockwise or undefined circulations, that is, during periods of low wave height. Shillington (1976) has computed the exceedence curves for wave heights at Melkbosstrand. Based on his observed relationship, $H = 1.2\ H_{mo}$, the percentage of waves exceeding $H_{mo} = 1.25$ metres may be evaluated as 70% (figure 5.14). Conditions unfavourable for waste disposal may be expected on only 30% of occasions. More relevant perhaps, is the persistence of such events. Figure 5.15 shows the

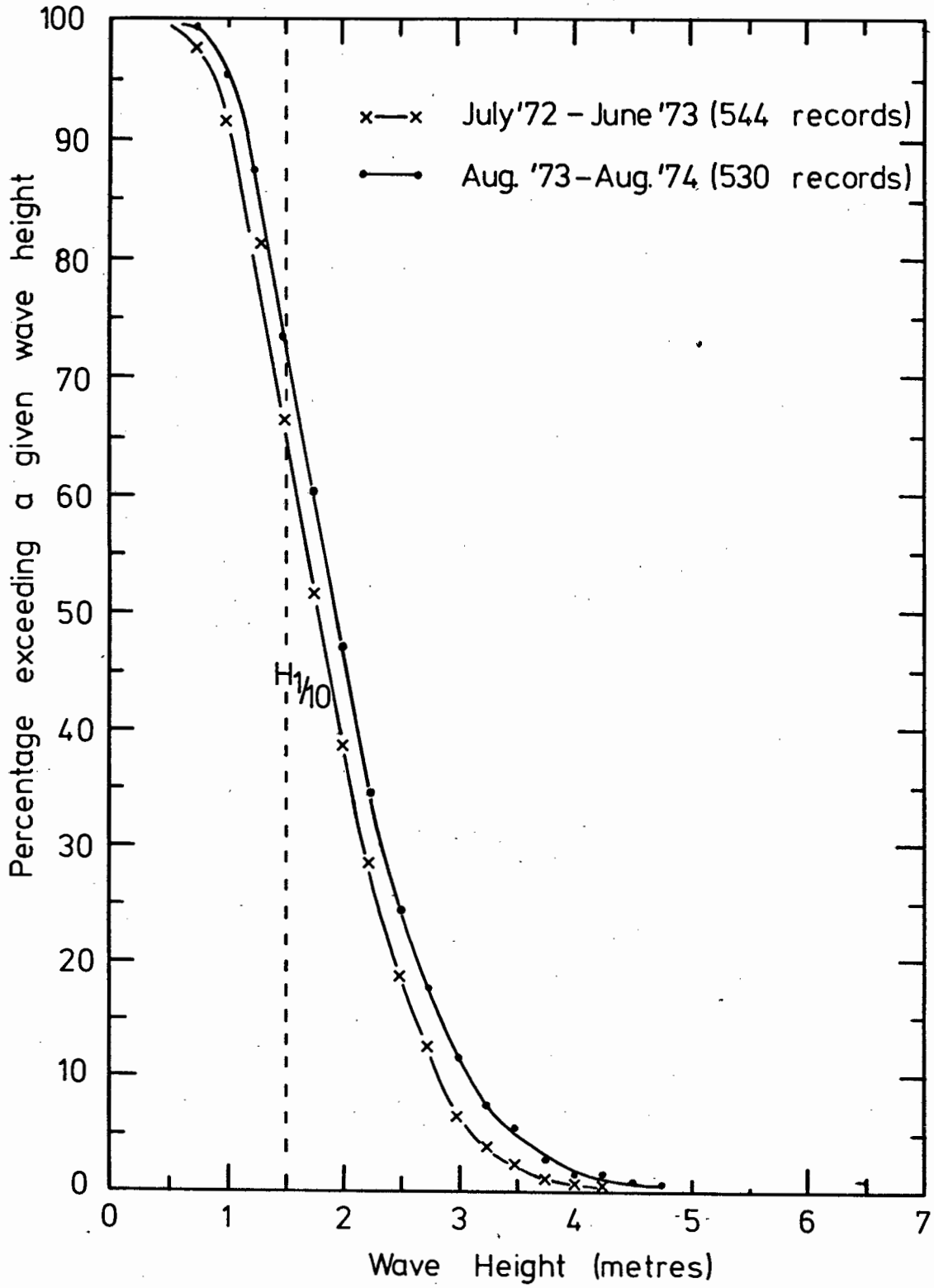

Fig. 5.14 Exceedence curves of wave height (after Shillington, 1976).

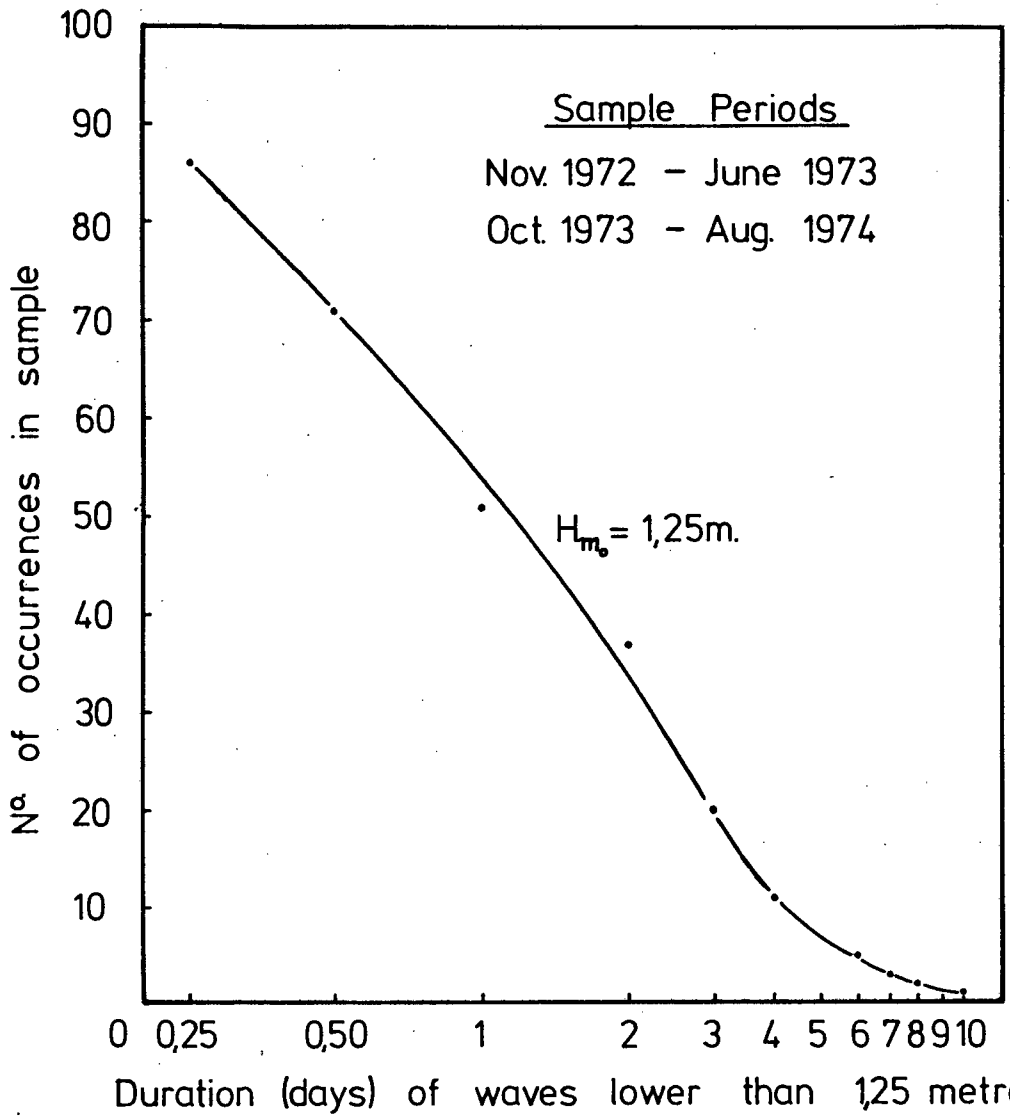

Fig. 5.15 Persistence of waves with $H_{m_o} \leq 1{,}25$ metres at Duynefontein.

persistence of waves with a height of less than 1.25 metres during a 19 month period. During the sample period, low wave conditions lasting for four days were experienced eleven times.

6. CONCLUSIONS AND RECOMMENDATIONS FOR FURTHER RESEARCH

Float tracking in Matroos Bay revealed two distinct circulation types. These were denoted "anticlockwise" and "clockwise". Circulation of the anticlockwise type was characterised by a longshore current flowing from the back of the bay towards the northern headland, where a prominent rip current was located. Circulation of the clockwise type was characterised by a longshore current flowing from the headland towards the back of the bay where a strong rip current was located. The data indicates that the circulation type observed depended both on the wave height and the wave period. Due to the small variation of the periods observed, the effect of wave period was, however, not well defined. Further measurements are required to clarify the effect of the wave period on the circulation type. The effect of wave height changes was more noticeable. Most anticlockwise circulation types were observed when the characteristic wave height, H_{mo}, was less than 1.25 metres. Most clockwise circulation types were observed when the wave height was greater than 1.25 metres.

Wave driven longshore currents are generally generated by either an oblique incidence of waves on a coastline or a longshore gradient of wave height. In a semi-circular bay the oblique incidence of the waves forces a longshore current to flow towards the centre of the bay. The wave height gradient forces a longshore current to flow away from the centre of the bay. The relative strength of these two forcing mechanisms at any position in the surf zone of the bay determines the direction of the longshore current flow, and thus, also determines the position of the rip currents. It was shown theoretically that the balance of these forces may be altered by a variation of the incoming wave height. In agreement with the field observations the rip current was predicted near the

headland during low incident wave heights whilst a central rip current was predicted during high waves.

The theoretical model used for this study was based on a linearization of the steady-state momentum equations. A solution was obtained for a semi-circular bay by assuming a simplified distribution of the wave height and angle of incidence around the bay and evaluating the longshore current at the mid-surf position. The forcing terms of the equation were balanced by the bottom friction. Much scope exists for the development of the theoretical models of the circulation in the bay. Numerical solutions of the refraction problem could be used to verify the applicability of the simplified wave height and angle of incidence terms and to evaluate the range of variables m_o, p and ϕ_o that may be experienced. Horizontal diffusion may be included in the equations of motion to obtain a more realistic distribution of the longshore currents across the surf zone.

The coastal current direction within one kilometre of the mouth of Matroos Bay was often sympathetic to the wind direction, particularly if the winds were moderate to strong. With the dominance of southerly winds in this region, north-flowing coastal currents were often observed. Little evidence was found of a south-flowing surface counter-current that had been mentioned in the literature. Such a current may, however, exist further offshore than the limit of the investigations of this study, approximately one kilometre from the shore.

A reasonable correlation was found between the circulation type and both the wind and the coastal current direction. The correlation of the wind with the nearshore circulation may result from the dependence of both the wind and the wave height on the atmospheric pressure distribution over the

South Atlantic Ocean. The correlation with the coastal current arises from the observed dependence of the coastal current direction, in the vicinity of Matroos Bay, on the wind direction.

A strong upwelling centre is located off Melkbosstrand, 15 kilometres to the south of Matroos Bay. The change in direction of the coastline that occurs at this point is responsible for the positioning of this upwelling centre. A similar change in direction of the coastline occurs at Matroos Bay but does not lead to the presence of a strong upwelling centre. Some evidence of upwelling was, however, found. The reason for the difference in the intensity of the upwelling occuring in the two regions may be a result of the small size of and strong wave driven circulation in Matroos Bay limiting the effect of the wind.

The response to the wind of the temperature and salinity of the water occurs primarily on a seasonal time scale. A weaker response was noted on a weekly time scale and poor response on a daily time scale. During summer, strong upwell-inducing south-easterly winds blow. The water temperature and salinity in this season were lower than during winter. The system responded rapidly to the first strong south-easterly winds of the summer. Heating of upwelled water in summer was greater than during winter. Dilution of the water, due to winter rainfal and runoff, was found to be negligible.

The range of surface temperature generally observed was sufficiently large that differences could be easily measured with a portable instrument. The salinity range was generally small. Density changes were usually the result of temperature variations rather than salinity variations. The density of the water lay between the σ_t values of 25 and 27.

On occasions, the distribution of the surface temperature contours was in response to the circulation, but on other

occasions no relationship was detected. It was not possible to predict the temperature distribution from the current patterns. A full understanding of the temperature and salinity relationships must be based on an understanding of the overall system, the Southern Benguela Upwelling System, of which Matroos Bay forms only a small part.

The influence of the coastal circulation on the nearshore circulation of the bay was not great, because of the strong wave induced currents generated in the bay. Only when the wave induced currents are weak are coastal currents likely to affect the circulation within the bay.

The strong outflowing rip currents found under high wave conditions, result in an active exchange of water from within the bay with the coastal currents. Under low wave conditions the exchange of water between the nearshore circulation of the bay and the coastal circulation is more restricted. The exchange of water between the embayment and coastal environments may thus be assisted by the wave induced circulation. The importance of upwelling in this region and the number of embayments that occur, points to the need for further investigations into the interrelationships between the nearshore circulation of these bays and the coastal circulation.

REFERENCES

ANDREWS, W.R.H. and D.L. CRAM, 1966. Combined aerial and ship board upwelling survey in the Benguela Current. Nature, 244, pp. 902-904.

ARTHUR, R.S., 1962. A note on the dynamics of rip currents. J. Geophys. Res., 67 (2), pp. 2777-2779.

BANG, N.D., 1972. Characteristics of an intense ocean frontal system in the upwell regime west of Cape Town. Tellus, 25 (3), pp. 256-265.

BANG, N.D., 1973. The southern Benguela system: finer oceanic structure and atmospheric determinants. Ph.D. Thesis, University of Cape Town.

BANG, N.D., 1976. On estimating the oceanic mass flux budget of lateral and cross circulations of the Southern Benguela upwelling system. 1st Interdisciplinary Conference on Marine and Freshwater Research in Southern Africa, S 122.

BATTJES, J.A., 1974. Surf similarity. Proc. 14th Conf. Coastal Eng., pp. 466-480.

BOWEN, A.J., 1967. Rip currents. Ph.D. Thesis, University of California, San Diego.

BOWEN, A.J., 1969a. The generation of longshore currents on a plane beach. J. Mar. Res. 27 (2), pp. 206-215.

BOWEN, A.J., 1969b. Rip currents 1: Theoretical investigations. J. Geophys. Res. 74 (23), pp. 5467-5479.

BOWEN, A.J., 1972. Edge waves and the littoral environment. Proc. 13th Conf. Coastal Eng., pp. 1313-1320.

BOWEN, A.J. and D.L. INMAN, 1969. Rip currents 2: Laboratory and field observations. J. Geophys. Res., 74 (23), pp. 5479-5490.

BREBNER, A. and J.W. KAMPHUIS, 1963. Model tests on relationship between deep water wave characteristics and longshore currents. Queens University, Civil Eng. Res. Rep. 31, pp. 1-25.

BRUUN, P., 1963. Longshore currents and longshore troughs. J. Geophys. Res., 68 (4), pp. 1065-1078.

CLOS-ARCEDUC, A., 1962. Effects de la reflexion sur un obstacle d'une houle de longeur d'onde. Photo Interpretation, Paris, No. 1-10.

CRAIG, H., 1957. The natural distribution of radiocarbon and the exchange time of carbon dioxide between atmosphere and sea. Tellus, 9 (1), pp. 1-17.

CSIR., 1976a. Field data analysis for the proposed ESCOM nuclear power station. CSIR Coastal Engineering and Hydraulics Division Report C/SEA, 7608.

CSIR., 1976b. Oceanographic investigation for waste disposal of Greater Saldanha. CSIR Report C/SEA, 7611.

DALRYMPLE, R.A., 1975. A mechanism for rip current generation on an open coast. J. Geophys. Res., 80 (24), pp. 3485-3487.

DEACON, E.L. and E.K. WEBB, 1962. Small scale interactions, in The Sea, V1, ed. Hill. Interscience, N.Y., pp. 43-87.

DOODSON, A.T., 1958. Oceanic tides. Advances in Geophysics. Vol. 5, Academic Press, N.Y., pp. 118-153.

DRAPER, L., 1966. The analysis and presentation of wave data - a plea for uniformity. Proc. 10th Conf. on Coastal Eng.

DUNCAN, C.P., 1967. Current measurements off the Cape Coast. S. Af. Div. Sea Fish., Bulletin No. 4.

DUNCAN, C.P. and J.H. NELL, 1969. Surface current off the Cape Coast. S. Af. Div. Sea Fish. Investigational Rep. No. 76.

EAGLESON, P.S., 1965. Theoretical study of longshore currents on a plane beach. Hydrodyn. Lab. Dept. Civil Eng. MIT. Rep. No. 82.

EKMAN, V.W., 1905. On the influence of the earth's rotation on ocean currents. Arkiv för Matematik, Astronomi och Fysik, 2 (11).

FUGLISTER, F.C., 1960. Atlantic Ocean Atlas of temperature and salinity profiles and data from the IGY of 1957 - 1958. Vol. 1. Woods Hole Oceanographic Institution, Woods Hole, Massachusetts.

GALVIN, C.J. Jr., 1967. Longshore current velocity: A review of theory and data. Rev. of Geophys., 5 (3), pp. 287-304.

GALVIN, C.J. Jr. and P.S. EAGLESON, 1965. Experimental study of longshore currents on a plane beach. Tech. Memo 10. U.S. Army Coastal Eng. Res. Centre.

GALVIN, C.J. Jr. and R.P. SAVAGE, 1966. Longshore currents at Nags Head, North Carolina. U.S. Army Coastal Eng. Res. Centre, Bulletin 2.

GOURLAY, M.R., 1974. Wave setup and wave generated currents in the lee of a breakwater or headland. Proc. 14th Conf. Coastal Eng., pp. 1976-1995.

GRIMSON, P., 1970. Mechanics and thermodynamics of fluids. McGraw - Hill, London.

GUZA, R.T. and D.L. INMAN, 1975. Edge waves and beach cusps. J. Geophys. Res., 80 (21), pp. 2997-3012.

HARRIS, T.F.W., 1964. The nearshore circulation of water. Symposium on Coastal Eng., Stellenbosch.

HARRIS, T.F.W. and C.A.R. BAIN, 1976. Coastal water movement study. Progress Report No. 2, Oceanography Department, University of Cape Town, p. 80.

HARRISON, W., E.W. RAYFIELD, J.D. BOON III, G. REYNOLDS, J.B. GRANT and D. TYLER, 1968. A time series from the beach environment. Land and Sea Interaction Lab., ESSA. Res. Lab., Tech. Memo 1., p. 28.

HART, T.J. and R.I. CURRIE, 1960. The Benguela Current. Discovery Reports, 31, C.U.P., pp. 123-298.

HINO, M., 1972. Theory on formation of shore current system and systematic deformation of coastal topography. Dept. Civil Eng. Tokyo Inst. Tech. Rep. No. 13, pp. 99-113.

HINO, M., 1973. Hydrodynamic instability theory on the formation of system of shore current and coastal topography, part II. Solution by Galerkin's procedure based on Hermitian polynomial expansion. Dept. Civil Eng. Tokyo Inst. Tech. 14, pp. 27-41.

HINO, M., 1974. Theory on formation of rip current and cuspidal coast. Coastal Eng. Jap., 17, pp. 23-37.

INMAN, D.L. and R.A. BAGNOLD, 1963. Littoral processes. In The Sea, Vol. 3, Wiley, N.Y., pp. 529-533.

INMAN, D.L. and W.H. QUINN, 1952. Currents in the surf zone. Proc. 2nd Conf. Coastal Eng., pp. 24-36.

JAMES, I.D., 1974a. Non-linear waves in the nearshore region: shoaling and setup. Estuarine and Coastal Marine Science, 2, pp. 207-234.

JAMES, I.D., 1974b. A non-linear theory of longshore currents. Estuarine and Coastal Marine Science, 2, pp. 235-249.

KIRWAN, A.D. Jr., G. McNALLY, M.S. CHANG and R. MOLINARI, 1975. The effect of wind and surface currents on drifters. J. Phys. Oc. 5, pp. 361-368.

KOMAR, P.D., 1971. Nearshore cell circulation and the formation of giant cusps. Bull. Geol. Soc. Am., 82, pp. 2643-2650.

KOMAR, P.D., 1975. Nearshore currents; Generation by obliquely incident waves and longshore variations in breaker height. Nearshore sediment dynamics and sedimentation, Hails, J. and A. Carr (eds). J. Wiley and Sons, pp. 19-45.

KOMAR, P.D. and D.L. INMAN, 1970. Longshore sand transport on beaches. J. Geophys. Res., 75, pp. 5914-5927.

KRAUSS, W., 1973. Methods and results of theoretical oceanography 1: Dynamics of the homogeneous and quasihomogeneous ocean. Gebrüder Borntraeger, Berlin.

Le BLOND, P.H., 1972. On the formation of spiral beaches. Proc. 13th Coastal Eng. Conf., pp. 1331-1345.

Le BLOND, P.H. and C.L. TANG, 1974. On energy coupling between waves and rip currents. J. Geophys. Res., 79 (6), pp. 811-816.

LONGUET-HIGGINS, M.S., 1970a. Longshore currents generated by obliquely incident sea waves, 1. J. Geophys. Res., 75 (33), pp. 6778-6789.

LONGUET-HIGGINS, M.S., 1970b. Longshore currents generated by obliquely incident sea waves, 2. J. Geophys. Res., 75 (33), pp. 6790-6801.

LONGUET-HIGGINS, M.S., 1972. Recent progress in the study of longshore currents in "Waves on Beaches", ed. Meyer. Ac. Press, pp. 203-248.

LONGUET-HIGGINS, M.S. and R.W. STEWART, 1960. Changes in the form of short gravity waves on long waves and tidal currents. J. Fluid Mech., 8, pp. 565-583.

LONGUET-HIGGINS, M.S. and R.W. STEWART, 1961. The changes in amplitude of short gravity waves on steady, non-uniform currents. J. Fluid Mech., 10, pp. 529-549.

LONGUET-HIGGINS, M.S. and R.W. STEWART, 1962. Radiation stress and mass transport in gravity waves, with application to surf beats. J. Fluid Mech., 13, pp. 481-504.

LONGUET-HIGGINS, M.S. and R.W. STEWART, 1963. A note on wave set-up. J. Marine Res., 21 (1), pp. 4-10.

LONGUET-HIGGINS, M.S. and R.W. STEWART, 1964. Radiation stresses in water waves; A physical discussion with applications. Dee Sea Res., 11, pp. 529-562.

MALLORY, J.K., 1970. Oceanographic investigations for the proposed ESCOM Nuclear Power Station, Duynefontein. Department of Oceanography, University of Cape Town. Progress Report No. 1, 1st January, 1969 - 31st January, 1970. Unpublished Report.

MALLORY, J.K., 1971. Progress Report No. 2, 1st February, 1970 - 31st May, 1971. Unpublished Report.

MALLORY, J.K., 1973. Progress Report No. 3, 1st June, 1971 - 30th November, 1973. Unpublished Report.

MALLORY, J.K., 1974a. Progress Report No. 4, 1st December, 1973 - 31st May, 1974. Unpublished Report.

MALLORY, J.K., 1974b. Progress Report No. 5, 1st June, 1974 - 31st August, 1974. Unpublished Report.

MALLORY, J.K., 1974c. Progress Report No. 6, 1st September, 1974 - 30th November, 1974. Unpublished Report.

MALLORY, J.K., 1975a. Progress Report No. 7, 1st December, 1974 - 28th February, 1975. Unpublished Report.

MALLORY, J.K., 1975b. Progress Report No. 8, 1st March, 1975 - 31st May, 1975. Unpublished Report.

MALLORY, J.K., 1975c. Progress Report No. 9, 1st June, 1975 - 31st August, 1975. Unpublished Report.

MALLORY, J.K., 1975d. Progress Report No. 10, 1st September, 1975 - 31st November, 1975. Unpublished Report.

MALLORY, J.K., 1976a. Progress Report No. 11, 1st December, 1975 - 29th February, 1976. Unpublished Report.

MALLORY, J.K., 1976b. Progress Report No. 12, 1st March, 1976 - 31st May, 1976. Unpublished Report.

MALLORY, J.K., 1976c. Progress Report No. 13, 1st June, 1976 - 31st August, 1976. Unpublished Report.

MALLORY, J.K., 1976d. Progress Report No. 14, 1st September, 1976 - 30th November, 1976. Unpublished Report.

MALLORY, J.K., 1977. Progress Report No. 15, 1st December, 1976 - 28th February, 1977. Unpublished Report.

MILLER, C.D. and A. BARCILON, 1976. The dynamics of the littoral zone. Rev. of Geophys. and Space Physics, 14 (1), pp. 81-91.

MURRAY, S.P., 1975. Trajectories and speeds of wind-driven currents near the coast. J. Phys. Oc. 5 (2), pp. 347-360.

NODA, E.K., 1972. Rip-currents. Proc. 13th Coastal Eng. Conf., pp. 653-668.

NODA, E.K., 1974. Wave-induced nearshore currents. J. Geophys. Res., 79 (27), pp. 4097-4106.

O'ROUKE, J.C. and P.H. Le BLOND, 1972. Longshore currents in a semi-circular bay. J. Geophys. Res., 77 (3), pp. 444-452.

PHYSICK, W.I., 1974. A numerical model and observations of the sea-breeze system over a gulf. Ph.D. Thesis, Flinders University of South Australia.

PUTNAM, J.A., W.H. MUNK and M.A. TRAYLOR, 1949. The prediction of longshore currents. Trans. A.G.U. 30, pp. 337-345.

RETIEF, G.de F. and A.P.M. VONK, 1974. A low-cost wave direction indicator. Proc. 14th Coastal Eng. Conf., pp. 212-224.

S.A.N., 1976. South African Tide Tables. Publication S.A.N. No. 2, Hydrographer, S. Af. Navy.

SASAKI, T. and K. HORIKAWA, 1975. Nearshore current system on a gently sloping bottom. Coastal Eng. Jap. 18, pp. 123-142.

SHANNON, L.V., 1966. Hydrology of the south and west coasts of South Africa. S. Af. Div. of Sea Fish., Inv. Rep. No. 58, pp. 1-52.

SHANNON, L.V., 1970. Oceanic circulation off South Africa. S. Af. Div. of Sea Fish., Fisheries Bulletin No. 6, pp. 27-33.

SHEPARD, F.P., K.O. EMERY and E.C. LA FOND, 1941. Rip currents: A process of Geological importance. J. Geol. 49 (4), pp. 337-369.

SHEPARD, F.P. and D.L. INMAN, 1950. Nearshore water circulation related to bottom topography and wave refraction. Trans. A.G.U., 31 (2), pp. 196-212.

SHEPARD, F.P. and D.L. INMAN, 1951. Nearshore circulation. Proc. 1st Conf. Coastal Eng., pp. 50-59.

SHILLINGTON, F.A., 1976. Surface waves near Cape Town: Measurement and statistics. 1st Interdisciplinary Conference on Marine and Freshwater Research in Southern Africa, S 122.

SHILLINGTON, F.A. and T.F.W. HARRIS, 1974. Surface waves near Cape Town, 11: Their associated atmospheric pressure distribution over the Southern Atlantic. Department of Oceanography, University of Cape Town. Unpublished Report.

SONU, C.J., 1972. Field observations of nearshore circulations and meandering currents. J. Geophys. Res., 77 (18), pp. 3232-3247.

SONU, C.J., J.M. McCLOY and D.S. McARTHUR, 1966. Longshore currents and nearshore topographics. Proc. 10th Conf. Coastal Eng., pp. 524-549.

STANDER, G.H., 1964. The Benguela Current off South West Africa. S.W.A. Marine Res. Lab. Investigational Rep. 12, pp. 1-43.

STANDER, G.H., 1967. The Benguela Current off South West Africa. S. Af. Div. Sea Fish., Fisheries Bulletin No. 4, pp. 1-7.

SUMMERS, L., 1975. Koeberg Nuclear Power Station - analysis of currents off Duynefontein coast. Unpublished Report of Sir William Halcrow and partners (pers. comm.).

TALJAARD, J.J., 1967. Development, distribution and movement of cyclones and anticyclones in the Southern Hemisphere during the I.G.Y. J. Appl. Meteor., 6, pp. 973-987.

TALJAARD, J.J., 1972. Synoptic meteorology of the Southern Hemisphere. In meteorology of the Southern Hemisphere, meteorological monographs, 13 (35), eds., van Loon, et.al. Am. Met. Soc.

TAM, C.K.W., 1973. Dynamics of rip currents. J. Geophys. Res., 78 (12), pp. 1937-1943.

van IEPEREN, M.P., 1971 Hydrology of Table Bay. Department of Oceanography, University of Cape Town. Unpublished Report. pp. 48 and Appendices.

APPENDIX A: CALIBRATION OF FLOAT/DROGUE SYSTEM

In order to determine the error induced into float tracking results by the wind acting on the float, calibration tests were performed in the wind/wave flume at the National Research Institute of Oceanology at Stellenbosch. The flume consists of an almost semi-circular wind tunnel of approximately 3 m. diameter and over 100 metres long. At the bottom of the tunnel is a water filled channel approximately 2 metres wide and one metre deep. This channel was only filled to a depth of 80 cm. with water, to prevent overlapping by the wind generated waves. Dampers built into the channel to reduce cross tank oscillation reduced the effective usable depth to only 50 cm. With this restriction a full sized drogue could not be used for calibration but only smaller drogues. The drag per unit area on these drogues was computed and results extended to the full size drogue.

The calibration technique employed was to determine the drag on the components of the float/drogue system separately and sum these to obtain the total drag. Steady state conditions were assumed. Floats were permitted to move for a few metres before timing commenced, thus, their acceleration was not recorded (Murray, 1975).

The following assumptions have been used in the analysis (i) the motion is steady, (ii) the water velocity is negligible with respect to the float velocity and the float velocity may be ignored with respect to the wind velocity, all are unidirectional, (iii) the "V^2" drag law applies and, (iv) the drag on the total system is equal to the sum of the drag on the components. Assumptions (i), (iii) and (iv) have been made by Kirwan et.al. (1975) in a theoretical analysis of float/drogue systems in situations where there was shear between wind and water velocities. By the assumptions made above, the balance of forces gives

$$\underline{F}_{FA} + \underline{F}_{WA} + \underline{F}_{TA} - \underline{F}_{TW} - \underline{F}_{WW} - \underline{F}_{DW} = 0 \qquad A1$$

where subscripts F, W, T, D refer to the components of the

system, flag, wire, tin and drogue respectively. A, W as secondary subscripts refer to the media of air and water. $\underline{F}$ is the vector of force acting on each component and by assumptions (i), (ii) and (iii) the force on the ith component of the system is

$$F_{im} = \tfrac{1}{2} \rho_{im} C_i A_i \underline{V}_i |\underline{V}_i| \qquad A2$$

where ρ_{im} is the density of the medium in which the ith component lies, C is the coefficient of drag, A the area of the article and V the velocity of the component relative to the medium, or by assumption (ii) simply the velocity of the component or medium.

To solve the equation A1, floats were made that consisted only of various parts of the whole system and hence the following simultaneous equations must be solved

Tin	$F_{TA} - F_{Tw} - F_{ww} = 0$	A3
Wire	$F_{wA} + F_{TA} - F_{Tw} - F_{ww} = 0$	A4
Flag	$F_{FA} + F_{wA} + F_{TA} - F_{Tw} - F_{ww} = 0$	A5
Drogue	$F_{FA} + F_{wA} + F_{TA} - F_{Tw} - F_{ww} - F_{Dw} = 0$	A6

The experimental results are illustrated in figure A1, where float velocities are plotted as a function of the wind velocities. The decreasing float velocities when drogues are attached is evident, whilst the increased velocities resulting from the flag is also quite marked. Differences in velocity were observed between flags made of loose cloth and flags of plastic or tightly bound cloth. The loose cloth flag flapped vigorously in the wind and this lead to an increased drag, consequently only flags prevented from flapping by dowelling attached above and below and connected to the wire support were used in field experiments. This analysis will deal only with these floats.

A decrease in the velocity of all the floats was observed between a wind speed of 4.0 and 4.8 $m.sec^{-1}$. Estimates of the Reynolds Number for the air and water flow typically

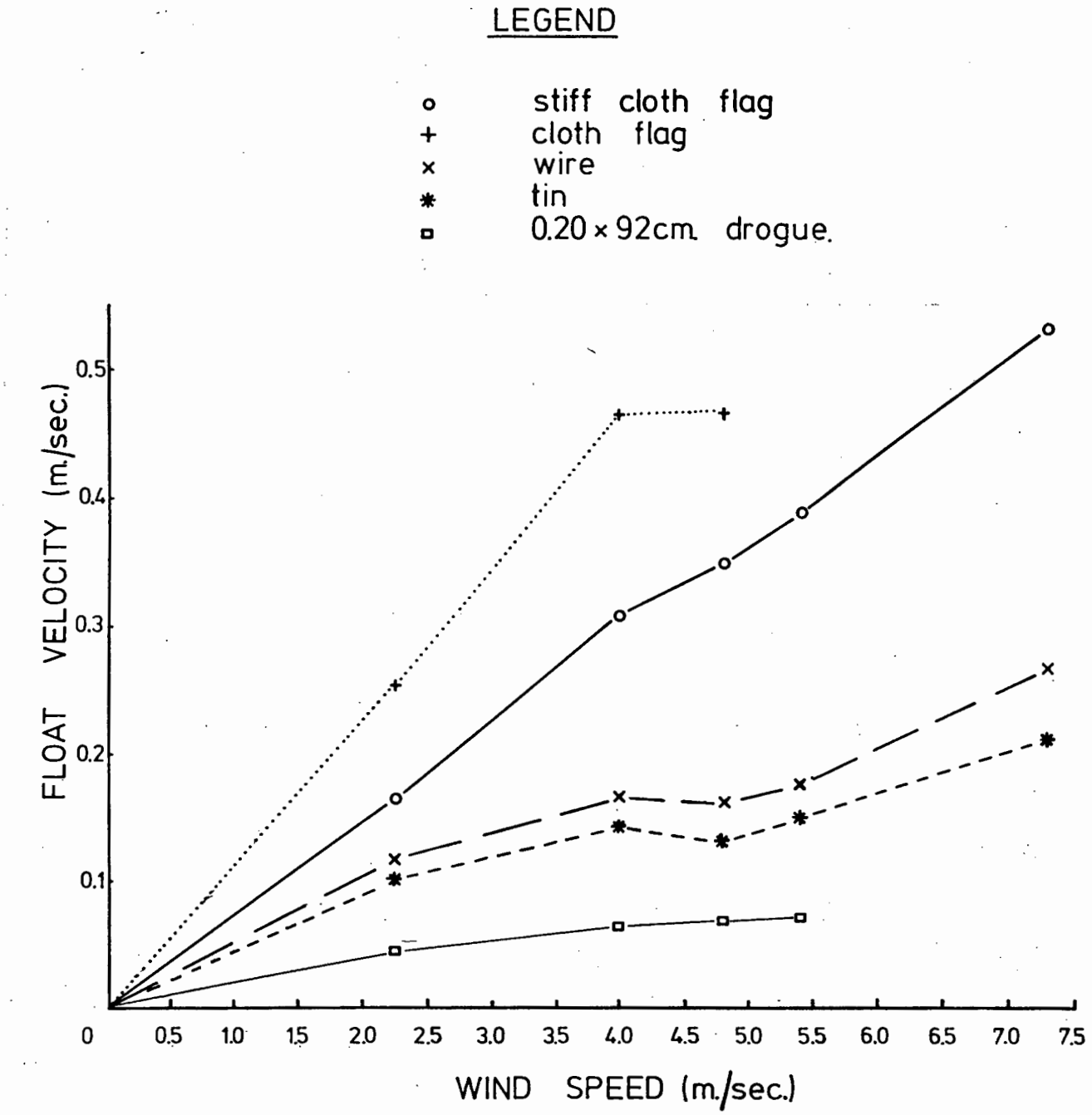

Fig. A.1 Relationship between float type and wind speed.

give results of the order 10^3 to 10^4, so it is unlikely that this represented a change from linear to turbulent drag, but, may represent a change in the wave drag (Grimson, 1970).

The wind velocities used represent the average of three measurements of wind run over 50 seconds. The anemometer was placed at the height of the flag of the float system, about .55 m. above the water surface. In determining the drag on the components of the float above the water, the velocity of the individual components was assumed to be equal.

Consider the first equation to be solved, equation A3, where the tin with lower wire support only was used. The coefficient of drag on a cyclinder is approximately 1.2 for Reynold's Number, Re, range $10^2 \leq Re \leq 10^5$. For the tin in air the Reynold's Number is approximately 5×10^4, for the tin in water 5×10^3, and for the wire in water 1.5×10^2, and so the range for which the drag coefficient is valid was not violated. Substitution of this value into equations A2 and A3 yields consistent results for the air: float velocity ratio for the five wind speeds used, especially for wind velocities greater than 4.8 $m.sec^{-1}$. Typically the ratio air velocity: float velocity was approximately 35 for wind velocities greater than 4.8 $m.sec^{-1}$, and 25 for lower velocities.

Similarly, substitution of the experimental results into equation A4, the case where the wire only exists, leads to an estimate of $C_{wA} A_{wA} \simeq 10^{-3}$. This contribution may be ignored compared to the drag on the tin.

Again substituting the results for the stiff flag into equation A5, yields $C_{fA} A_{fA} \simeq 317$. Substituting this result into the final equation, equation A6, leads to an estimate of $C_{Dw} A_{Dw}$ of 2×10^3. As the area of the drogue was $.2 \times .92$ m^2 the drag coefficient of the drogue, $C_{Dw} = 1.1$.

Consider now the ratio of the drag experienced on the parts in the water, with a full size drogue:

Tin	:	Wire	:	Drogue
60	:	10	:	10^4

thus, the drogue was clearly the most important component, and the drag on the tin may be neglected as a first approximation. This result suggests that, even if a velocity shear exists in the water, the float-drogue system will give a good indication of the velocity at the depth of the drogue. Due to the size restrictions imposed by the experimental conditions the string connecting the float with the drogue was eliminated and the drogue attached directly to the float. The inclusion of this string in the prototype will lead to some error but this was not believed to be significant when the length was kept to 4 m., as it was in deep drogues.

The drag experienced on the components exposed to the wind is in the ratio:

Flag	:	Tin
5	:	1

and thus the drag on the tin cannot be neglected with respect to the tin. For the system used a combined drag term $CA \simeq 380$ was appropriate.

For a 1 m. drogue system $V_f / V_a \simeq .6\%$, and so, in general, the wind velocity imparts a velocity of .6% onto the float. This wind velocity, however, was that observed .55 m. above the water surface.

Conversion of wind flume results to 10 metres: As a separate experiment, profiles of wind velocity were measured above the water surface for three wind speeds in the NRIO wind/wave flume. The results of this experiment were plotted with a logarithmic height scale and linear velocity scale, as illustrated by figure A2. Wind speeds recorded below 1.0 metre approximate the straight lines expected in atmospheric boundary layers. The results obtained above 1.0 metres do

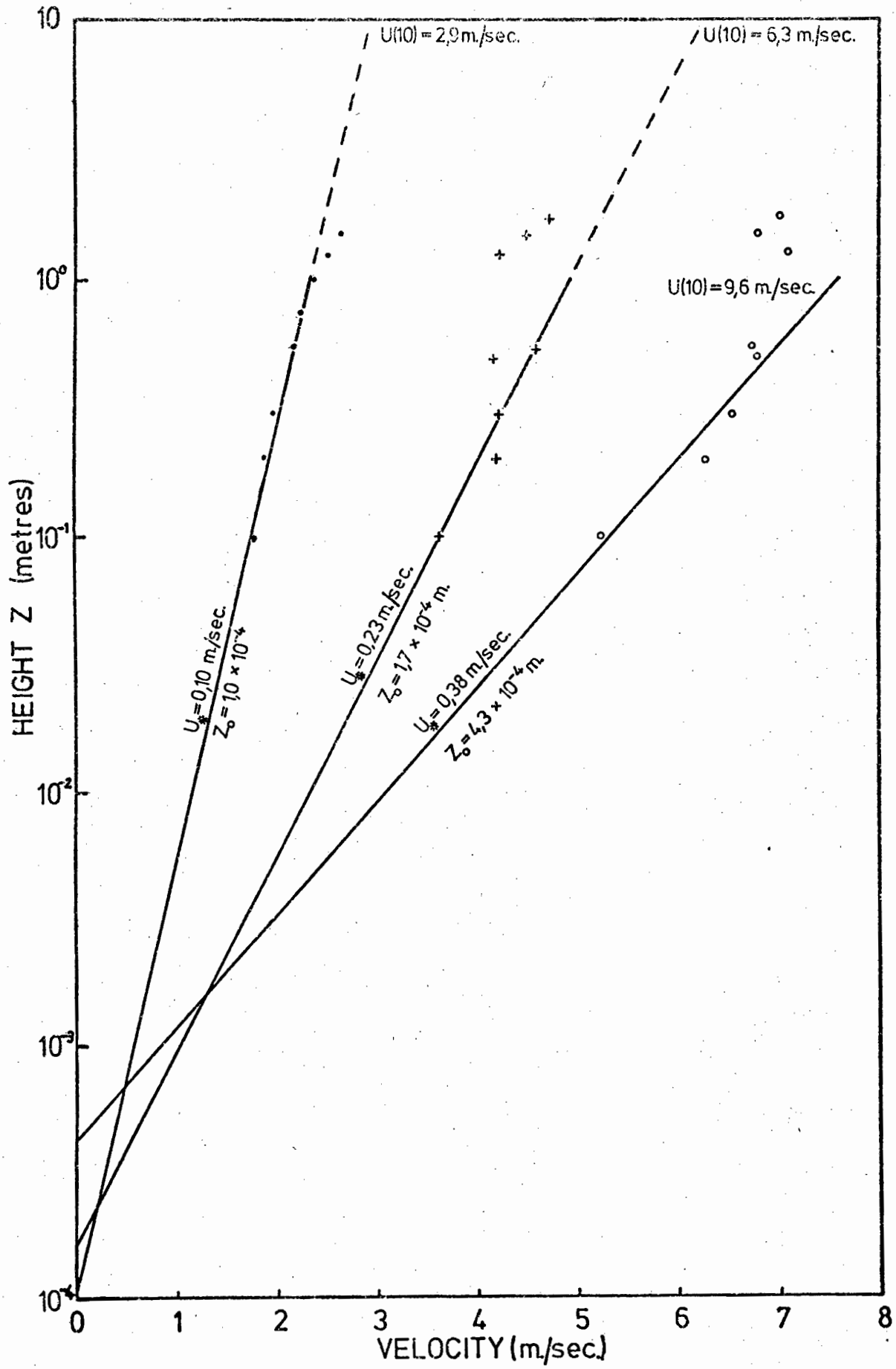

Fig. A.2 Logarithmic profiles observed in the wind – wave flume.

not fit this curve and it is suggested that the physical dimensions of the flume itself have inhibited the growth of the boundary layer above this height. As a result, these values have been ignored in the following analysis.

The roughness length, z_o, for each wind speed was determined and found to have a value of the order of 10^{-4} metres. This value increased slightly with increasing wind speed (table A1) and this may be interpreted as resulting from the higher waves generated by the higher wind speeds. The positioning of the anemometer near to the source of the wind would limit the size of the waves observed. The friction velocity, u_*, was computed from the slope of the best fit straight lines of figure A2. The friction velocity increased with increasing wind speed. This may be expected if the friction velocity is interpreted as the velocity of a typical turbulent velocity fluctuation.

Having computed both z_o and u_* the wind speed at a height of 10 metres, u_{10}, was calculated using the logarithmic profile equation (Deacon and Webb, 1964)

$$u(z) = \frac{u_*}{k} \ln \frac{z}{z_o} \qquad A7$$

where k is von Karman's constant and was taken equal to .4. Alternatively, u_{10} may be estimated directly from figure A2. Having performed this computation the ratio of the wind speeds at levels .55 metres and 10 metres above the sea-surface was estimated with results found to lie around 0.7. Another estimate may be made using equation A7 in the form

$$\frac{u_{.55}}{u_{10}} = \frac{\ln .55 - \ln z_o}{\ln 10 - \ln z_o} \qquad A8$$

where it may be seen from equation A8, that the roughness length will affect the final result whereas the friction velocity will not directly influence the result. (It will

TABLE A1 : Interface parameters computed for various wind speeds in the NRIO wind/wave flume

WIND SPEED		RATIO	ROUGHNESS LENGTH	FRICTION VELOCITY	RATIO
.55 metres	10 metres (calculated)				
$u_{.55}$ m.sec^{-1}	u_{10} m.sec^{-1}	$\frac{u_{.55}}{u_{10}}$	z_o metres	u_* m.sec^{-1}	$\frac{u_*}{u_{10}}$
2.2	2.9	.72	1.0×10^{-4}	.10	.034
4.6	6.3	.70	1.7×10^{-4}	.23	.037
6.8	9.6	.70	4.3×10^{-4}	.38	.040

of course, determine the slope of the curve and thus the position at which the curve intersects the height axis, z_o). Substituting the range of z_o values yields only a small range of $u_{.55}/u_{10}$

$$.70 \leq u_{.55}/u_{10} \leq .72 \qquad \text{A9}$$

Thus, the velocity at the height of the flag of the float/drogue system was approximately 70% of the 10 metre wind velocity. Thus the error induced in the calculation of the current velocity will amount to .7 x 6% = .4% of the wind speed at 10 metres.

Conclusions here may only really be taken to order of magnitude as, wind gusts, tilting of the float, shear and waves, may all impose errors. Hence, rather than routinely subtract wind error vectors from all data, the data was left untouched and care taken in the interpretation on days of high wind velocity.

APPENDIX B : MATROOS BAY OBSERVATIONS, 14th April, 1976

LOCATION :	Matroos Bay
DATE :	14th April, 1976
CHARACTERISTIC WAVE HEIGHT (H_{mo}) :	0200 hours 0.67 metres 0800 hours 0.62 metres 1400 hours 0.69 metres 2000 hours 0.70 metres
PEAK PERIOD (T_p) :	0200 hours 7.3 seconds 0800 hours 7.9 seconds 1400 hours 7.3 seconds 2000 hours 7.0 seconds
WAVE DIRECTION :	D.O.S.O. Record 0200 hours 228°
TIDES (TABLE BAY) :	HIGH: 0255 : 1.93 m. LOW: 0914 : 0.06 m. 1525 : 1.83 m. 2116 : 0.12 m.

WIND CONDITIONS : Light winds persisted during the 14th April. Winds were from the east during the first 6 hours of the day, after which variable winds or windless conditions persisted until 1800 hours when a south-east to easterly direction was dominant until 2300 hours. The average wind speed during the day did not exceed 4 $m.sec^{-1}$.

TIMES OF DATA COLLECTION :	FLOAT TRACKING: 0806-1600 hrs. (approx) TEMPERATURE/ SALINITY: A.M.0800-1000 hrs.(approx) P.M.1430-1600 hrs.(approx)
DATA QUALITY :	Good, reliable data.

DISCUSSION : The float paths show that the northern rip was the dominant feature of the circulation in Matroos Bay on the 14th April, 1976. Floats moved onshore in the centre of the bay, northwards around the coast to the rip current and out of the bay in this rip. They then moved offshore in the rip and described a clockwise gyre once offshore. The rip current in the northern end of the bay was the typical circulation feature experienced during periods of low wave height whilst the clockwise gyre may be due to a northerly flowing coastal current. The moored buoy system indicated northerly flowing currents. The highest speeds observed occurred where the longshore current met the northern rip. Here, speeds upto .71 $m.sec^{-1}$ were recorded. Speeds within the rip dropped slowly with distance from the

shore to .15 to .20 m.sec^{-1} where the floats commenced their gyre. Whilst turning inshore speeds were only around .10 m.sec^{-1} but higher again, about .15 m.sec^{-1}, when moving inshore.

In front of the more southerly of the two theodolite stations a weak rip current was observed. This rip was in the position of the central rips that were dominant on days when high waves are present. Although it did not penetrate far into the bay, velocities of upto .40 m.sec^{-1} were observed in this rip and the effect of the rip on the rapid northerly longshore movement is shown by the path of one float.

In the southern part of the bay a weak clockwise gyre was indicated, with velocities only about .05 m.sec^{-1}. The sheltering effect of the blinder may have been responsible for the weak circulation in this part of the bay.

Surface temperatures recorded in the morning of the 14th April show a large area of water with a temperature of less than 14.0°C in the bay and extending offshore in a south-westerly direction, along the path of the rip current. Warmer water, upto 15.0°C, lay to the north and to the south of this ridge. The temperature profiles showed that the offshore water was very stratified with temperatures dropping from near 14.0°C at the surface to 11.0°C at about 15 metres. Below this depth water was fairly uniform in temperature. At station 12 the water had a temperature of 13.2°C for the upper 10 metres and this is ascribed to the rip current transporting the well mixed and hence, isothermal water out of the bay. The depth of the rip current was about 10 metres; below this depth was a well developed thermocline leading to the cool, isothermal deep water. The profile across the mouth of the bay shows stratified water near the middle and southern regions and more uniform, less stratified water in the northern part of the bay. This indicates that water entering the bay near the centre was mixed as it moved towards the northern part of the bay.

The surface salinities also show a ridge of low salinity (≃34.72 ‰) extending south-west from the northern part of the bay. The offshore and southern water had a salinity around 34.725 ‰ and so the difference was not really significant. On the profile perpendicular to the coast a low salinity area occurred between the higher salinity surface and bottom waters and thus formed a wedge approximately 5 metres thick, centred at about 5 metres deep, suggesting that a verical transport was also occurring. Re-examination of the temperature section strengthens this opinion. The salinity section between the headlands shows water with a salinity range between the surface and bottom of .01 ‰ occurred near the southern end of the bay, whilst near the northern end the range was smaller. The value of about 34.72 ‰ occurring near the northern end of the bay does not however appear to be a product of simple mixing of water in the southern end, as this water had an average value nearer 34.73 ‰. A gradual change was probably occurring with inflow of more saline water from the south.

In the light of evidence for subsidence the float paths may be reinterpreted where they turn and flow north outside the bay. Having moved out in the rip, the floats found that the rip water subsided to a deeper layer, leaving the floats on the surface. Here they took up the northward motion of the coastal current and were entrained back into the rip current.

Consideration of the density supports the possibility that subsidence was occurring. The water at 15.0 metres depth had a density of 26.4 to 26.6. The offshore water was lighter having a density of about 25.8. The water entering the bay on the surface in the southern end of the bay had a density of 26.0 whilst at the bottom the density reached 26.5. Upon mixing, a water of about 13.0°C and a density of about 26.2 was produced and this density was that observed both on the surface in the rip and at 5 to 10 metres further offshore.

By the afternoon temperatures had increased throughout the region with lowest temperatures occurring within the southern part of the bay. The ridge of cold water protruding from the north was not so evident as in the morning, possibly due to a high temperature recorded at station 8, 17.0°C. This may only have been a parcel of entrained warmer, but as yet unmixed, water from the warm water to the north.

Thus, close agreement was observed between the float paths and the temperature and salinity data, the temperature and salinity data aiding the interpretation of vertical motion that could not be followed by float paths.

The low wave height was responsible for the northern rip and has already been mentioned. A description of the mechanics of the motion is found in Section 5. In general, wave heights were too low to be recorded by the D.O.S.O.. However, a short record was obtained at 0600 hours indicating that the swell was from the south-west to south-south-west.

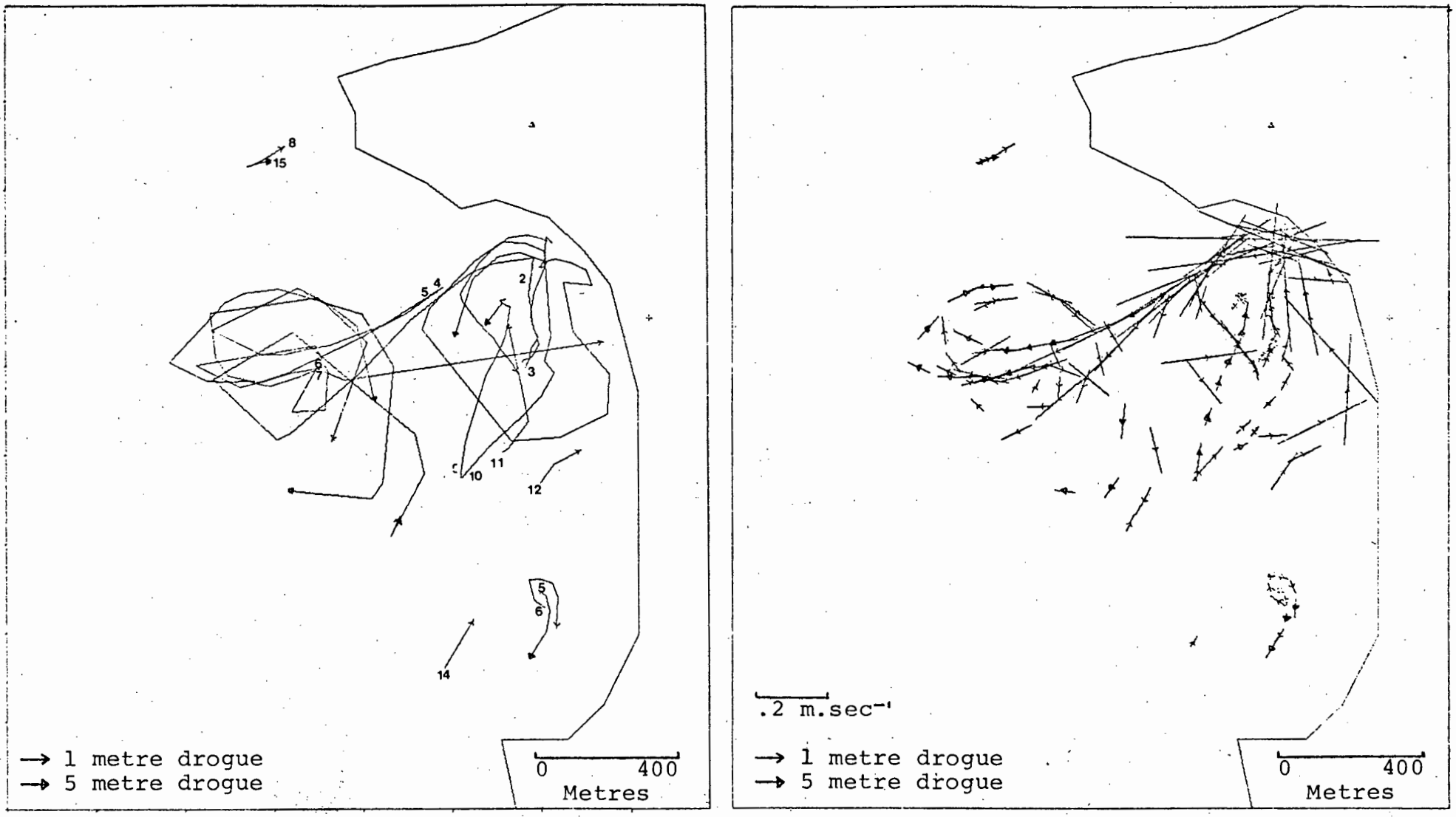

Fig. B.1 Float paths and velocity vectors, 14-04-76.

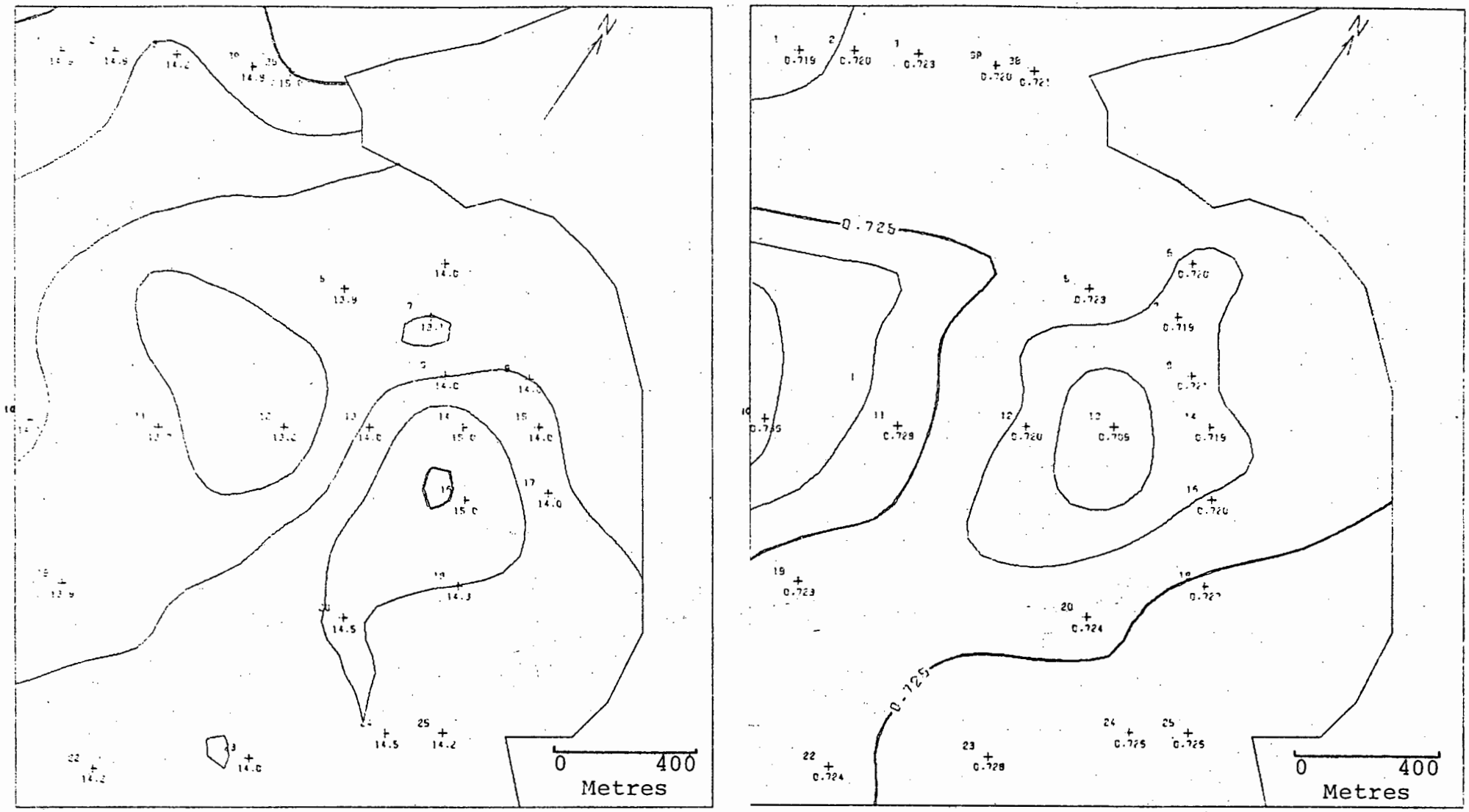

Fig. B.2 Surface temperature and salinity, 14-04-76, A.M.

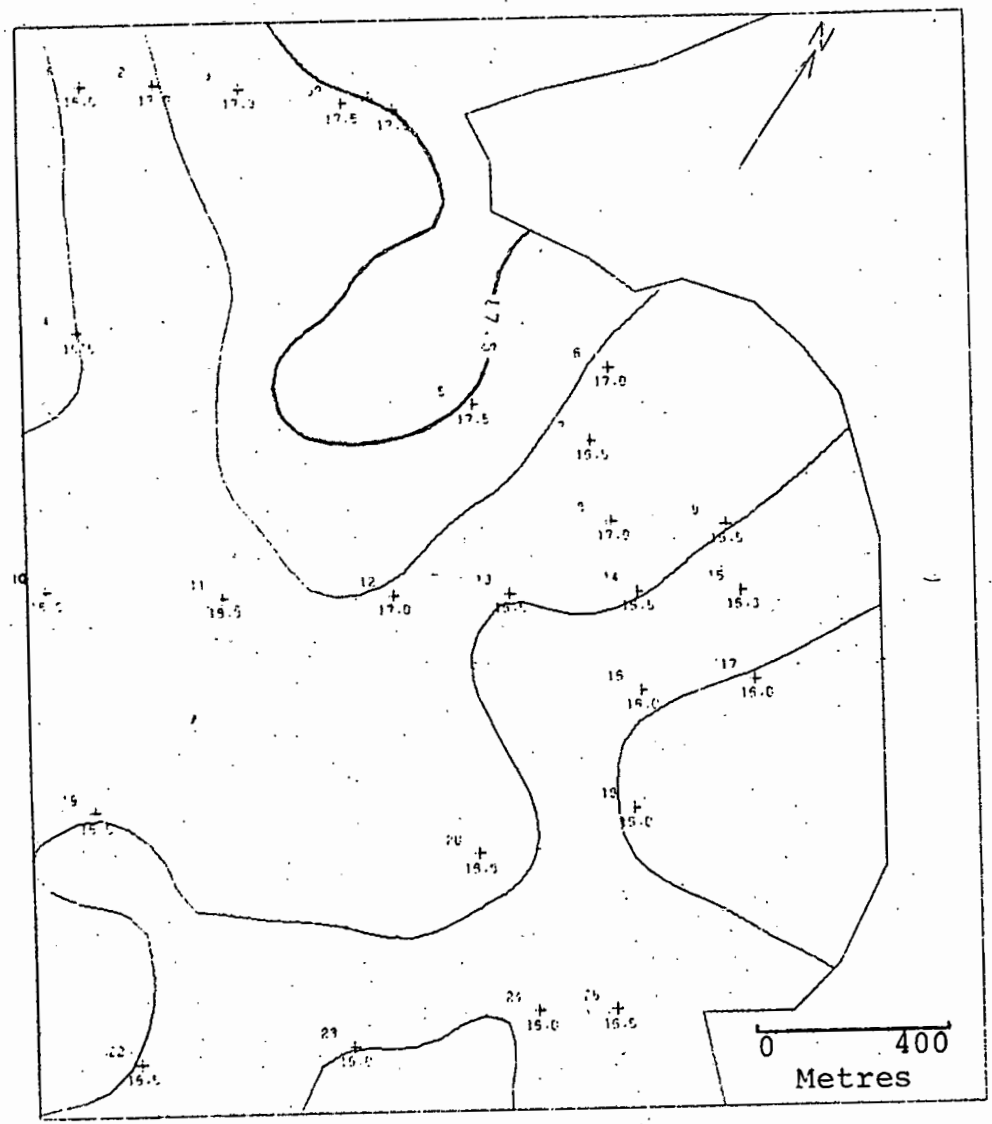

Fig. B.3 Surface temperature, 14-04-76, P.M.

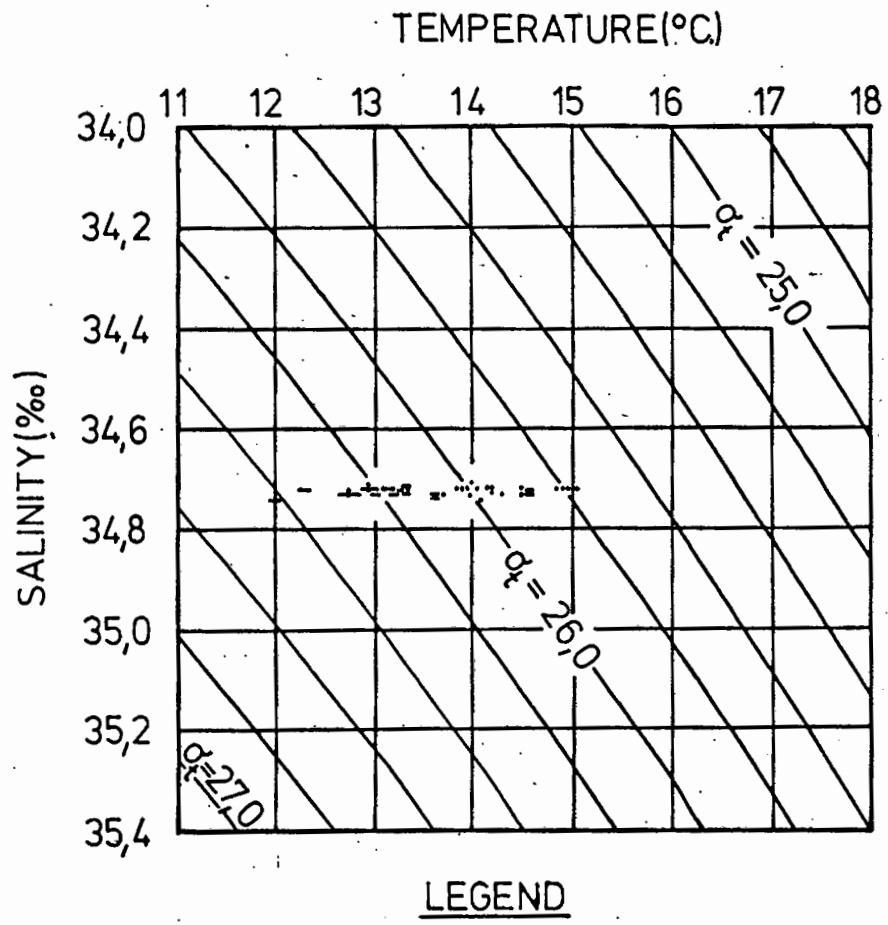

Fig. B.4 T-S diagram, 14-04-76, A.M.

APPENDIX C : MATROOS BAY OBSERVATIONS, 18th April, 1976

LOCATION :	Matroos Bay
DATE :	18th April, 1976
CHARACTERISTIC WAVE HEIGHT (H_{mo}) :	0200 hours 1.84 metres 0800 hours 2.55 metres 1400 hours 2.43 metres 2000 hours 2.36 metres
PEAK PERIOD (T_p) :	0200 hours 8.8 seconds 0800 hours 10.4 seconds 1400 hours 9.8 seconds 2000 hours 9.9 seconds
WAVE DIRECTION :	0200 hours 192° 0800 hours 210° 1400 hours 192° 2000 hours 200°
TIDES (TABLE BAY) :	HIGH: 0553 : 1.64 m. LOW: 1212 : 0.35 m. 1826 : 1.57 m.

WIND CONDITIONS : A light south-south-westerly breeze of less than 4 $m.sec^{-1}$ was recorded between 1000 and 1800 hours clearing the coastal mist. At other times conditions were calm.

TIMES OF DATA COLLECTION :	FLOAT TRACKING: 1039-1520 hours TEMPERATURE/ SALINITY: A.M. 1055-1215 hrs.(approx) P.M. 1400-1500 hrs.(approx)

DATA QUALITY : Good, reliable data. Waves too high to permit floats to be deployed far inside the bay.

DISCUSSION : The pattern of float paths shows the strong central rip current characteristic of high wave conditions. Float number 1 was carried inshore near the northern headland and reached speeds in excess of .60 $m.sec^{-1}$ as it was transported around the coast and out in the rip current. Other floats over 800 metres offshore, were observed moving with speed over .30 $m.sec^{-1}$. Inflow occurred near the northern headland and to the south of the rip, although here the inflow appeared to be mainly entrainment into the rip current. Inflow may have taken place closer to the southern headland. Inflow speeds were generally around .10 $m.sec^{-1}$.

Floats moving out in the rip turned towards the right and moved up the coast, following the coastal current. At a distance of approximately 1.5 to 2.0 kilometres offshore speeds varied from .10 to .25 $m.sec^{-1}$.

Surface temperature contours in both the morning and afternoon were almost perpendicular to the coast with cooler, 14.0°C water being flanked to the north and south by warmer, 15.0°C water. By the afternoon the 15.0°C isotherms had moved slightly north in response to the coastal water movement. The northerly swing of the floats, as they moved out of the bay, was not indicated by the surface temperatures and some vertical motion may have been involved. Warmer water appears to have entered from the south whilst in the northern part of the bay, temperatures remained more uniform, possibly due to the recycling motion indicated by several of the floats.

The temperature section, 10 - A, obtained in the morning showed a gradual drop in temperature for the first 10 metres to 13.0°C. This surface water may have represented the mixed water moving outwards to a depth of 10 metres in the rip current. Below this, a thermocline occurred with a temperature drop of 1.5°C over 5 metres. A more gradual drop occurred from there to the bottom. The thermocline persisted in the afternoon but oscillations in depth were observed. These oscillations may have been present during the morning but not observed due to missing data. The upper 10 metres of water was again almost isothermal due to the transport of well mixed water from the bay by the rip current.

A temperature difference of 1.5°C between the central and southern waters was more intense than indicated, occurring over a few metres. The boundary was marked by a distinct colour difference and a foam line.

Two stations in the morning and three stations in the afternoon were all that were occupied of the seven stations between the headlands. The resulting sections do not reveal much about the water movement and are not presented here.

The morning surface salinities show an orientation of the isohalines perpendicular to the shore, similar in direction to that of the isotherms. In this case, higher salinity water ($\simeq$ 34.64 ‰) was surrounded by water of lower salinity ($\simeq$34.63 ‰). In the afternoon a similar pattern existed, but the isohalines had moved north allowing less saline water to penetrate into the southern end of the bay. The salinity of the water in the northern part of the bay had increased to over 34.66 ‰, higher than that observed in the morning. The origin of this water is not known.

The salinity on the offshore side of the foam line was 34.633 ‰ in the 15.0°C dark green offshore water. The salinity was 34.679 ‰ in the 13.5°C brown nearshore water. It was observed that foam lines often mark boundaries of distinct water masses.

The temperature - salinity curve shows the distinction between the central water mass and that to the north and south. The temperature was the more important factor in determining the density, the central mass having a density, σ_t, of about 25.9 and the coastal water 26.7.

The high swells left strong records on the D.O.S.O. and indicated that the swell was from the south-south-west.

The transport of water out of the bay took place at the rate of 600 $m^3 sec^{-1}$, sufficient to empty the bay in a matter of hours. Float 5, deployed on the 17th April was recovered within the bay. It may have been grounded, but the possibility of the long residence times due to recirculation does exist.

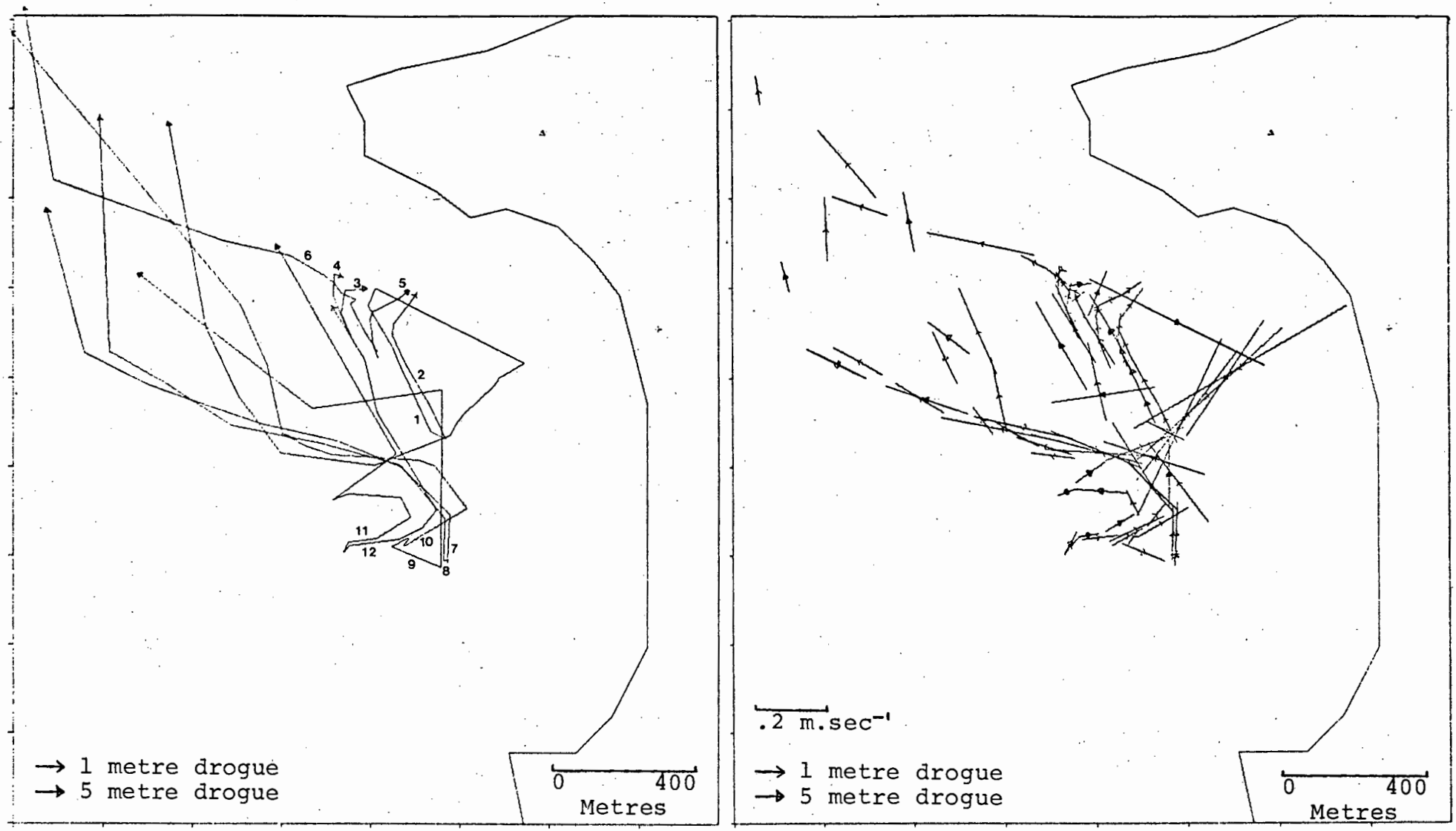

Fig. C.1 Float paths and velocity vectors, 18-04-76.

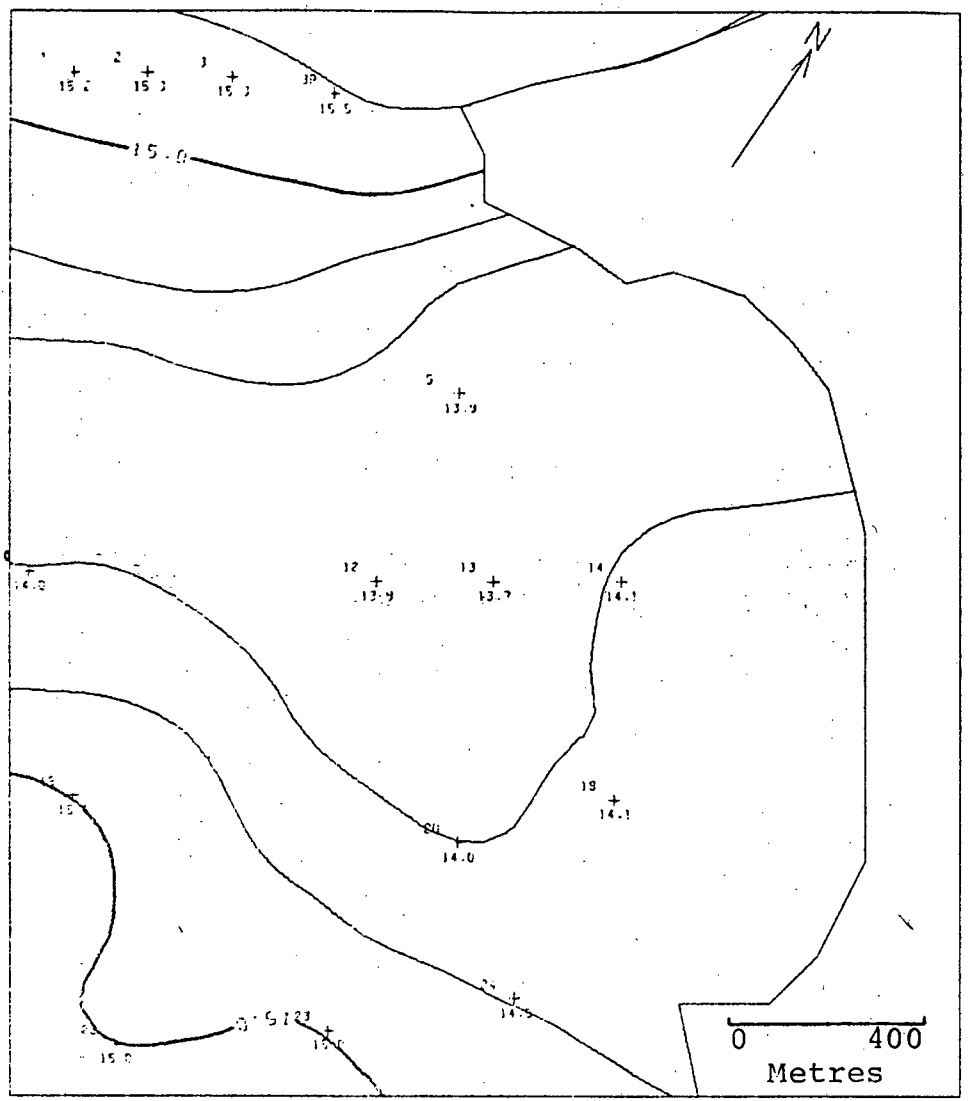

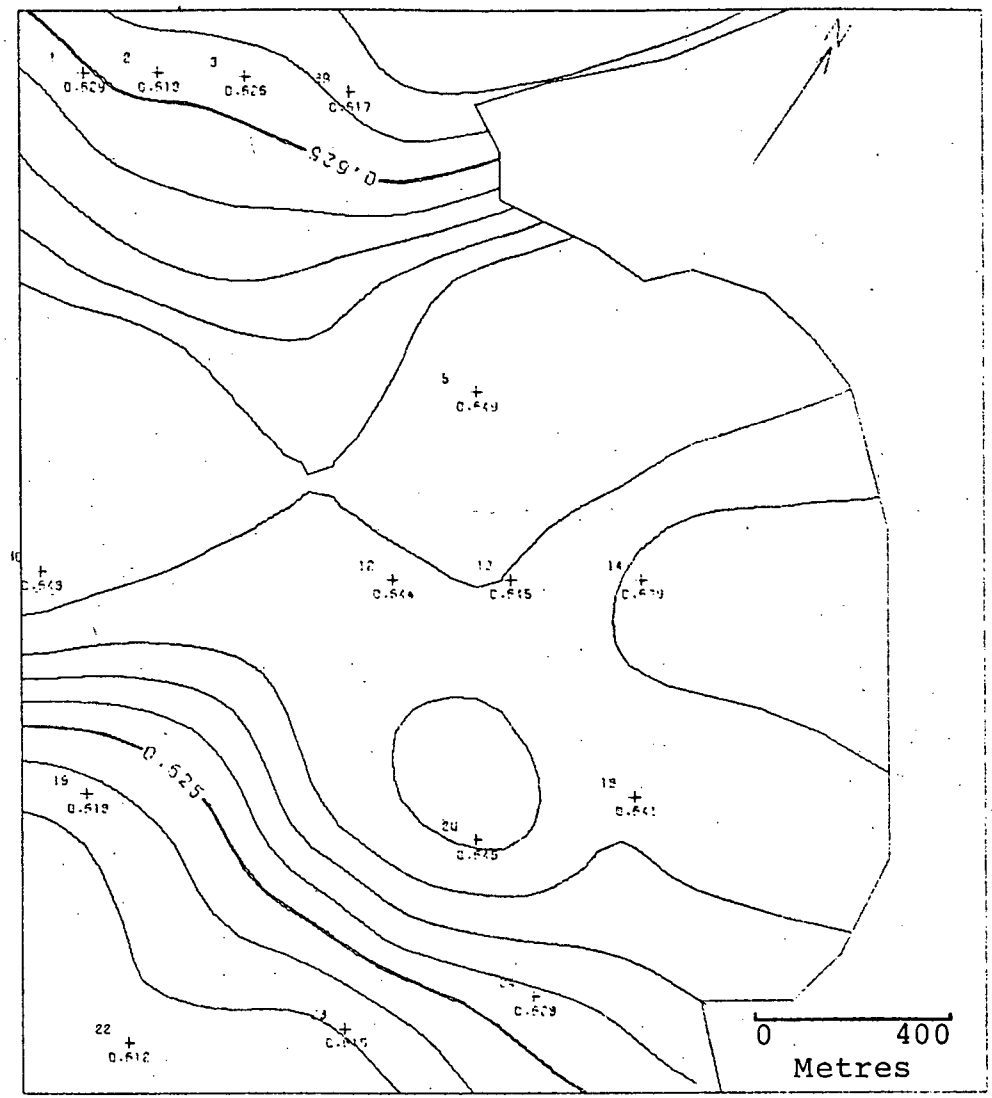

Fig. C.2 Surface temperature and salinity, 18-04-76, A.M.

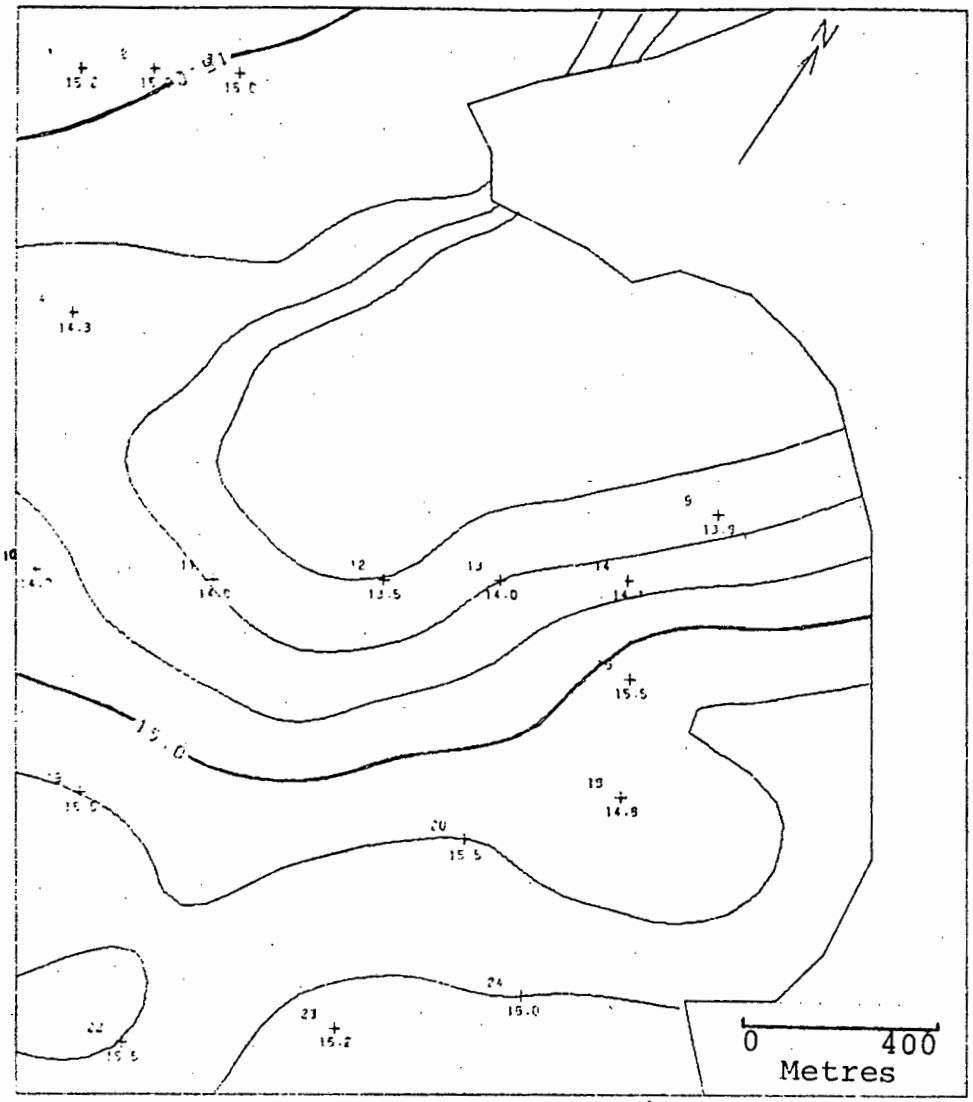

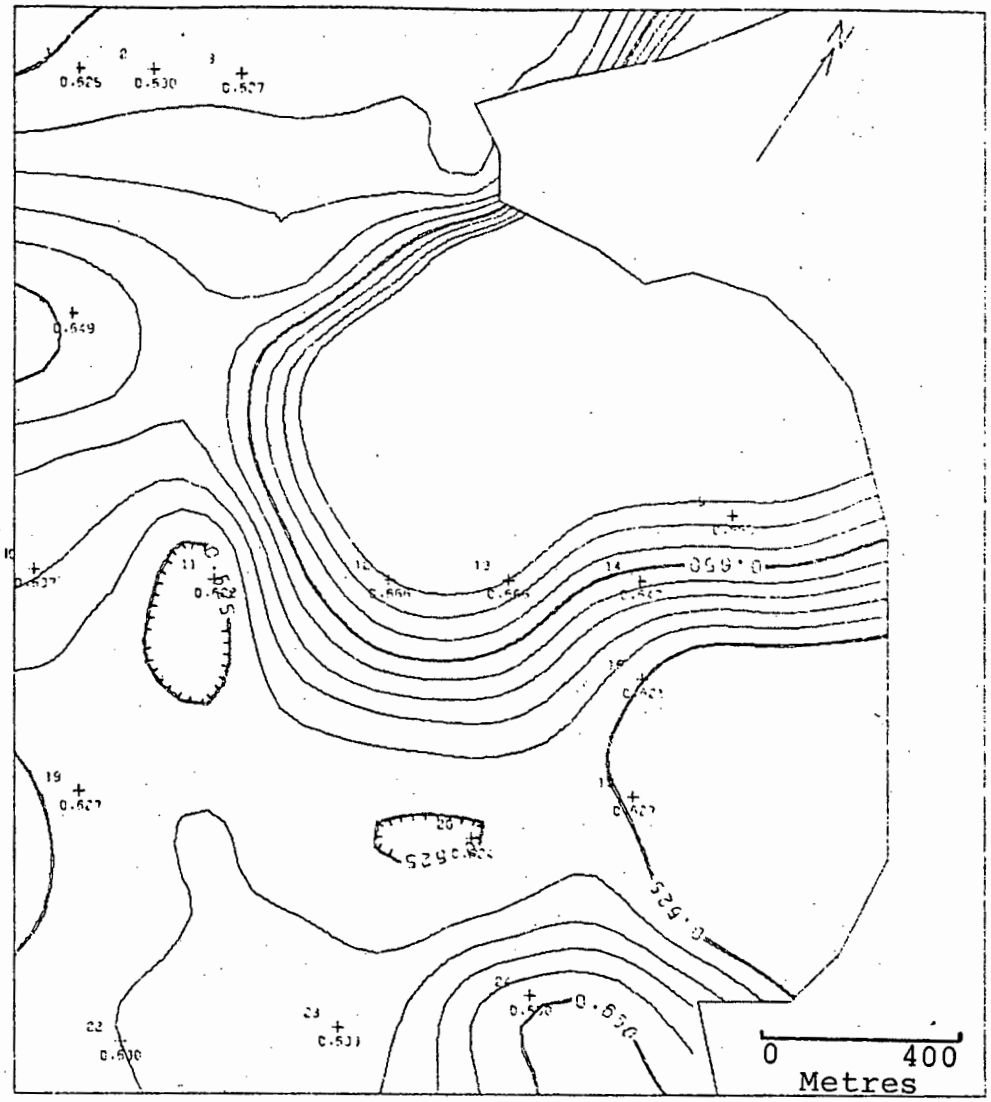

Fig. C.3 Surface temperature and salinity, 18-04-76, P.M.

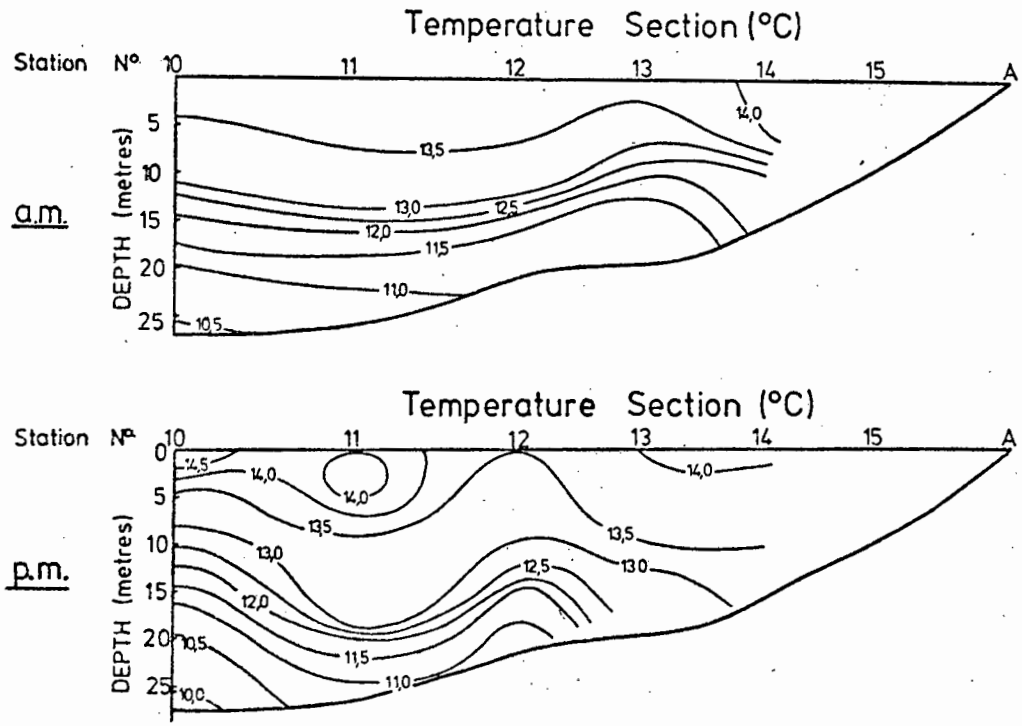

Fig. C.4 Temperature sections, 18-04-76.

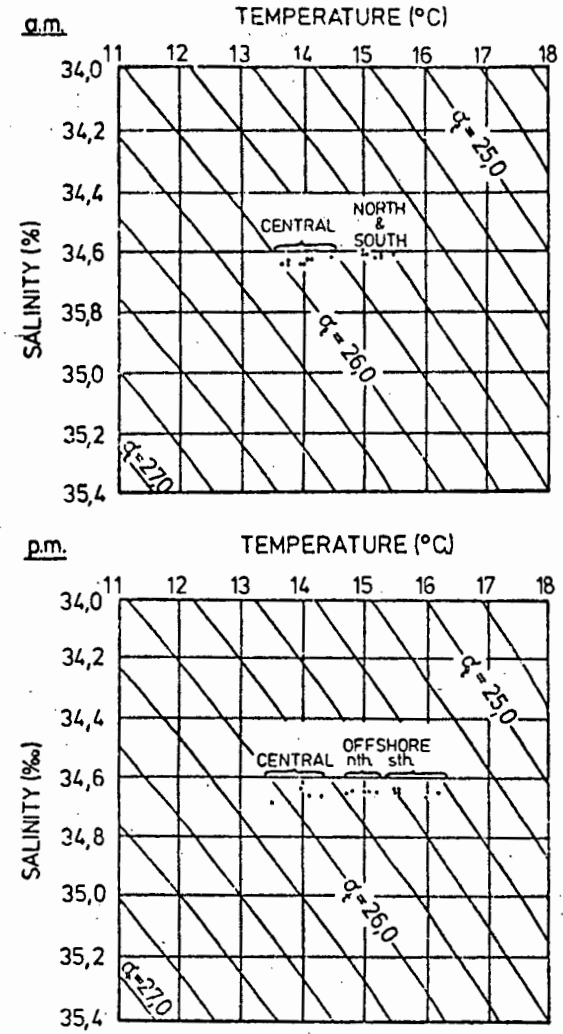

Fig. C.5 T-S diagrams, 18-04-76.

APPENDIX D : MATROOS BAY OBSERVATIONS, 03rd September, 1976

LOCATION :	Matroos Bay
DATE :	3rd September, 1976
CHARACTERISTIC WAVE HEIGHT (H_{mo}) : (Waverider "E")	0200 hours 0.65 metres 0800 hours 0.64 metres 1400 hours 0.55 metres 2000 hours 0.56 metres
PEAK PERIOD (T_p) :	0200 hours 9.6 seconds 0800 hours 9.0 seconds 1400 hours 6.0 seconds 2000 hours 6.6 seconds
WAVE DIRECTION :	No records available
TIDES (TABLE BAY) :	HIGH: 1151 : 1.34 m. LOW: 0535 : 0.60 m. 1811 : 0.61 m.

WIND CONDITIONS : Winds throughout the day were light, never exceeding an hourly average of 5 $m.sec^{-1}$. The direction of the wind swung slowly from east-north-east at midnight to north at 0600 hours and west-south-west at 1700 hours, when, after a short period of calm, north-easterly winds were again experienced.

TIMES OF DATA COLLECTION :	FLOAT TRACKING: 1122-1740 hrs. TEMPERATURE/ Noon 1300-1400 hrs.(approx) SALINITY: P.M. 1600-1715 hrs.(approx) DYE PHOTOGRAPHY: 1048-1413 hours

DATA QUALITY : Good, reliable data. Both float tracking and dye photographic techniques were used to give details of the circulation present.

DISCUSSION : Two cusps were visible along the coastline and three rip currents. From the shore neither the central nor the northern rip appeared to dominate the circulation, but rather the currents within the bay appeared to have consisted of three individual cells. An anticlockwise cell driven by the northern rip current was located in the northern part of the bay. This was separated by a narrow region of large horizontal shear from another anticlockwise cell driven by the central rip current, with a third, clockwise cell in the southern end of the bay. Float paths revealed that only two cells were in fact present, a large anticyclonic

cell in the northern end of the bay and a weaker cyclonic cell to the south.

The path of float number 8 demonstrates the area of the northernmost anticlockwise gyre. Maximum speeds of .20 $m.sec^{-1}$ were reached within this gyre in the longshore current and at the base of the rip. Speeds of only about .05 $m.sec^{-1}$ were recorded during inflow. Floats 3 and 4 initially moved south around the outside of this northern gyre before moving inshore and commencing to move in what appeared to be a central gyre. This gyre, also anticlockwise in its rotation, was not as vigorous as the northern gyre and floats moved with a maximum speed of only about .10 $m.sec^{-1}$. In fact, these two gyres really formed only one larger anticlockwise gyre, the rip current near the centre of the bay being only a remnant from a clockwise circulation, or generated by the presence of the cusp. It did not dominate the circulation of the bay and merely deflected water offshore. The diagram of the float velocities illustrates this. The circulation was in accord with the circulation pattern experienced on days of low wave height.

The paths of floats 5, 6 and 2 indicate that a slow clockwise gyre may have existed in the southern end of the bay, with inflow of surface water into the bay taking place between this gyre and the anticlockwise gyre.

Conditions on the day were such that downwelling was active and, in particular, a front separating warm saline, offshore water from cooler, less saline, upwelled nearshore water was observed to move rapidly inshore. Two distinct types of motion of the offshore floats were observed in front of and behind this front. It is convenient to separate the float paths into two diagrams, the first illustrating the paths taken before 1440 hours, prior to the floats passing

the front, the other after 1440 hours when the floats were on the offshore side of the front. The circulation within the bay itself appeared to be virtually independent of the time except near the southern headland.

Prior to 1440 hours, floats near the mouth of the bay exhibited a slow motion (less than .05 $m.sec^{-1}$). Floats 1 and 2 moved inshore with a slight down the coast motion, float 2 eventually entering the bay as mentioned above. Float 1 however, swung offshore and started to move away from the coast, still with a southerly tendency. This motion was repeated with floats 9 and 10 and was probably a response to the downwelling. As such, it was not surprising that the deep float moved more rapidly than the shallow float.

By 1440 the front had moved to be on the inshore side of most of the floats outside the bay. Significant differences in the motion of the floats were noted. Floats moved almost parallel to and up the coast. The floats with drogues at 1 m. tended to have an onshore component to the movement, floats with drogues set to 5 m., an offshore component. The onshore movement of the surface floats was associated with the return flow of the warmer water that had been displaced by the upwelling winds. The 5 m. drogues continued their offshore movement as their drogues were beneath the inflowing surface water (as will be seen later when temperature profiles are considered). The speed of the water movement was about .05 to .10 $m.sec^{-1}$.

The northward, or up the coast, component may have been due to the motion imparted by the southerly winds that resulted in the upwelling.

The apparent change in the motion of the floats before and after 1440 hours therefore, was not so much a change in the

movement of water, but rather, a change in water mass in which the float was located. Here, clearly, the inability of the floats to take part in the vertical motion was responsible for what may have appeared somewhat confusing at first sight.

It was possible to compare the velocity of the drogue and the dye patches under these almost windless conditions. The two were found to be very similar with a difference of only about 10 metres occurring in over an hour.

The contours of surface temperatures drawn from the morning readings, show that cooler water, less than 10.5°C existed within Matroos Bay and near the northern and southern headlands. Water with a temperature in excess of 11.0°C was located offshore and to the south.

The morning temperature section between station 10 and the shore showed the layer of water with a temperature greater than 11.0 C to be only about 3 metres thick. Below this, at about 5 metres, was a thermocline in which the temperature dropped rapidly from 10.0°C to below 9.0°C in only a few metres. Temperatures then fell more gradually to the bottom where temperatures as low as 7.7°C were recorded.

The section between the headlands recorded in the morning also showed the thermocline but indicated that it, infact, sloped from near the surface in the southern part of the bay to 3 to 5 metres in the centre. The reason for this was not clear, but may have been due to the inflow of surface water observed near the centre, whilst to the south, the water was more isolated. Water below a depth of 5 m. in the southern part of the bay was almost isothermal with a temperature of between 8.5 and 8.0°C, although at station 18 a temperature of 7.6°C was recorded. In the northern

part of the bay the temperature at depths below 5 m. were slightly warmer, varying between 8.5 and 9.0°C.

The surface salinity contours of the morning showed a similar pattern to that of the isotherms. Low salinity water, less than 34.64 ‰ was found in the bay and near the two headlands, whilst more saline water (salinity in excess of 34.84 ‰) was found offshore.

By the afternoon the veneer of warmer surface water had extended into the bay and now only two stations were found with a temperature of 11.0°C or less (stations 9 and 15), the north and central inshore stations in Matroos Bay. Outside the bay and in the southern end of the bay water was almost isothermal with a temperature of about 12.2°C. By comparing the morning and afternoon maps, the northward advance of the contours may be clearly seen. The 11.0°C isotherm, for example, had advanced approximately 600 metres during the day, a speed of approximately .20 $m.sec^{-1}$. (c.f. .05 to .10 $m.sec^{-1}$ computed from float observations).

The section of temperatures taken perpendicularly to the shore in the afternoon showed that the inflowing warmer water was still only a thin surface layer. The 11.0°C contour lay at only 3 m. The water was almost horizontally stratified with temperatures falling with depth to be below 8.0°C at 20 metres.

From the section taken across the bay in the afternoon, the warmer surface water was seen to have penetrated into the bay with a resultant deepening of the contours. Temperatures near the surface were, of course, warmer than in the morning, but at depth, a temperature of 8.0°C was still found. The temperature range between the surface and the bottom was therefore greater than in the morning.

The afternoon surface salinity readings, although incomplete due to a shortage of sample bottles, illustrated that the higher salinity water had moved onshore.

Although rapid onshore flow of warm surface water was occurring, the layer was so thin that very little downward motion was required to compensate for this inflow. Contours, in general, fell only 3 metres. In fact, in deep water at some offshore stations, temperature contours were observed to rise.

The temperature - salinity relationships show the differences of both temperature and salinity that existed between the offshore water and the nearshore, upwelled water. Although both the temperature and salinity varied considerably, the density was not markedly different. The offshore water had a density, σ_t, of between 26.5 and 26.6 and the nearshore water 26.6 and 26.7.

At 1048 hours the boat commenced to lay dye trails across the bay. Three trails were laid in all. A red line between the headlands, and two green lines approximately $\frac{1}{3}$ and $\frac{2}{3}$ of the way into the bay. Rhodamine B was the red dye and fluorescein the green dye. Photographs were taken at irregular intervals by the observer stationed at the Trigonometric Beacon on the northern headland. A 35 mm. ASAHI PENTAX camera with a 55 mm. lens and Agfa CT18 slide film was used. The slides have been reproduced as plates D1 to D4. Although the altitude from which the photographs were taken prohibits rectification, it was possible to get a qualitative indication of the water movement by observing the relative motions of the dye lines.

Plate D1 was taken looking offshore (south-west) at the start of the dye laying, 1048 hours. It shows the distinct colour difference that was observed at the front.

Plate D2, 1115 hours, illustrates the irregularities which had already started to appear in the two green lines. The offshore deflection of both lines near the northern end (foreground) of the bay was due to the offshore motion of the northern gyre (described earlier). Several slicks were observed and these are believed to be associated with regions where downwelling was taking place. The outer red line, in fact, lies off such a slick and moved little during the day. The dark blue, warmer water is just visible at the top right hand corner.

Plate D3, 1129 hours, shows that the outward flow of water near the bottom of the picture had deflected the green lines still further from the shore. A similar deflection of the more inshore of the lines was observed nearer the centre of the bay. This deflection was due to the central rip current described earlier. This rip current moved offshore from the southern side of the cusp on the shoreline. On the northern side of the cusp, inflow occurred.

The cusps in the bay had been present at least since the 1st September. Although they may have been modified by the waves, they were relics from past wave conditions. The cusps may have formed in the lee of the dominant central rip observed at this time.

It is interesting to consider what changes may have occurred in the wave conditions to give the assymetrical current pattern on either side of the cusp that was observed.

The simplest suggestion is that the wave direction had swung more to the south. This would have increased the angle of incidence of the waves on the beach to each side of the cusp, leading to northward flowing longshore currents in this region. At the same time the angle of incidence on the southern side of the cusp was reduced, on the northern side

increased. Such a change would lead to the current pattern observed (not considering any counter-acting or assisting forces resulting from the wave height differences).

Returning to the consideration of Plate D3, the red line had sheared near the southern headland. This was in accord with the inshore surface motion of the floats near the centre of the bay and offshore motion further south. The red dye near the northern headland had moved inperceptibly since deployment at 1048 hours.

The darker blue offshore water was still visible offshore and to the south.

Further photographs were taken until 1153 hours showing the deformation of the dye lines within the bay. These have not been included as they show similar patterns but the dye, of course, becomes fainter as it was dispersed. Additional dye patches were placed in front of the advancing boundary and these disappeared rapidly. It is inferred that they were downwelled beneath the advancing front. The distance between the red and green lines in the northern part of the bay was decreasing rapidly. Dye placed between these lines disappeared quickly. It was assumed to have been downwelled beneath the slicks that were observed between the red and green lines.

Plate D4, shows the boundary between the light and dark blue water at 1413 hours. By this time the boundary was almost between the headland at which point its inward advance slowed considerably.

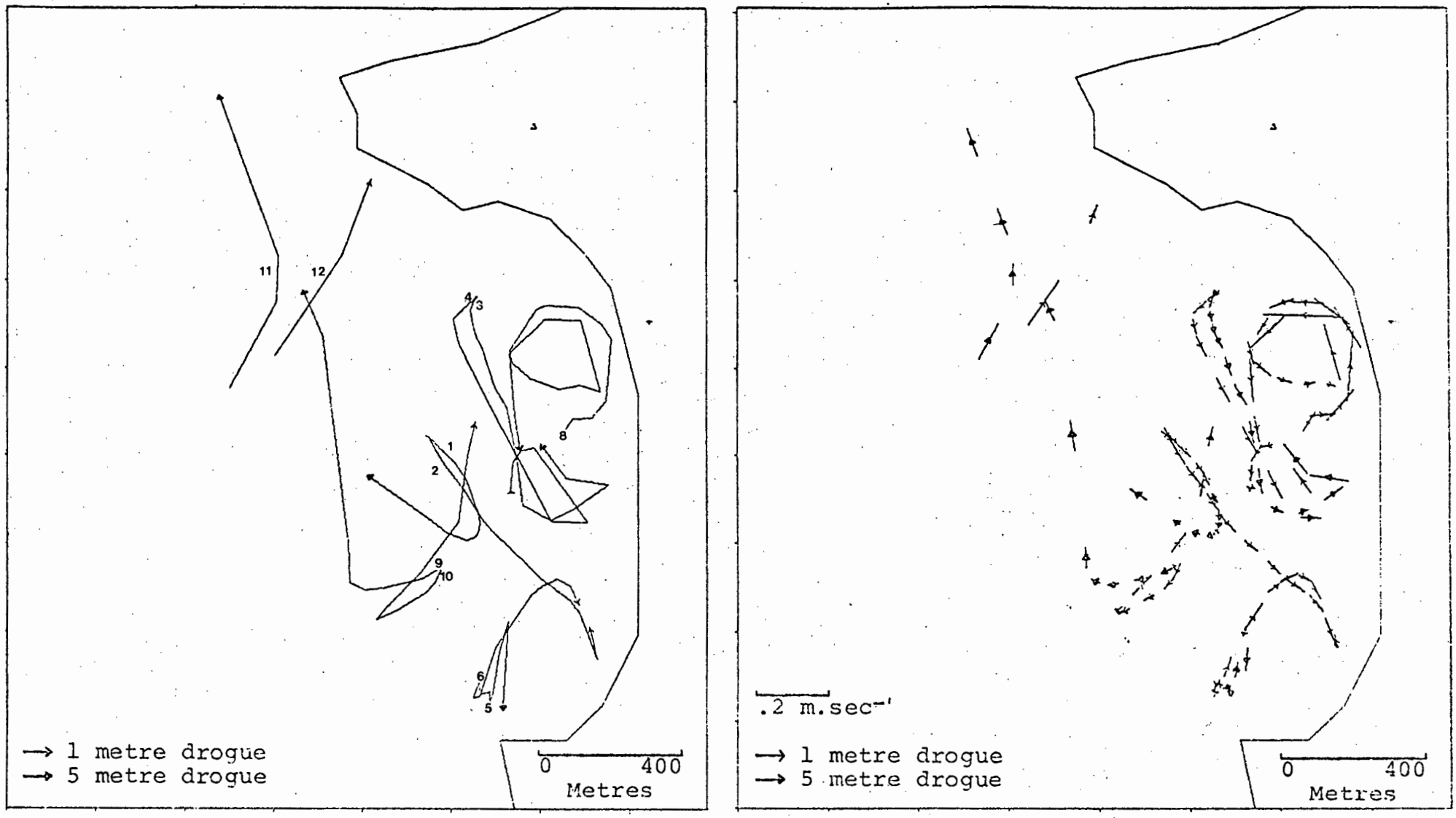

Fig. D.1 Float paths and velocity vectors, 03-09-76.

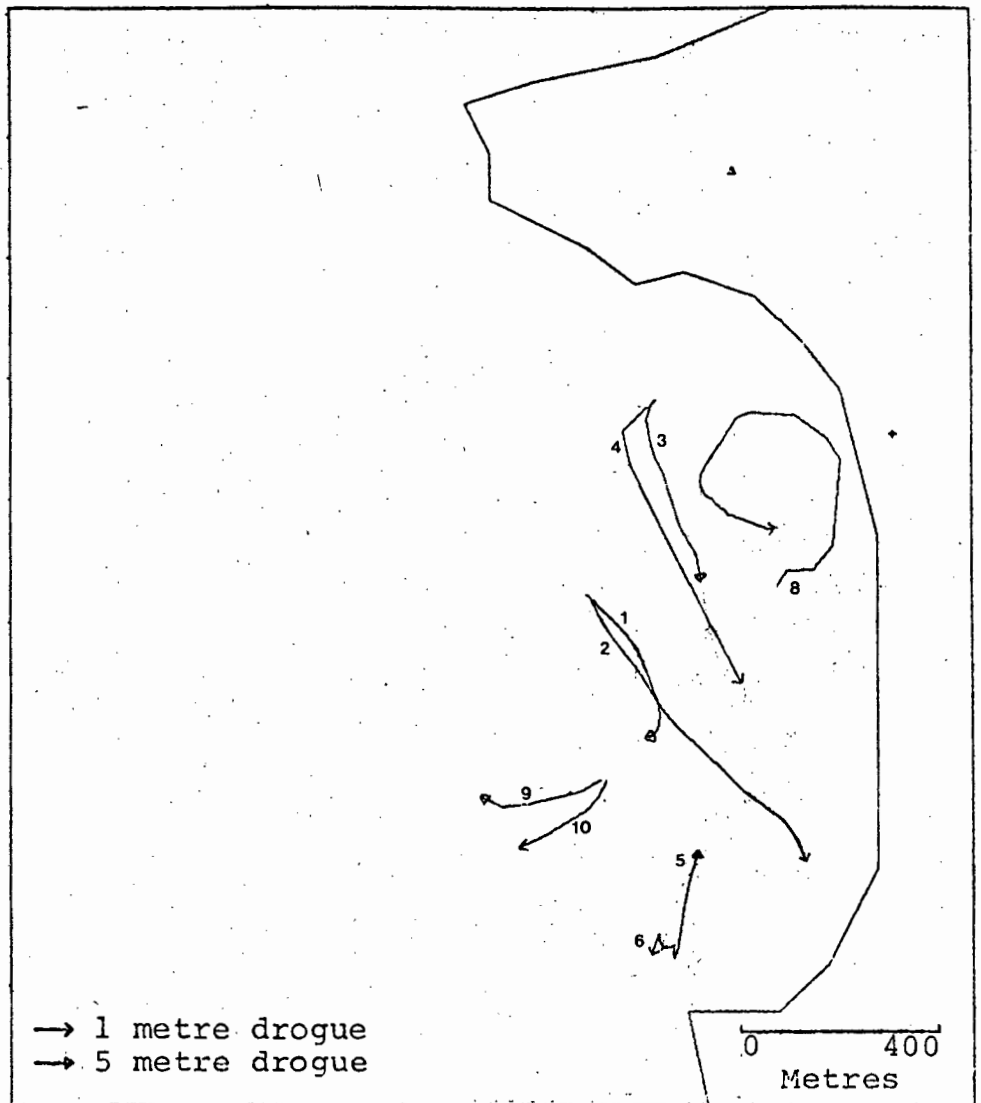

(A) before 1440 hours

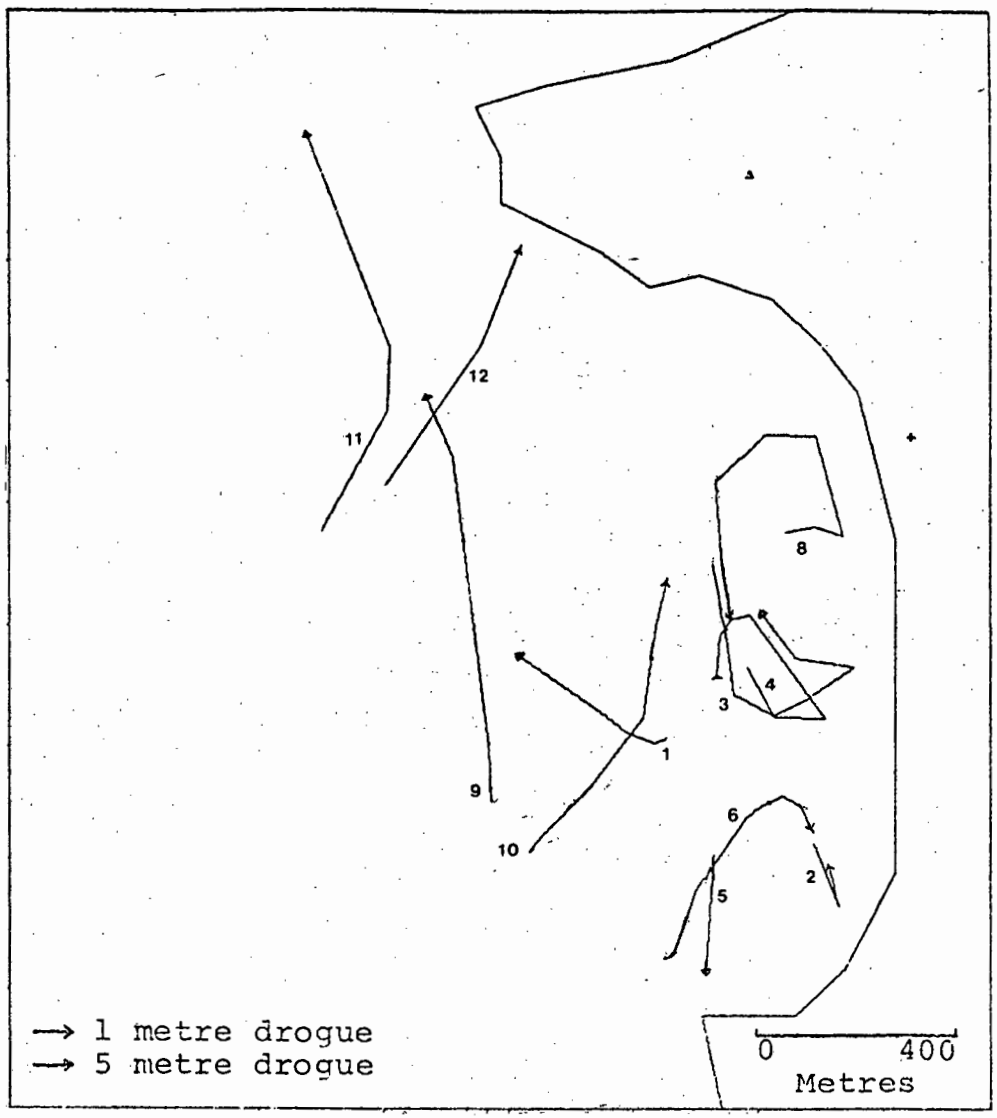

(B) after 1440 hours

Fig. D.2 Float paths before and after 1440 hours, 03-09-76.

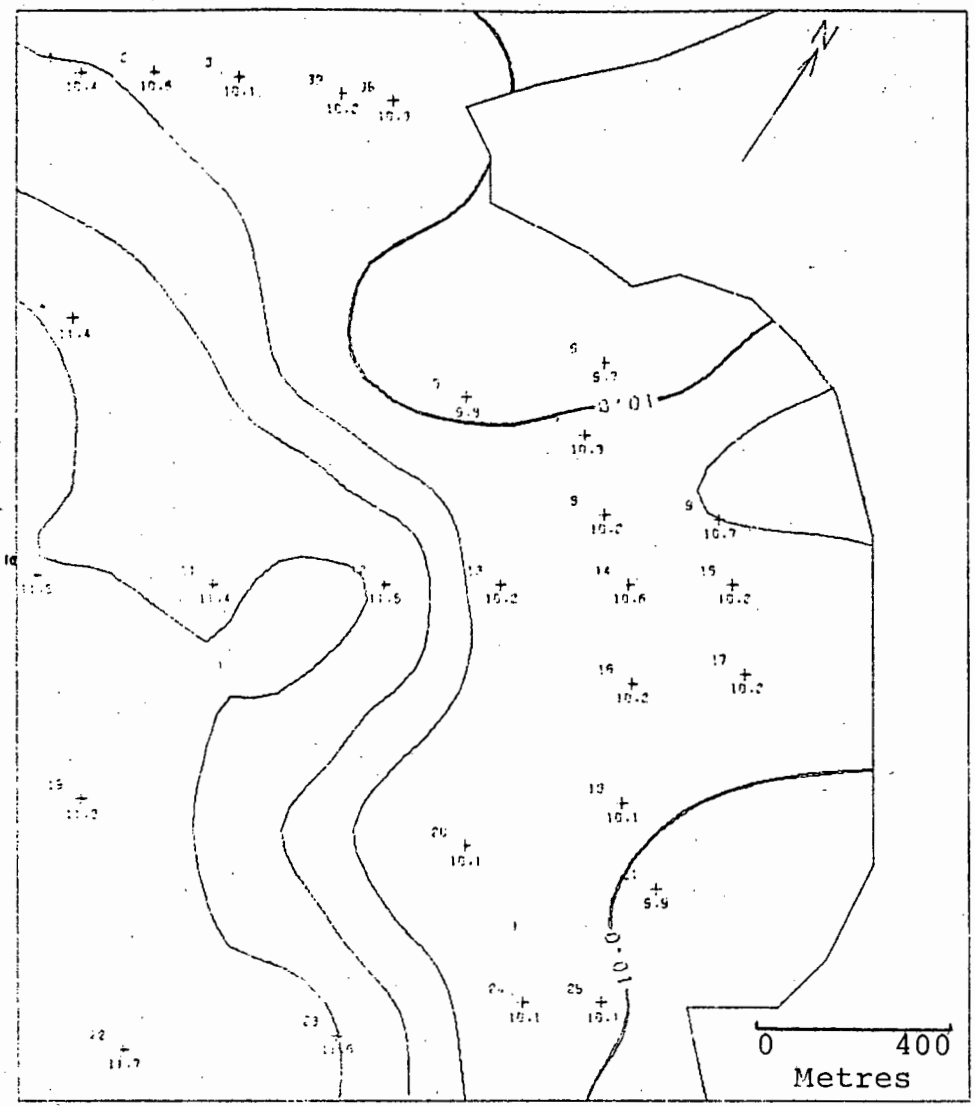

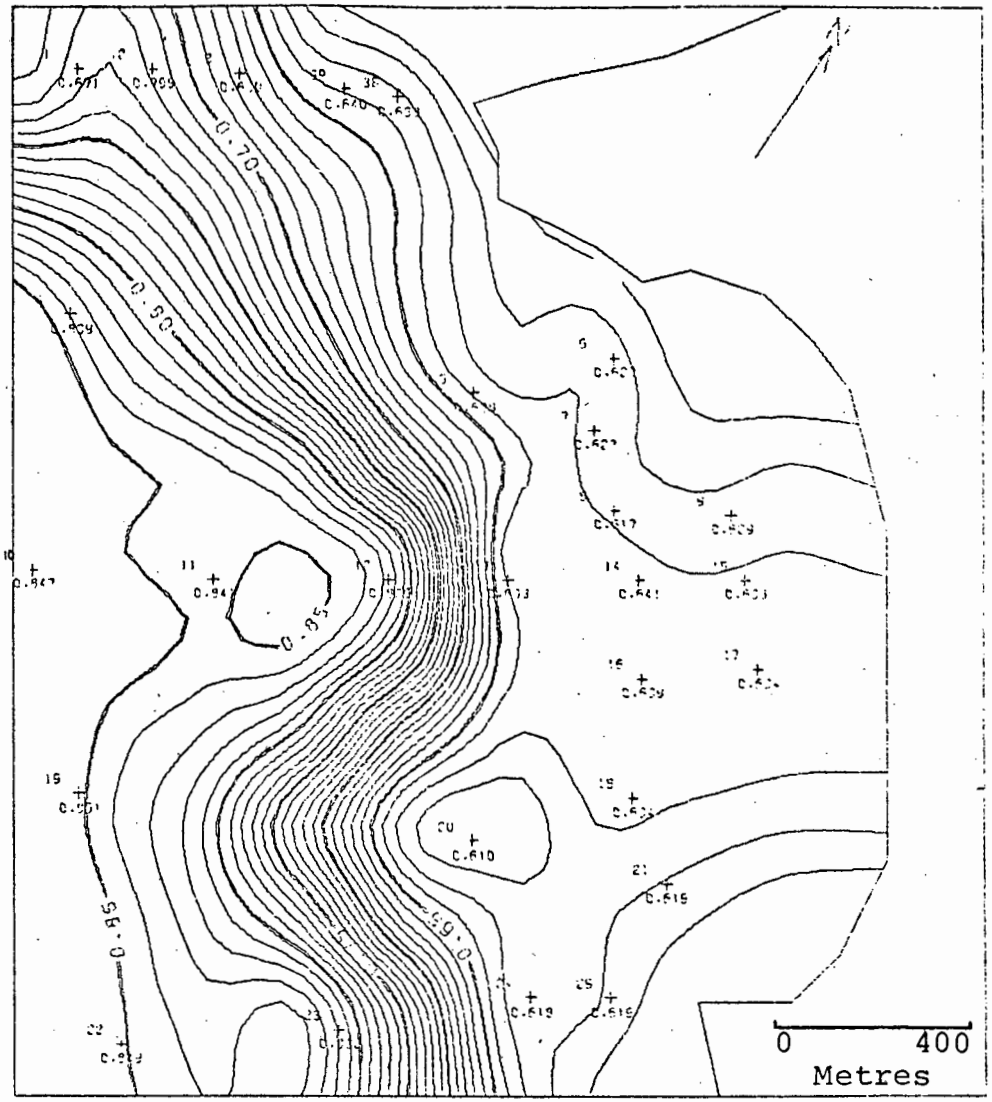

Fig. D.3 Surface temperature and salinity, 03-09-76, A.M.

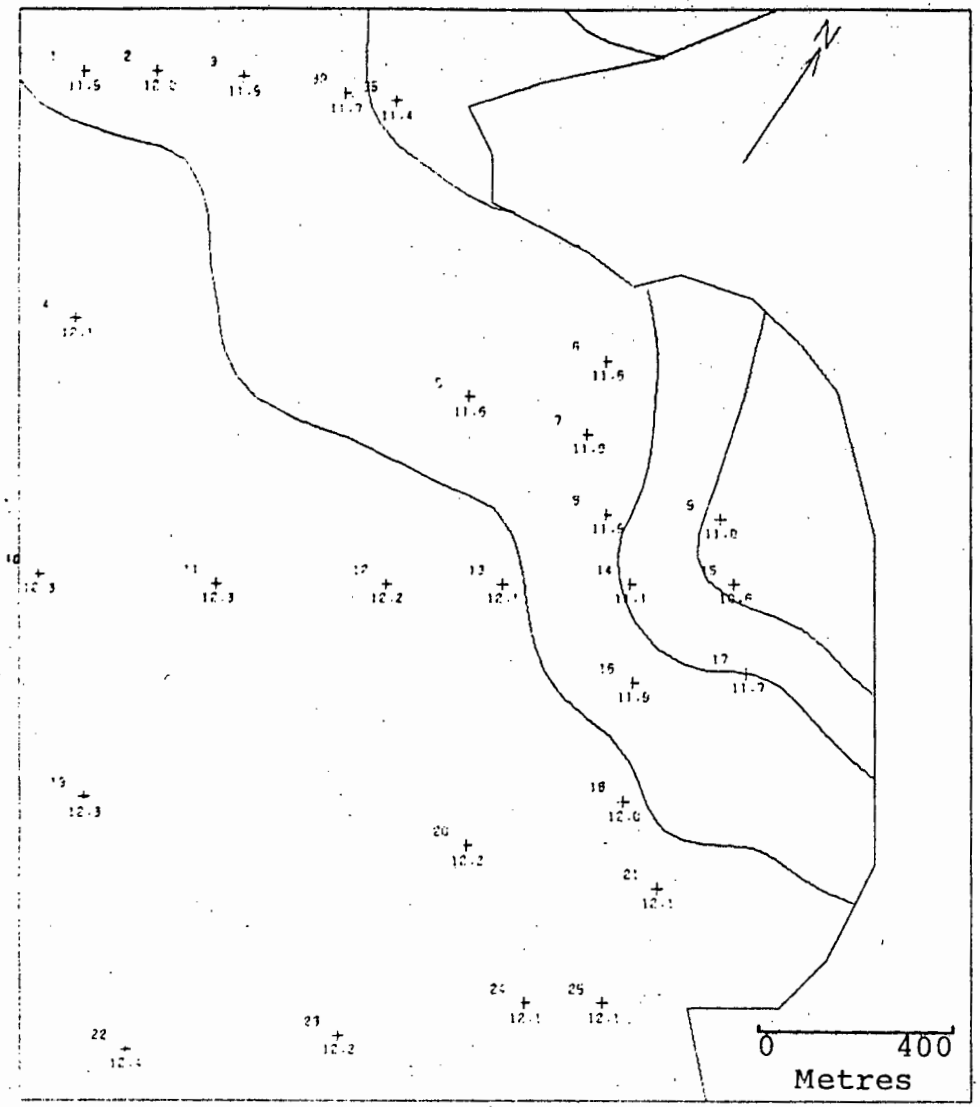

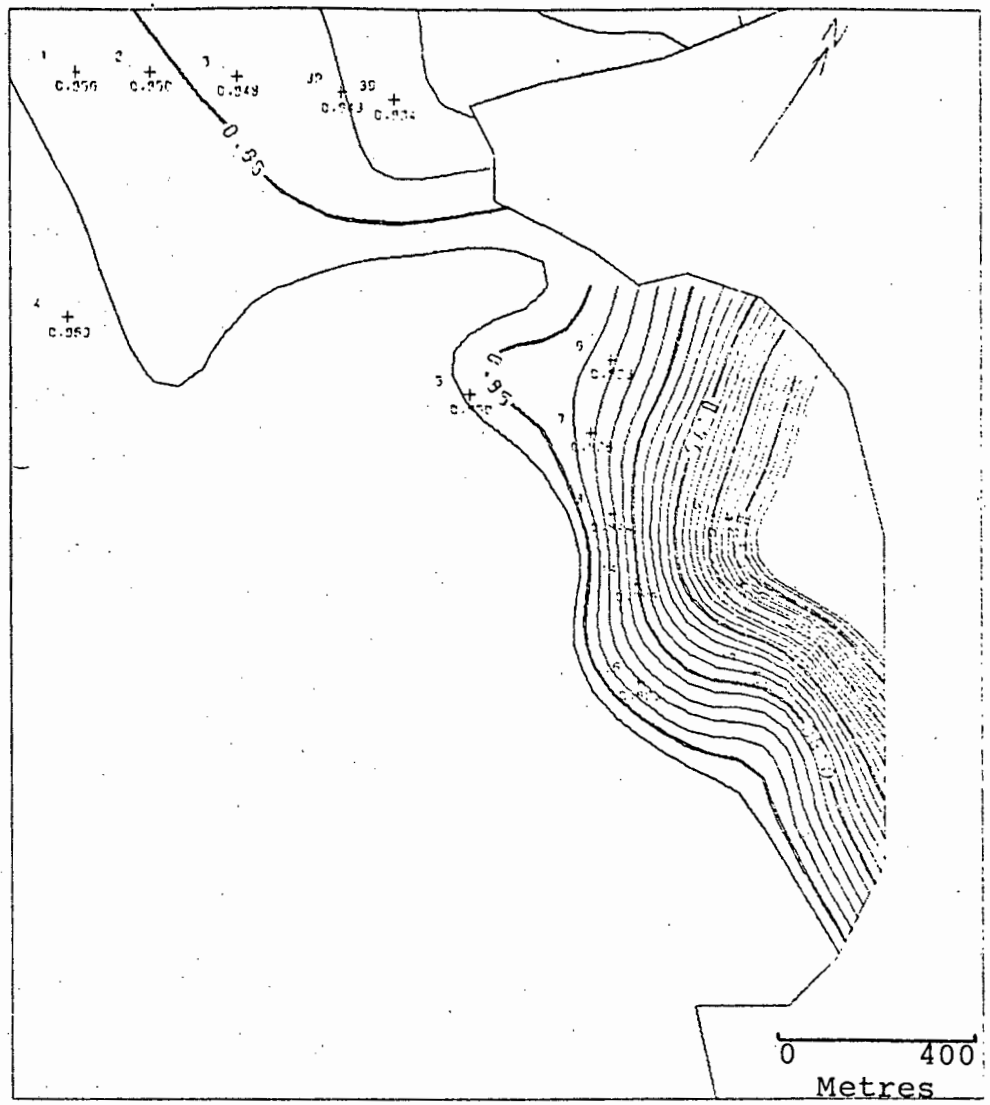

Fig. D.4 Surface temperature and salinity, 03-09-76, P.M.

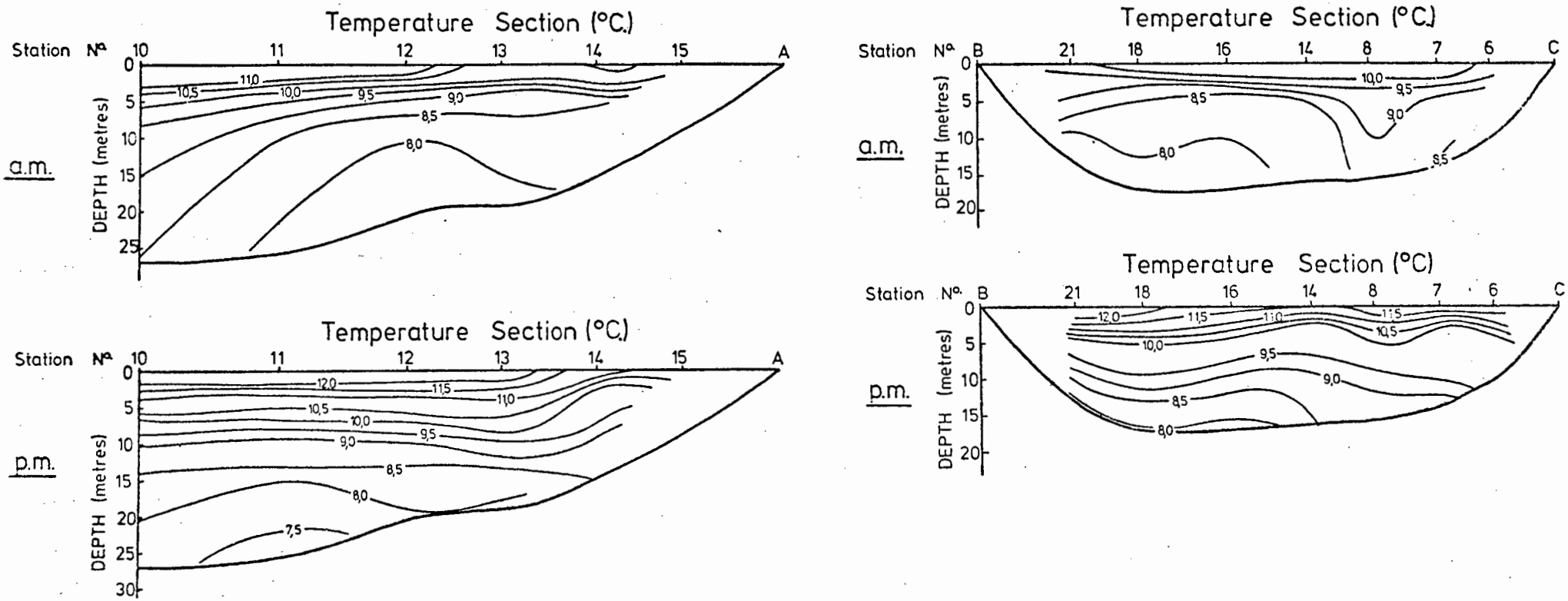

Fig. D.5 Temperature sections, 03-09-76.

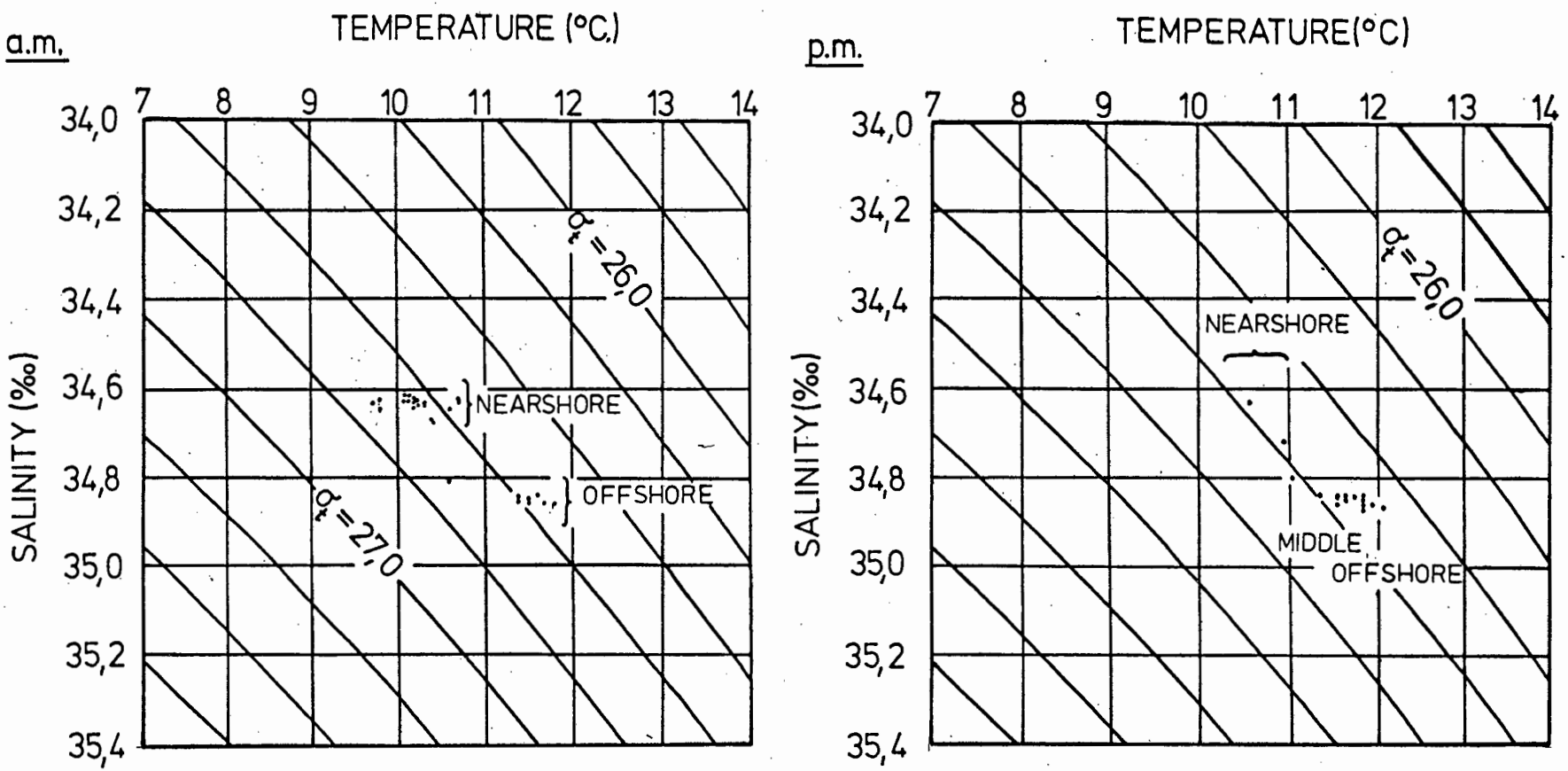

Fig. D.6 T-S diagrams, 03-09-76.

Plate D.1 South-west view from the northern headland of Matroos Bay, 1048 hours, 03 September, 1976. Note the distinct offshore colour difference, indicating the presence of the front.

Plate D.2 Southerly view from the northern headland of Matroos Bay, 1115 hours, 03 September, 1976.

Plate D.3 Matroos Bay, 1129 hours, 03 September, 1976. Note the cusps on the beach, the deflection of the dye resulting from the circulation and the offshore colour diffenence.

Plate D.4 Matroos Bay, 1413 hours, 03 September, 1976. Note the proximity to the shore of the colour change (front).